Copyright

by

Paul Bujalowski

2015

The Dissertation Committee for Pawel Bujalowski Certifies that this is the approved version of the following Dissertation:

The UNC-45 molecular chaperone:
Its interactions with myosin and its thermosensing properties

Committee:

Andres Oberhauser, PhD, Mentor

Kyung Choi, PhD, Chair

Jose Barral, M.D., PhD

Marc Morais, PhD

Giulio Taglialatela, PhD

Piotr Marszalek, PhD

Dean, Graduate School of Biomedical Sciences

The UNC-45 molecular chaperone:

Its interactions with myosin and its thermosensing properties

by

Paul Bujalowski

Dissertation

Presented to the Faculty of the Graduate School of

The University of Texas Medical Branch

in Partial Fulfillment

of the Requirements

for the Degree of

Doctor of Philosophy

The University of Texas Medical Branch

2015

Acknowledgements

My special thanks are to my family, particularly to my parents Jacek Bujalowski and Arleta Bujalowska whose support over all these years kept me going and helped me to overcome any difficulty. Without their support I would have never been able to complete my doctoral research. Their encouragement guided me for many years.

I am extremely grateful to Wlodek Bujalowski and Maria Jezewska for their invaluable help and advice before and during my graduate studies. I would like to acknowledge with gratitude, Bozena Bujalowska who has been my intellectual inspiration since my childhood. My curiosity of the world truly flourished thanks to her influence.

I own particular thanks to my mentor, Dr. Andreas Oberhauser. He has been an incredible source of inspiration and information during my doctoral research. I will be always grateful for our long discussions about science and other topic. His love of science and natural curiosity combined with his intense desire to solve scientifically important problems was and will always be an inspiration for me.

I would also like to thank my committee members, Drs. Barral, Choi, Marszalek, Morais, and Taglialatela who have been very supportive of my research and guided me during my thesis work. Their discussion and ideas always motivated me and provided me with new ways of solving problems.

I also thank my friend that I met at the UTMB as well as those that I left in Europe. Especially, I would like to thank lab college Paul Nicholls for his help in carrying out the research and forth most long discussions about wiled variety of topics

ranging from English culture and nuances of English language to theoretical physics. I also thank Michal Szymanski for his friendship and his advises on science and other topics.

The UNC-45 molecular chaperone:
Its interactions with myosin and its thermosensing properties

Publication No._____

Paul Bujalowski, PhD

The University of Texas Medical Branch, 2015

Mentor: Andres F. Oberhauser

In order to perform their biological functions, proteins must fold into a defined structure which is termed the "native state". In some cases proteins can acquire the native structure spontaneously; however for others additional assistance of molecular chaperones is needed. The molecular chaperones are proteins which through interactions with the client proteins, prevent the formation of aggregates and promote the folding process without being present in their final structure. One of the most biologically significant proteins which require assistance of chaperones are myosins. These are motor proteins responsible together with actin for muscle contraction process. The UNC-45 protein is a chaperone that has been identified to be involved during the myosin folding process.

During my thesis research, I have addressed the energetics of interactions of the UNC-45 chaperone and its domains with myosin. My results indicate that the myosin

motor domain possesses two binding sites, which engage two different domains of the UNC-45 chaperone, namely the UCS and the Central domain. Interactions between the domains in the complex affect the UNC-45 chaperone affinity for myosin. Moreover, the experiments showed that the UCS domain alone is responsible for chaperone-like activity of UNC-45. I have also discovered that the chaperone-like UCS domain possesses thermosensing properties.

I have found that the UCS domain undergoes significant structural rearrangements within the physiological temperature ranges of 38-41°C when the hydrophobic protein surfaces that were once deeply buried inside of protein core become accessible to solvent. These changes are results of alterations within the tertiary but not the secondary protein structure. Most importantly, the temperature which triggers the chaperone conformational changes is also the temperature of the myosin aggregation. Therefore, the results suggest that the UCS domain significant structural flexibility is required for the chaperone function.

TABLE OF CONTENTS

List of Figures

	molecule AFM based assay.	

List of Abbreviations

BADAN	6-Bromoacetyl-2-Dimethylaminonaphthalene
Hsp90	Heat shock protein 90
Hsp70	Heat shock protein 70
ANS	8-Anilinonaphthalene-1-sulfonic acid
PBS	Phosphate buffered saline

Introduction – Chapter 1

Molecular Chaperones

Proteins are structurally very complex macromolecules and function as instruments by which genetic information is expressed. These biological macromolecules are built of hundreds or thousands amino acid but contain only 20 different amino acid types. Thus, the sequence of amino acids must be one of the major determinants of protein biological activities. Moreover, the three dimensional structure that the protein molecule acquires in space is of fundamental importance in the expressing the activities of the molecule. There are thousands of different proteins in the cell each carrying out specific and strictly defined functions. They catalyze reactions in cells (enzymes), are involved in transports of other molecules (*e.g.*, hemoglobin, myoglobin, serum albumins), are sources of nutrition (*e.g.*, storage proteins), act as structural proteins that strengthen and protect biological structures, or as contractile and/or motor molecules which have the ability to contract or move about (*e.g.*, myosins, actins, tubulins). They also defend organism from invasion by other species (*e.g.*, antibodies, fibrinogen, thrombin), or regulate cellular and physiological activity (*e.g.*, hormones, repressors). The versatility of the protein structure allows the molecules to be directly involved in almost all biological processes.

To perform their biological functions, proteins must fold into proper three-dimensional structures or conformations called the "native state". Moreover, the native state of a protein molecule is an ensemble of structurally closely related three-

dimensional entities. Furthermore, to function properly, the molecule structure possesses a certain degree of conformational flexibility. In other words, the structure is not completely rigid but dynamic. Therefore, the native state of a protein is only marginally thermodynamically stable under the relevant physiological conditions.

Since proteins are large macromolecules, for decades scientists were wondering how complicated folding processes occur. In 1961, Anfinsen showed that ribonuclease A, initially denatured in 8 M urea, can spontaneously refold to its native structure and regain its catalytic activity upon diluting of the urea concentration (1). These pioneering experiments suggested that information required for the folding of ribonuclease A is incorporated in its amino acid sequence. It had also lead to formulation of the "Anfinsen dogma", which stated that native structures of small globular proteins are purely determined by their amino acid sequences (2).

In late 1960s, Cyrus Levinthal observed that since unfolded protein chains have very large number of degrees of freedom, they might exist in enormous number of possible conformations ("Levinthal's paradox"). For example, a protein composed of 100 amino acids would have $\sim 3^{198}$ possible conformations. It was immediately noticed that if the folding process involved sampling all possible conformations, the reaction would take more time than the age of the universe. Hence, the actual protein folding process must be controlled by some factors that tremendously speed it up. In this context, small proteins can spontaneously fold on the time scale of microseconds (3).

Highly complex protein folding reactions depend on the coordination of many weak and non-covalent interactions.

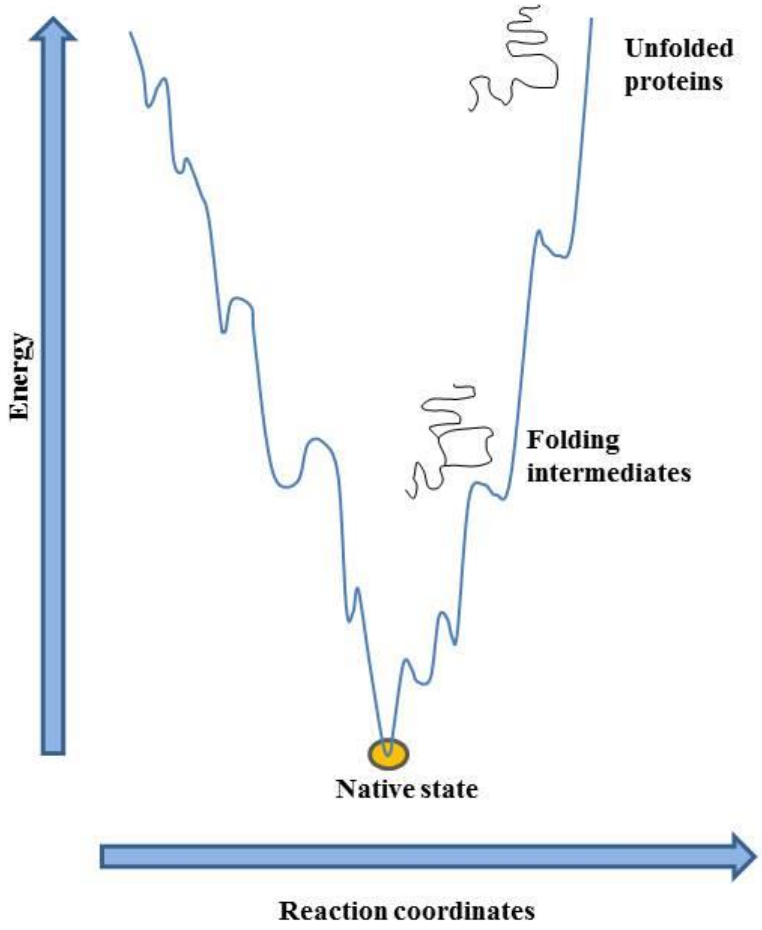

Figure I-1. Schematic representation of folding funnel. The unfolded protein is characterized by both high entropy and high free energy. During the folding process, the Gibbs free energy of the protein and the number of available conformational states decreases. The protein reaches its native state when Gibbs free energy is at the minimum (bottom of the funnel).

.

Mechanistically, hydrophobic forces are thought to plays a central role here because they are driving the burial of non-polar amino acid residues within the interior of the protein (4). Therefore, hydrophobic interactions seem to be critical for protein chain collapse into certain conformations on the way to and in the native structure. Short-range hydrogen bonds can also impose specificity in formation of the initial local structures, as well as in the final entity. As a result, formations of the local structures narrow the number of possible folding pathways. The entire folding process is believed to occur through the "folding funnel" where polypeptide chains explore narrowed yet still large number of pathways directed towards the native state, the state at which the protein is the most stable, has the lowest Gibbs free energy, and can perform its biological functions (**Figure I-1**) (5).

Many small proteins fold spontaneously into their native state and do not require other components or energy sources (6). On the other hand, some proteins need additional help from other proteins to fold efficiently within biologically relevant timescale. These "helping" proteins are named molecular chaperones and are characterized by their ability to interact with, stabilize and prevent aggregation, or even assist a client protein to acquire its functionally active conformation, without being present in its final structure. Studies of molecular chaperones have a long history spreading for more than 30 years. The term "chaperone" was first introduced by Laskey who reported the ability of nucleoplasmin to prevent aggregation of folded histones during the nucleosome assembly process (7). The binding of nucleoplasmin decreases the strong positive charge on histones and only then the addition of the negatively charged DNA at physiological ionic strength results in formation of nucleosomes. These results

showed that nucleoplasmin is required for the proper nucleosome assembly but is not part of the nucleosome final structure. Therefore, nucleoplasmin activity is to promote proper interactions between histones and DNA and prevent the aggregation process. During the following years, studies of heat shock protein 70 and heat shock protein 90 suggested their involvement in other proteins assembly and disassembly processes occurring in the cell (8). That led R. John Ellis to propose the existence of a new class of cellular proteins that promote proper folding and assembly of other proteins, which gave birth to the term "molecular chaperones" (9).

In the context of performed functions, one might divide chaperones into two classes (10). The first class is composed of chaperones that interact with the client protein, stabilize its structure, and prevents misfolding and aggregation, but do not actively promote the refolding of the protein. They are sometimes referred in literature as "holdases" (10). Most of holdases are small heat shock proteins. Classical examples are Hsp33 (heat shock protein) and DnaJ (heat shock protein 40). They recognize solvent exposed hydrophobic amino-acid side chains of proteins in non-native states, bind to them and thus prevent aggregation. The second class consists of chaperones that promote client protein folding and hence are called foldases. They draw on energy obtained from ATP binding and hydrolysis to switch from low- to high-affinity state, form a complex with the client protein, and accelerate rate determining steps along the folding pathway. Moreover, besides the ATP regulated binding/hydrolysis cycles, they promote folding through interactions with additional protein cofactors and often in collaboration with small heat shock "holdases". Foldases are usually large molecules with classical examples being the Hsp70, Hsp90 systems and chaperonins. Although both heat shock

protein systems and chaperonins are foldases, the mechanisms of client protein folding are different. After the action of the Hsp70 and Hsp90 systems, the client protein is released to fold in the bulk cell environment, while chaperonins developed an alternative approach, where folding of client proteins occurs inside of the chaperonin cage, thus it is separated from the rest of the cell environment.

The Hsp70 and Hsp90 systems

The classical example of a foldase is the Hsp70 protein. The mechanism of its action was studied and described using eubacterial homologue the DnaK protein, its co-chaperone DnaJ (Hsp40) protein, and nucleotide exchange factor, GrpE (**Figure I-2**)(11). The DnaK chaperone is composed of two domains: the ATP-binding domain and the peptide-binding domain. The latter domain recognizes the typical features of most of nascent peptide chains, mainly exposed hydrophobic protein side chains with accessible polypeptide backbone (12). It is made of β-sandwich subdomain and α-helical latch-like segment. The peptide-binding domain has strictly defined target and recognizes seven residues long, hydrophobic peptides, usually possessing leucine or isoleucine residue. Rapid peptide binding occurs in the ATP-bound state when both the β-sandwich subdomain possessing a peptide binding cleft and α-helical latch like segment are in open conformation. Hydrolysis of the bound ATP to ADP and Pi induces conformational transitions that are closing the latch and thus trapping the substrate (close conformation). The transition between open and close conformations is controlled by DnaJ (Hsp40) and GrpE proteins (11, 13).

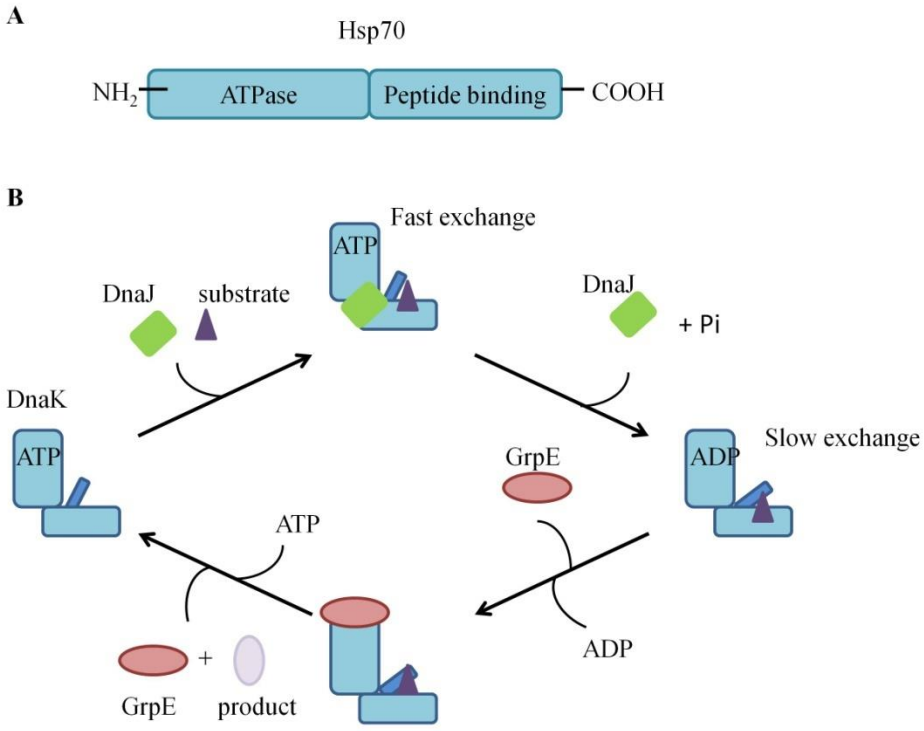

Figure I-2. Mechanism of the Hsp70 action. **A**) The Hsp70 chaperone is composed of N-terminal ATPase domain and C-terminal peptide-binding domain. **B**) Simplified reaction cycle of the DnaK (Hsp70) chaperone. Adapted with permission from (4).

Binding of N-terminal domain of DnaJ to DnaK accelerates the ATP hydrolysis, whereas the C-terminal domain of DnaJ can identify hydrophobic patches, thus can bring the nascent chains in close proximity to DnaK. Subsequently, GrpE binds to the formed DnaK complex, which triggers release of ADP. Next, binding of ATP to the complex releases GrpE and the targeted peptides, therefore the cycle is completed. The Hsp70 protein family is a very widely spread system and was found in eubacteria, eukaryotes, and some Archaea. In addition to cytosol, its presence has been reported in eukaryotic organelles such as mitochondria and endoplasmatic reticulum.

Another example of a molecular chaperone belonging to the heat shock protein family is Hsp90. It is made of three domains, the N-terminal domain (NTD, 25 kDa) where the ATP-binding site is located, the middle domain involved in the client protein binding (MD, 40 kDa), the C-terminal domain responsible for Hsp90 dimerization (CTD, 12 kDa) and the charged linker region connecting the N-terminal domain with the middle domain. Hsp90 is mainly involved during late stages of protein folding where it functions to stabilize near native-state forms of client proteins. It receives the unfolded protein through co-chaperone Hop (Hsp70/Hsp90 organizing protein) which links Hsp70/Hsp40 system with Hsp90. The Hop co-chaperone uses its TPR domains, which bind to Hsp70 and Hsp90 to bring both chaperones together. Interestingly, Hop also inhibits folding properties of Hsp90 during the transfer process between two chaperones that is restored by Aha1 (14). This ubiquitous molecular chaperone is involved in folding of hundreds of client proteins, including nuclear receptors, cell-cycle kinases, telomerases, and myosin in late stages of folding. Because of its functional diversity and

significant number of client proteins, the Hsp90 chaperone is an important therapeutic target.

Chaperonins

Over the last decades another class of chaperones, chaperonins have been extensively studied. The feature that distinguishes them from other chaperones is the mechanism of their action. Chaperonins provide a special compartment that separates a single polypeptide chains from the cell environment and thus allow undisturbed protein folding reaction to occur. The studies of chaperonins started in the last 1980s when the collaborative work of R. John Ellis's, Roger W. Hendrix's, and Sean M. Hemmingsen's laboratories revealed that Rubisco subunit binding protein (located in chloroplasts) and GroEL (*E. coli*) protein are evolutionary homologues and they play critical role in proper assemblies of other proteins (15). Similarity in sequence and function of these two molecules so different in biological origin (chloroplast and bacteria) suggested existence of a new class of proteins assisting in proper assembly of polypeptides. They were named chaperonins. Finally, the combined work of Franz-Ulrich Hartl's and Arthur Horwich's laboratories showed that the mitochondrial Hsp60 chaperonin is essential for folding of proteins that are imported into mitochondria and that the process is ATP-dependent (16-18).

Chaperonins are a class of molecular chaperones that forms large oligomers (800-900 kDa) built of 60 kDa subunits (4, 15, 19). They form two distinct rings where the center of each ring contains a certain space termed "cage" where the protein folding process occurs. They can be divided into two groups. Group I chaperonins form seven-

unit rings and cooperatively interact with the Hsp10 protein (4). They are also referred sometimes as the Hsp60s and their most notable examples are GroEL-GroES systems found in bacteria and in organelles of endosymbiotic origin (mitochondria and chloroplast). The group II chaperonins are built of eight-unit rings and are independent of Hsp10. They are also sometimes referred as the TCP-1 subfamily and their most typical examples are thermosomes discovered in *Archaea* and TRiC found in eukaryotic cytosol.

The most studied chaperonin is the GroEL-GroES system in *E. coli*. Until now, more than 50 cytosol proteins have been identified as GroEL client proteins. Each GroEL subunit is composed of three domains: equatorial domain which possess the ATP-binding site, the hinge-like domain, and the apical domain. The apical domain possesses the hydrophobic residues, which can interact with hydrophobic residues on the targeted protein. The folding reaction starts with binding of client polypeptide to the available apical domain, which is not associated with GroES (uncapped). Binding of ATP molecules (one per subunit) to equatorial domains and simultaneous binding of GroES to the end of GroEL ring releases the substrate into newly formed cage (**Figure I-3**). The process involves significant structural rearrangements of GroEL, resulting in creation of highly hydrophilic and negatively charged environment inside the ring. The polypeptide chain has 10-15 seconds to fold during which ATP is hydrolyzed to ADP and Pi. Then ADP is released from the ring, which triggers dissociation of GroES and allows the polypeptide chain to leave the GroEL cage. Often the folding process is not completed in one cycle.

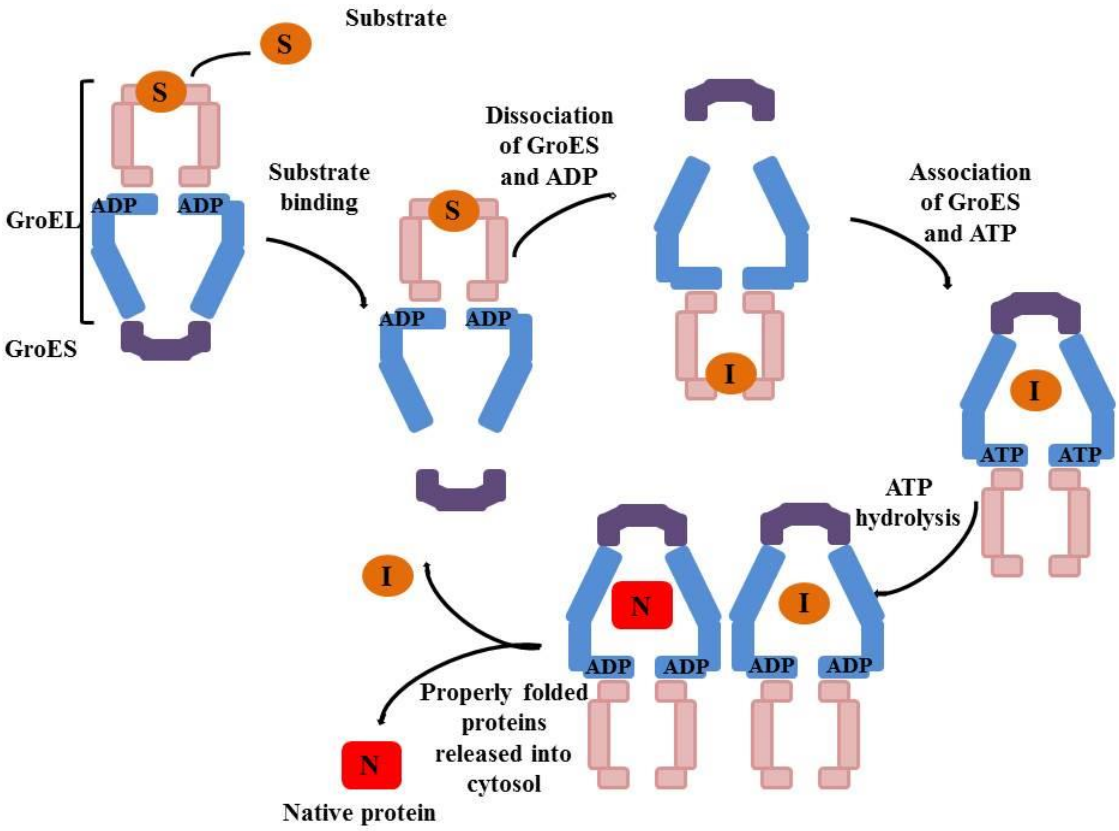

Figure I-3. Folding reaction catalysed by GroEL-GroES system in the chaperonins GroEL-GroES cage. Folding intermediates bind to the apical domain of GroEL moving them into the chaperonin cage where the folding occurs. For most substrates, many rounds of chaperonin action is need before the protein obtains its native structure. Adapted with permission from (4).

If that is the case, the polypeptide chain, which still possesses the exposed hydrophobic residues will bind again to GroEL and the process will continue until the protein native form is reached.

The UNC-45 protein within the UCS protein family

The *unc-45* gene was discovered by Henry Epstein in 1974 as a single recessive, temperature-sensitive mutant allele designated as *e286 in Caenorhabditis elegans (C. elegans)(20)*. The mutant show a decreased body movement and disorganized myofilaments (filaments of myofibrils built of sarcomers) arrays at 25°C, but display a wild-type phenotype at 15°C. At that point, it was suggested that the product of *unc-45* gene, UNC-45, might possess catalytic function necessary for formation of proper myofilament arrays (20). Although these pioneering studies were performed on *C. elegans* model organism, subsequent numerous genetic and biochemical experiments identified many UNC-45 homologues in various organisms and showed a strong linkage of UNC-45 to the myosin functions.

Current data indicate that UNC-45 is a member of the UCS (UNC-45, Cro1, She4p) family of proteins and is one of the chaperones involved in the myosin folding(21). It is essential for the *in vivo* assembly of myosin into myofibrils (**Figure I-4**). UNC-45 is composed of three domains: the UCS domain, the Central domain, and the TPR (tetratricopeptide repeat) domain (22, 23). The UCS domain is the most conserved protein structural unit through metazoa and fungi kingdoms with the sequence homology to *Homo sapiens* ranging from 98% (*Mus musculus*, metazoa) to 39% (*Saccharomyces cerevisiae*, fungi). Up today, it is the only domain known to interact with myosin.

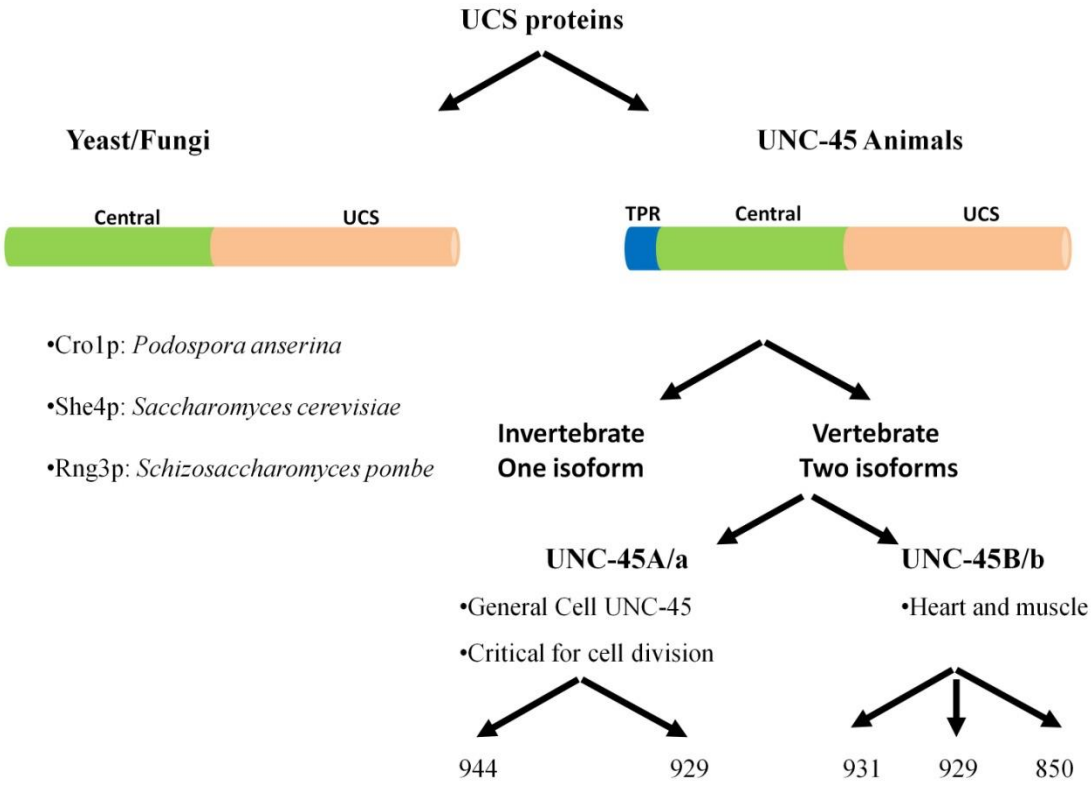

Figure I-4. Different forms of identified UCS proteins. Fungi UCS proteins contain highly conserved UCS domain and poorly conserved central domain. However, they do not possess the TPR domain. UCS proteins found in metazoa are termed UNC-45 proteins and possess all three domains: UCS, central, and TPR domains. In invertebrates, there is one form of UNC-45 protein, whereas in vertebrates there two forms: sarcomeric and non-sarcomeric UNC-45. The numbers of amino acid residues for identified isoforms are indicated in the figure.

Contrary to the UCS domain, very little is known about the UNC-45 central domain. Nothing is known about its functions. Its interactions with other proteins have never been even addressed.

Interestingly, the Central domain is highly conserved in metazoa. However, its fungi homologue is severely truncated and has very low sequence homology to its metazoa counterparts (*e.g*., less than 4% for *S. cerevisiae)*. Finally, the TPR domain is only present in metazoa UCS proteins and it has been found to interact with the heat shock protein, Hsp90.

The fungal UCS proteins, She4p (*Saccharomyces cerevisiae)*, Cro1 (*Podospora anserine)*, and Rng3p (*Schizosaccharomyces pombe)* are composed of the conserved UCS domain and the truncated central domain. Nevertheless, they lack the TPR domain (**Figure I-4**). The Rng3p protein was identified in actin gliding experiment as an essential factor for proper myosin II activity *in vitro* (24). During cytokinesis both domains of the protein colocalize in the contractile ring, but only the full-length Rng3p supports the contractile ring function (25). Interestingly, although most UCS proteins interact with myosin II, only yeast protein She4p was found to be critical for activities of other myosins, namely belonging to myosin classes I and V (26). In this context, four point mutations in myosin I (Myo5p) eliminate the requirement of She4p for proper myosin function (27). Additional experiments clearly indicated the crucial role of UNC-45 protein in muscle functions. UNC-45 knockdowns in *Drosophila melanogaster* resulted in disorganized sarcomeres and reductions in the amount of thick filaments (28)(myosin filaments). Noticeably, it seems that the cell requires an optimal concentration of UNC-

45. Thus, experiments with *C. elegans* showed that overexpression of the protein decreased the worm mobility and diminished the amount of present myosin (21).

A more complex situation occurs in vertebrates where the UNC-45 protein has two distinct functions (29, 30). First, it is required for cytokinesis and second, it is essential for proper muscle development. Therefore, there are two genes for the homologues. One in the striated muscle form (SM UNC-45 or UNC-45B) and the other one is the general cell form (GC UNC-45 or UNC-45A)(29). Crucial biochemical studies of these homologues were carried out using the C2C12 skeletal myogenic cells. The knockdown of the striated muscle isoform UNC-45B affects the sarcomere organization, while the knockdown of the general cell isoform UNC-45A reduces cell proliferation and fusion (29). Moreover, UNC-45B acts as a molecular chaperone protecting myosin from thermal aggregation (23).

The first high-resolution crystal structure of the UCS protein was obtained for yeast She4p from *S. cerevisiae* (31)(**Figure I-5**). The molecule is composed of 16 helical repeats that are organized into an L-shaped superhelix, with the N-terminal helix hanging off the short arm. The helical repeats are around 40 amino acid residues long and form a classical armadillo repeats structure. The authors suggested that She4p protein undergoes a dimerization process. The first UNC-45 crystal structure from the animal kingdom was determined for the *Drosophila* protein (32). Only the structure of the small N-terminal TPR domain was missing, due to the low electron density in that region, suggesting high flexibility of the domain. Both crystallography and SAXS solution data indicated that the protein exist as a monomer.

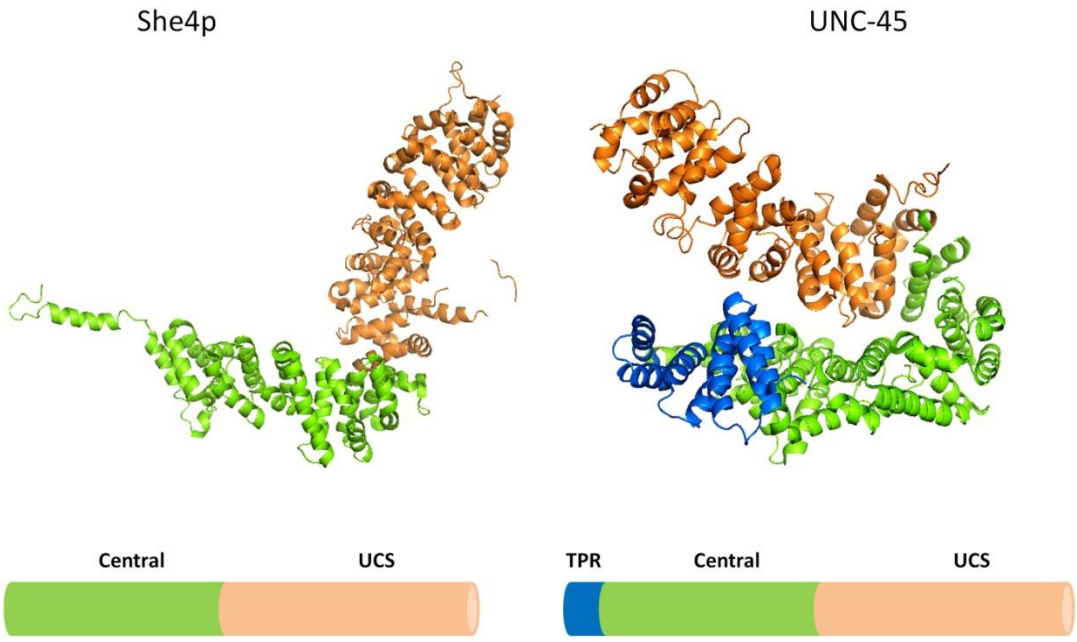

Figure I-5. Crystal structures of She4p (3opb.pdb) and UNC-45 (4i2z.pdb) proteins. Modified with permission from (31, 33) using 3opb.pdb and 4i2z.pdb files. The images were done using PyMOL (34).

The most recent crystal structure was obtained for UNC-45 from *C. elegans (33)*. These are refined data, which include the TPR domain. The authors also proposed a novel model for conformational arrangement of UNC-45 and its co-chaperone Hsp90 in sarcomere during the last stages of myosin folding. Moreover, they suggested that UNC-45 molecules form oligomers that can act as a scaffold for Hsp90 and Hsp70, thus bringing all chaperones in close proximity to myosin. Furthermore, it has been suggested that the UNC-45 oligomers can serve to regulate alignment of myosin heads. These conclusions were based on analysis of crystal structures and additionally supported by solution studies showing formation of short oligomers detected by cross-linking methods.

Medical importance of chaperones and involvement of UNC-45 in human diseases.

Understanding protein-misfolding diseases is becoming one of the most studied and medically significant challenges in health research today (35-37). The misfolding diseases result from the inability of relevant proteins to reach their native state, which lead to accumulation of the aberrantly folded molecules. The disorders like Alzheimer's disease, the prion disease (Creutzfeld-Jakob syndrome), Huntington's disease, and variants of Parkinson disease are caused by a gain of toxic function of misfolded proteins (35, 37). Although unknown in each and every case, the toxicity may be induced by the imbalance between the production of harmful protein species and the capacity of the chaperone machinery to counteract the misfolding process. In other words, the disorders might occur when the production of misfolded species overwhelms the ability of the chaperone systems to prevent protein misfolding. Mutations in a molecular chaperone may result in a protein that is incapable to facilitate the folding of a client protein. The

Hsp70 protein family is an example of chaperones which are associated with the diseases caused by the misfolded client protein (38, 39). Expression of Hsp70 and Hsp40 in the yeast model of Huntington's disease reduces the toxicity that results from the presence of the toxic mutant protein, huntingtin (cause of Huntington's disease)(40). On the other hand, a mutation in the mitochondrial chaperonin Hsp60 may be an example of the genetically defected chaperone involved in the hereditary disease of spastic paraplegia, SPG13 (41). Thus, it has been found that the human mitochondrial Hsp60 and its co-chaperone Hsp10 can moderate the effect of deletion of GroEL/ES operon in *E. coli*, while mutated Hsp60 cannot (42).

The UNC-45 protein has been identified as a factor that might play a critical role in several disease syndromes such as congenial heart diseases and cancers. For instance, the expression of general cell isoform UNC-45A was found elevated in ovarian tumors (43). Moreover, UNC-45A overexpression increased the rate of proliferation of ovarian cancer cell and increased their spreading ability (43). The significance of UNC-45A was also reported in breast cancer studies (44). Thus, enhanced levels of UNC-45A were reported in human breast carcinomas and the cell lines derived from breast carcinoma metastases (44). Two UNC-45A isoforms were identified, one which is 929 amino acids long and the other, which has the additional proline-rich 15-amino-acid sequence localized near the amino-terminus. Experiments performed in breast carcinoma cell lines revealed that the shorter 929 amino acid residues isoform is expressed at higher level than the 944 residues isoform. The observed difference resulted from the faster degradation of 944 residues isoform, which happened most likely due to presence of additional fragment

of 15-amino-acids. Thus, the human breast carcinomas involve changes in the relative ratio of different UNC-45A isoforms.

Furthermore, combination of genome-wide linkage analysis and targeted DNA deep sequencing identified first human UNC-45B mutation (45). The data was obtained from family with juvenile cataract, linking the UNC-45 protein with the disease and showing that UNC-45B is expressed not only in heart and skeletal muscle tissue but also in human embryo eyes. The mutation substitutes 805Arg with Trp residue in the conserved UCS domain. The studies performed in zebrafish model organism showed that UNC-45B steif mutant exhibits deficiencies in eye formation, *i.e.*, reduced lens size. The phenotype is partially rescued by injection of RNA encoding the human wild-type UNC45B protein into embryo. On the other hand addition of RNA encoding the mutant UNC-45B into wild-type embryos yields similar phenotype to steif mutant. The results of the research showed that UNC-45B colocalize along non-muscle myosin II therefore suggesting that presence of mutant UNC-45b affects non-muscle myosin II function which prevents proper lens formation.

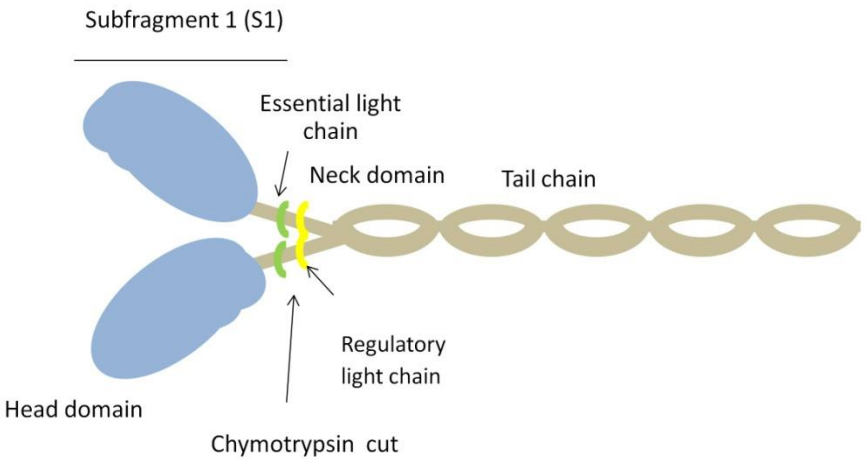

Figure I-6. Structure of muscle myosin II. Myosin II is composed of myosin heads attached to the neck domain associated with the essential and regulatory light chains and the tail domain. The chymotrypsin digestion site is localised in the neck domain and yields the myosin subfragment 1 (S1).

Myosins

The name myosin was introduced by Wilhelm Kuhne in 1864 and, at that time, the term described proteins extracted from muscle that were believed to be responsible for muscle vigor and generally linked to movement (46). Much later, experiments carried out mainly by Albert Szent-Gyorgyi showed that what was called "myosin" was in fact a mixture of two entities. One was termed myosin A and was characterized by low viscosity and the other was termed myosin B and was characterized by high viscosity. Moreover, it was also noticed that the high viscosity of myosin B could be reduced by addition of ATP (47). Furthermore, Szent-Gyorgyi group demonstrated that an additional protein is present in myosin B. They called it "actin" since it was responsible not only for myosin high viscosity but also for contractility, *i.e.*, the activation of movement properties. Thus, it was established that two proteins, myosin and actin, are responsible for muscle contraction.

Subsequent studies aimed at elucidation of the myosin structure. The trypsin digestion experiments showed that myosin is composed of two different components, the light meromyosin components and heavy meromyosin components (48). Later experiments identified that the light meromyosin as is built of two fragments named S1 and S2 (49)(**Figure I-6**). Electron microscopy revealed existence of two myosin globular heads (50) . The heavy meromyosin components were associated with the tail domains.

Until today, up to 24 different classes of myosins have been identified (51). They are all motor proteins that convert chemical energy obtained from ATP hydrolysis into mechanical work and play essential roles in a wide variety of cellular motility processes, ranging from muscle contraction to cleavage furrow ingression during cytokinesis. The

most studied member of the protein family is the "conventional" myosin II. It is found in both muscle and non-muscle cells. Muscle myosin forms thick filaments (around 400 hundred molecules), whose interaction with actin thin filaments results in muscle contraction. The myosin II molecule is composed of three domains: head domain, neck domain and tail domain (**Figure I-6**). Myosin motor properties are localized in the head domains. Globular heads are responsible for interactions with actin and have the actin-activated ATPase site. Neck domain links the head domain to the tail domain and has essential and regulatory light chains attached to it. Dimerization of tail domain results in formation of classical dimeric myosin molecule. In sarcomere, myosins form long filaments (thick filaments) that together with thin filaments (actin) form the dominant element of muscle contraction system (**Figure I-7**). Contraction of sarcomere, the major structural and functional muscle unit, is a result of movement of myosin heads along actin filaments which is generated by conformational changes in the myosin motor domain induced by ATP binding and hydrolysis.

Non-muscle myosins II play a critical role during cytokinesis where at the end of mitosis, myosin II and actin filaments form a contractile ring that pulls plasma membrane progressively inwards thus narrowing the center of the cell and finally leading to cell division (**Figure I-8**). Among non-conventional myosins, myosins I, V and VI are the most intensively studies proteins. Myosins I contain a globular head group that can function as a molecular motor but has a short tail domain and therefore does not form dimers. Its main function is to transport cargo inside the cell using its capability of moving along actin filaments. Myosins V and VI play important roles in both cargo transports and organelle movements (**Figure I-8**).

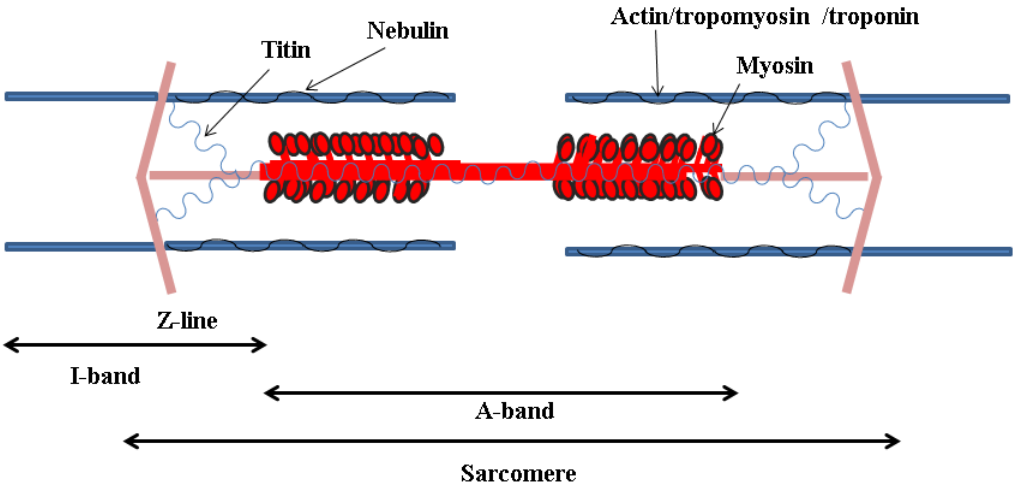

Figure I-7. Schematic structure of the sarcomere. Actin filaments together with tropomyosin and troponin form thin filaments while myosins form thick filaments. The nebulin protein is thought to regulate the length of the thin filaments. The giant titin molecule connects the thick filaments to Z-line and in the I-band region functions as a molecular spring.

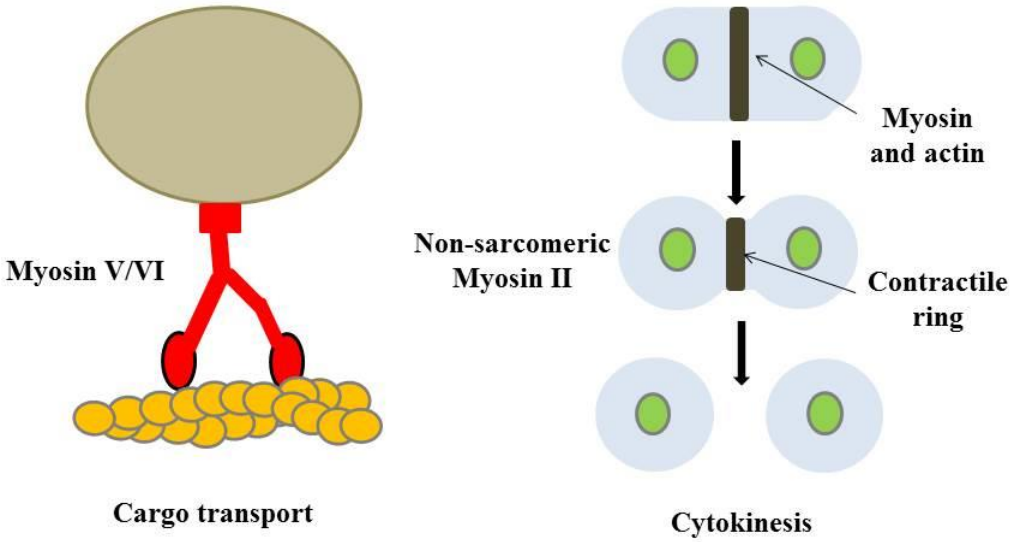

Figure I-8. Examples of the functions of different myosins. Myosins V and VI are involved in cargo transport inside the cells (left). Non-sarcomeric myosin II forms a contractile ring with actin during cell division process.

Molecular chaperones as thermosensors

As discussed above, some chaperones are heat shock proteins which mean that their expression is induced by an increase in temperature. The best studied examples of the group include Hsp60, Hsp70 and Hsp90 as well as some small heat shock proteins such as Hsp26. Moreover, in the case of small heat shock proteins it was shown that they can undergo functionally relevant, structural changes under thermal stress. Therefore it is of great importance to investigate how environmental conditions affect the properties of chaperones.

All chemical reactions occur under certain temperature conditions. Temperature changes can speed up, slow down, and even practically stop the reaction. Therefore, alteration of temperature can function as a gear initiating or inhibiting the chemical process. For most chemical reactions increase of temperature by 10 ^{0}C double the rate of the reaction (52).

The biochemical reactions taking place in living organism had to be tuned to very specific conditions. They occur in a very crowded environment with availability of multiple binding partners, in a very high viscosity, changing pH, and temperature ranging from a few Celsius degrees to 40 ^{0}C, or even in case of *thermophiles* to 122 ^{0}C (53). Therefore, cells of living organism developed an intricate network of protective mechanisms to tame changing environmental circumstances including the temperature.

From that perspective, it should be of no surprise that under these circumstances some macromolecules including proteins and nucleic acids evolved to function as

thermosensors whose activities could be mobilized by temperature changes. The thermo-sensitive RNA molecule was identified for the first time for mRNA of bacteriophage cIII gene (54). The macromolecule exists in equilibrium of two conformations. Alterations of temperature (or magnesium) shift the equilibrium towards one of conformations thus determining the rate of translation. Since then, many more heat shock or cold shock proteins whose expression is controlled by RNA thermosensors (sometime referred as RNA thermometers) have been identified (55).

Similar thermosensing properties have been observed in some small heat shock proteins. A good example is heat shock protein 26 (Hsp26), which undergoes subtle structural rearrangement with the increasing temperature that enhances its activity(56). The Hsp26 middle domain was determined to act as a thermosensor changing its binding properties with temperature alterations (56). Furthermore, Cryo-EM studies showed existence of two conformations that are at equilibrium. It was determined that switching from close to open conformation enhances the number of binding protein clients (56).

In addition to temperature other factors like chemical stress can also activate the specific macromolecule. For instance, the heat shock protein 33 (Hsp33) activity was shown to be controlled by the redox reaction. The protein is not active in its reduced state, however upon oxidation it undergoes partial unfolding creating flexible loop that can bind to many folding intermediates of its client protein. Removal of oxidative conditions results in reduction of disulfide bonds and return of disordered region to fully structured alpha helices (57). Despite different forms of activation, both Hsp26 and Hsp33 undergo structural changes in response to environmental stress, generating

disordered region capable of binding to many client proteins during folding processes (56).

Activations by the temperature or environmental stress are very desirable properties for some molecular chaperones. Thus, *in vivo* studies performed on *Danio rerio* (Zebrafish) suggested that UNC-45 can function as a thermosensor (58). In a mature sarcomere, UNC-45 is localized in the Z-line (ends of sarcomere). However, upon induction of heat stress, the chaperone migrates into the center of sarcomere towards the A-band, where its client protein myosin is localized (58). Since increase in temperature results in shuttling of the UNC-45 chaperone in the sarcomere, it is possible that these migrations are accompanied by changes of biochemical properties of the chaperone. Therefore temperature seems to be a critical factor in activating this chaperone. Notice that higher temperature can induce a number of conformational changes within the myosin proteins and each of these structural rearrangements can potentially lead to aggregation (23). Therefore, under stressful conditions the UNC-45 chaperone should have a significant structural flexibility that can accommodate the diversity of client's structures, *e.g*., myosin.

Application of single molecule methods to study of chaperone function.

Over the past decades, the force spectroscopy and fluorescence single-molecule techniques have been used to examine the structure and mechanisms of chaperones action (59-61). One of the major advantages of the single molecule techniques lies in the ability to detect the rare events, reaction intermediates and subpopulations that otherwise could not be observed in the bulk studies (59, 62, 63). In the other words, the single molecule

methods provide additional information about the heterogeneity of the studied biological system. In the case of the chaperone-assisted protein folding the transient intermediate conformations which protein acquires during the exploration of the folding pathway and which are critical for understanding of the entire process, cannot be detected using classical bulk approaches. Therefore, the single molecule techniques are powerful tool to study important biological process such as chaperone-assisted protein folding.

Within the last twenty years, the single-molecule force spectroscopy techniques have been used to investigate chaperones structure and function in context of protein folding (60, 64, 65). The growing popularity of the techniques arises from the fact that the methods allow the mechanical perturbation of the studied proteins (60, 62). Single-molecule Atomic Force Microscopy (AFM) is one of the most common techniques to study mechanical properties of proteins and was also used to address the effect of chaperones on protein folding (66-69).

The central part of the AFM instrument is cantilever, which ends with a sharp tip that is used to pick up the proteins (59). The pulling force is measured by determining the deflection of cantilever form its initial position. The sensitivity of the instrument is so large that cantilever bending of only 10 Å results in change of force of 100 pN. The AFM instrument is capable of measuring forces of a few pico-newtons and distances of only a few Ångstroms. Over the last decades, the AFM has been used to address mechanical features of diverse array of macromolecules. For example the technique was applied to measure the interaction forces between proteins (70, 71), to image single molecules in physiological conditions (72, 73), to or to map the cell surface receptors (74-76) as well as to obtain the high-speed imaging of molecular motors in action (77).

In the context of chaperone studies the AFM techniques have been mainly used to image the chaperones structure. For example, the AFM was used to gain structural insight of GroEL and GroES proteins (78). The AFM imaging technique allowed direct observation of the seven subunits of the GroEL ring structure. Moreover, the technique is sensitive enough to distinguish between the GroEL and GroEL-GroES structures. The AFM techniques were used not only to image the structure but also to detect interactions between chaperone and its client proteins. In the experiments, GroEL was immobilized on mica surface while mutant of citrate synthase and beta-lactamase were attached to the AFM tip. The study determined that the presence of ATP decreased the interacting forces between the substrates. Moreover, in case of the native-like proteins the interaction forces are lower than for the fully denatured ones (79). Similar technique was used by another group which reported observation of GroES binding to and dissociating from the GroEL protein(80). In the experiments multiple cycles of GroEL-GroES complex formation were detected in real time. Therefore the method can be used to investigate protein dynamics at single molecule level.

Furthermore, the AFM force-spectroscopy methods were applied to track chaperone – myosin interactions (67). In this approach I27 domains function as a molecular reporter for the myosin domain folding. In the absence of the UNC-45 chaperone, the characteristic I27 saw-tooth pattern was detected only in the initial unfolding cycle, thus strongly suggesting that the misfolded myosin motor domain affects the refolding of the I27 domains. The presence of the chaperone restores the refolding of the I27 domains. This effect is likely a result of UNC-45 binding to the myosin which prevents motor domain misfolding. The following approach could be applied to elucidate

chaperone–substrate interactions of other biological systems. Another study highlighting the importance of the chaperones for the proper muscle function were done using small heat shock protein, alfaB-crystallin which was showed to protect cardiac titin from damage (81). The presence of the chaperone resulted in lowering the persistence length of the titin N2B-Us (sequence in N2B element of titin) and decreasing the probability of the Ig domain unfolding.

Moreover, the AFM was also used to elucidate the mechanism of chaperone-assisted luciferase refolding (61). The experiments showed that if only the N-terminal domain of luciferase is folded the whole protein refolds robustly without the chaperones assistance. When luciferase is completely unfolded the chaperones are required to complete the refolding process. The researchers suggested that the chaperones function in this system is to physically separate protein domains which allow them to fold independently.

Another widely used single molecule force spectroscopy method that allows the investigation of mechanical properties of macromolecules is optical tweezers, also sometimes referred as optical traps. This technique is based on the discovery showing that small dielectric particles (in the experiments called beads) can be trapped by using a focused laser. A good example representing the application of optical tweezers in the context of chaperone action is the investigation of SecB chaperone induced changes of the maltose binding protein (MBP) folding pathways (65). In absence of the chaperone, the MBP forms molten globulike compacted state which then folds into a stable core structure. The presence of SecB inhibited the tertiary interactions during the transitions into the core state but did not affect the transitions into the native state. The SecB

chaperone blocks the stable aggregation interactions between the MBP proteins. Therefore, the application of the optical tweezers technique allowed probing the behavior of the folding transitions of a single molecule in presence and absence of the chaperone molecule.

Optical tweezers techniques were also applied to study the effect of the Trigger Factor on the exploration of different conformations by polypeptides during the folding process (64). The experiments were performed using the single domain and repeat construct of maltose binding protein (MBP). The data indicated that the Trigger Factor binds and stabilizes small, partially folded structures which then eventually will reach native conformation. Furthermore, experiments performed on MBP repeat construct indicated that the presence of the Trigger Factor enhances the folding reaction. Therefore, the studies imply that the Trigger Factor can affect the conformational search of the polypeptide for its native state.

The technique was also used to demonstrate that ribosome in addition to synthesis of polypeptides also affects the folding process (82). The special experimental system was design where nascent polypeptides were attached to single ribosome. The study showed that the folding process of the studied protein (T4 lysozyme) is slowed down in close proximity of ribosome and that the ribosome prevents the misfolding of incompletely synthesized polypeptides. The results suggest that ribosome may bias the conformational search of the protein and thus contributes to efficient *de novo* folding.

Furthermore, the mechanism of action of the ClpXP unfoldeases was addressed using optical tweezers by two independent groups (83, 84). The ClpXP is composed of

ClpX that recognize and unfolds the targeted proteins and ClpP which is responsible for the client degradation. Both groups showed that ClpX and ClpXP apply the mechanical force to client protein and translocate polypeptides through its central pore in highly cooperative manner implying that the unfolding process includes simultaneously the application of mechanical force and transient stochastic reduction in the stability of the targeted protein domain. Moreover, the formation of the ClpP-ClpX complex increases the unfolding efficiency.

Single molecule techniques that are applied to study chaperones effect on proteins are not limited to force spectroscopy techniques but includes the single molecule fluorescence methods as well. In a typical experiment, the studied protein is labeled with fluorophores at specific positions which allows taking advantage of Forster resonance energy transfer (FRET) to address the structural and conformational changes within the protein which results from the chaperone action. For example, this approach was used to address how GroEL facilitate protein folding. In absence of GroEL, the maltose binding protein (substrate) collapses into a compact state while in presence of chaperonin, proteins start to unfold and form expanded and heterogeneous conformations (85). Moreover, the presence of GroEL speeds up the folding process about 10 times. Furthermore, single molecule FRET experiments examining chaperonins effect on the domains of the protein rhodanese indicated that the chaperonins effect depends on substrate (86). The chaperonins affected the folding of the C-terminal domain of the protein but did not have any effect on the folding process of the N-terminal domain. The single molecule FRET technique was also used to investigate conformational dynamics of the Ssc1 chaperone, mitochondrial member of the Hsp70 family (87). The studies

revealed that the chaperone conformations are surprisingly uniform in ATP- bound state while the chaperone in the ADP-bound state exists in heterogeneous conformations. Hence, single molecule fluorescence methods are typically used to address different biological problems which include the chaperone–assisted protein folding, examination of the different role of the substrate domains or analysis of the conformational dynamics of the ATP and ADP-bound state of the chaperone.

Furthermore, the single-molecule fluorescence spectroscopy was applied to elucidate the effect of the DnaJ-DnaK chaperone system on the conformational changes of the denatured rhodanese protein (88). The data indicate that the substrate protein undergoes a significant ATP-driven expansion when DnaK binds to rhodanese–DnaJ complexes. During the process the intramolecular contacts in the substrate protein are disrupted which may function as a method of rescuing misfolded proteins from kinetic traps, thus preventing the conditions which can lead to aggregation.

Chapter 2

Tracking UNC-45 chaperone-myosin interaction using single molecule AFM technique

Modified from:

2212 Biophysical Journal Volume 102 May 2012 2212–2219

Tracking UNC-45 Chaperone-Myosin Interaction with a Titin Mechanical Reporter

Christian M. Kaiser,[†] Paul J. Bujalowski,[‡] Liang Ma,[†] John Anderson,[†] Henry F. Epstein,[†‡§] and Andres F. Oberhauser[†‡§*]

[†]Department of Neuroscience and Cell Biology, [‡]Department of Biochemistry and Molecular Biology, and [§]Sealy Center for Structural Biology and Molecular Biophysics, University of Texas Medical Branch at Galveston, Galveston, Texas

INTRODUCTION

In order to function properly, all proteins must acquire a defined three dimensional structure (89). In case of many small proteins the process is usually spontaneous, however for larger protein additional help is needed. Since myosin motor domain is structurally very complex it requires presence of molecular chaperones during the folding process(21). The UNC-45B chaperone has been identified as essential for proper folding and assembly of myosin into muscle thick filaments (21)(for simplicity, in the text, we will refer to the UNC-45B isoform as UNC-45). It belongs to UCS (UNC-45/Cro1/She4p) family of proteins (22). Several independent research groups showed that proteins containing the UCS domain play a critical role in proper folding of myosin (21, 22, 90-92). Studies *in vivo* performed with temperature-sensitive UNC-45 mutants in examined worm organisms showed disordered muscle thick filaments (22, 93).

Myosins compose a large superfamily of motor proteins (94). They hydrolyze ATP and use the energy from the hydrolysis process to perform mechanical work, *i.e.*, they are motor proteins (94). The motor properties allow them to be involved in many critical processes in the cell, linked with motility. The most studied myosins include the proteins are involved in muscle contraction, cytokinesis, and cell crawling. Currently, due to diversity of their function, one can distinguish 24 classes of myosin(51).

Our studies focused on sarcomeric myosin II. It is large macromolecule (monomer of 225 kDa) composed of an N-terminal globular head domain and a C-terminal rod domain (chapter 3). The motor properties are confined within myosin heads, where actin- and ATP-binding sites are located. The contraction of the sarcomere is

achieved by myosin movement along the actin filaments. The model of the process was proposed by Huxley and refined later by plethora of structural and functional studies (95, 96). Altogether, these works showed that myosin power stroke is governed by coordinated structural rearrangements within the motor domain, where ATP-binding, hydrolysis and release, actin binding and release, as well as force-generating structural changes occur in sequential manner.

The UNC-45 chaperone is built of three domains: C-terminal UCS domain, the Central domain and the TPR domain (chapter 3). The UCS domain (400 amino acids) is known to interact with myosin, the central domain (400 amino acids) function is completely unknown and the TPR domain binds to Hsp90. The UNC-45 protein was shown to prevent the aggregation of thermally denatured myosin subfragment 1 (23)(motor domain) (chapter 3).

Examination of myosin properties and functions, in the context of its interactions with the chaperone, on a single molecule level was hindered by the lack of suitable mechanical fingerprints (67)(chapter 3). Here, we describe a novel method to analyze chaperone - myosin interactions at the single molecule level using the atomic force microscopy (AFM). The great feature of AFM is its ability to mimics the directionality of the *in vivo* folding pathways and to capture misfolding events (59). Nevertheless, as we stated the major challenge in using the AFM technique was dearth of clearly defined mechanical fingerprint of myosin, *i.e.*, a clear force extension pattern. We addressed this problem by chemical coupling the titin I27 octamer to the motor domain of myosin. This approach allowed us to treat titin domains as a "mechanical reporter", since the domains provide a specific attachment point and a well-characterized mechanical fingerprint in

AFM measurements. Moreover, our method can be applied to other molecular systems to investigate chaperone - client protein interactions.

MATERIALS AND METHODS

Construction, expression, and purification of the myosin-titin protein-I27 chimera and UNC-45 chaperone

Myosin was purified from rabbit skeletal muscle using previously described protocol(97) (chapter 3). The myosin Subfragment-1 (S1) was obtained by digestion of full-length myosin using chymotrypsin as described in chapter 3 (98). The myosin S1-I27 protein chimera has been synthesized by coupling the titin I27 octamer (which contains an N-terminal cysteine residue and a C-terminal His_6 tag) to the myosin S1. The reaction was achieved *via* the reactive cysteines (SH1/SH2) within the motor domain (99). Briefly, the I27 tandem repeat protein (50 μM) was first incubated with a 20-fold excess of a homo-bi-functional thiol-reactive cross-linker ($BM(PEG)_3$, Pierce, MN) and purified by gel filtration over Sephadex G-25 column. The activated I27 titin octamer was mixed with a 1.5-fold excess of the myosin S1. The reaction yields a product with a covalent linkage between the N-terminal cysteine in the I27 and the reactive thiols of the myosin motor domain.

Expression and purification of the UNC-45 chaperone have been described in chapter 3.

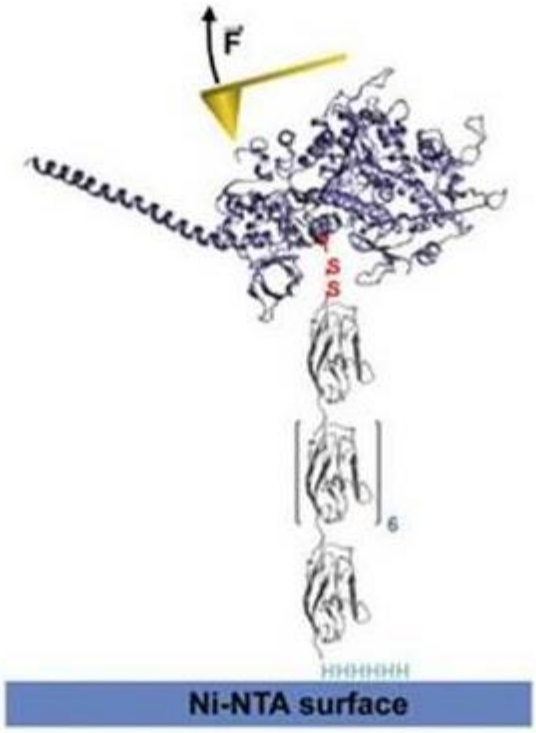

Figure II-1. Schematic structure of myosin S1 - I27 protein chimera placed in the context of the AFM experiment. The myosin motor domain (blue) is chemically coupled with the tandem repeat I27 polyprotein (gray) containing the N-terminal cysteine residue and C-terminal His_6 tag. Coupling of both proteins was carried out *via* the reactive cysteines (SH1/SH2) within the motor domain. On the other hand, coupling of the titin I27 polyprotein to Ni-NTA surface (coverslip) occurs through the site-specific attachment point, His_6 tag. The cantilever (yellow), of the AFM instrument, through which the force, F, is applied, is show at the top of the panel. Adapted from (67) with permission.

Single-molecule Atomic Force Microscopy

The home-built single molecule AFM instrument was used to analyze the nano-mechanical properties of tested proteins, as previously described (59, 66, 100-103). The equipartition theorem was used to calculate the spring constant of each individual cantilever (MLCT or Olympus OBL, Veeco Metrology Group, Santa Barbara, CA). Each experiment was carried out as followed. A small aliquot of the studied proteins (~1 - 5 µl, 10 - 100 µg/ml) was allowed to adsorb to a clean glass coverslip (in the case of full-length myosin and myosin S1) or to Ni-NTA coated glass coverslip (in the case of the S1-$(I27)_8$ and $(I27)_8$ constructs). The myosin molecules were incubated for about 5 - 15 min, and then the coverslip was rinsed with myosin buffer (600 mM sodium acetate, 600 mM KCl, 25 mM imidazole, 4 mM $MgCl_2$, and 1 mM dithiothreitol (DTT), pH 7.4). In the experiments involving S1-I27 protein chimera, the system was incubated for about 15 min and then rinsed with the PBS, pH = 7.4. In a typical experiment, the cantilever tip was pressed down onto the sample until it reached targeted proteins. Proteins are attached to the tip of the cantilever by adsorption forces.

The probability of picking up a protein and stretching it from end-to-end was very low. Most likely some proteins may be non-specifically attached to the coverslip surface, *via* I27 domains. In many experiments involving S1-I27 chimera, we have established that the number of I27 unfolding events observed in the force-extension curves was typically much smaller than the total number of I27 domains, *i.e.*, less than eight. Thus, often, obtaining the force-extension curve requires a careful accumulation of a large set of data. The AFM experiments were performed at room temperature (~25^{o}C), with

pulling speed of unfolding and refolding experiments in the range of 0.5-0.7 nm/ms(59, 67) .

Measuring the Fraction of Refolded I27 domains

The fraction of refolded domains was determined by application of the two-pulse unfolding/refolding protocol (59, 69). In a typical approach, first, a single polyprotein is stretched and it is allowed to relax for different time intervals. Second, the polyprotein is stretched again and, this time, the number of refolded domains is counted (59).

Analysis of Force extension curves

The worm-like chain (WLC) model of polymer elasticity was used to analyze the elasticity of the stretched proteins (99, 101):

$$F(x)=\frac{kT}{p}\left[\frac{1}{4}\left(1-\frac{x}{L_c}\right)^{-2}-\frac{1}{4}+\frac{x}{L_c}\right] \qquad \text{(II-1)}$$

where F is the applied force, x is the end-to-end length, *p* is the persistence length, and L_c is the contour length of the stretched protein. The adjustable parameters are *p* and L_c.

RESULTS

Mechanical fingerprint of myosin unfolding

The specific design of AFM stretching experiments allows the application of force to the single protein molecule thus enabling the direct observation of folding and unfolding processes (59). The experiments can reveal specific mechanical properties of the targeted protein, forces required to unfold the protein or its domain, or the contour length of the protein. Our aim is to apply the method to study the effect of the chaperone binding on myosin, or any client protein.

In the case of the UNC-45 effect on the myosin folding, in order to be able to analyse AFM data, we have to obtain the characteristic mechanical fingerprint of myosin unfolding. Therefore, the full-length myosin was placed on the glass coverslip and physically stretched in the AFM experiments. A typical "mechanical fingerprint" of the full-length myosin is shown in **Figure II-2**. The obtained force extension curves display two features. An initial long plateau is observed up to around 30 pN. The plateau is only observed in experiments with the full-length myosin, not when the myosin S1 is stretched, as shown in **Figure II-3**. The results corroborate other reports, which suggested that the long plateau is associated with the rod domain (104-106). We have also determined the contour length of these two proteins. Our results (n number of analyzed experiments) show that the average contour length for the full-length myosin is 316 ± 83nm (n = 40).

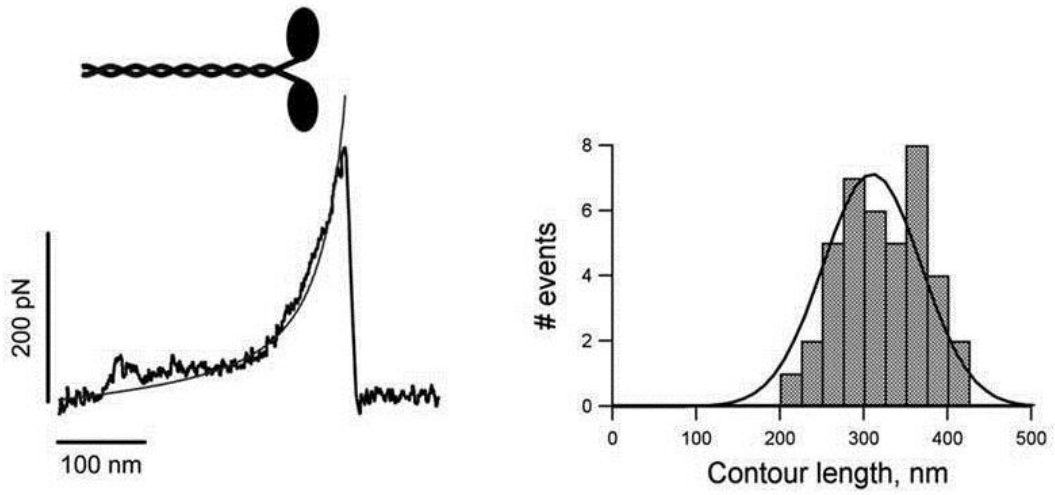

Figure II-2. The force–extension trace of the full length myosin unfolding. The left panel shows a representative example of a single full-length myosin molecule unfolding trace obtained by AFM. The myosin molecule was nonspecifically attached to glass surfaces and stretched. The right panel represents a histogram for contour lengths obtained from 40 different unfolding experiments. The mean value of the contour length, L_c = ~315 ± 83 nm. The thin line in the right panel represents a fit to the worm-like chain equation using a persistence length, p = 0.26 nm (equation II-1). Adapted from (67) with permission.

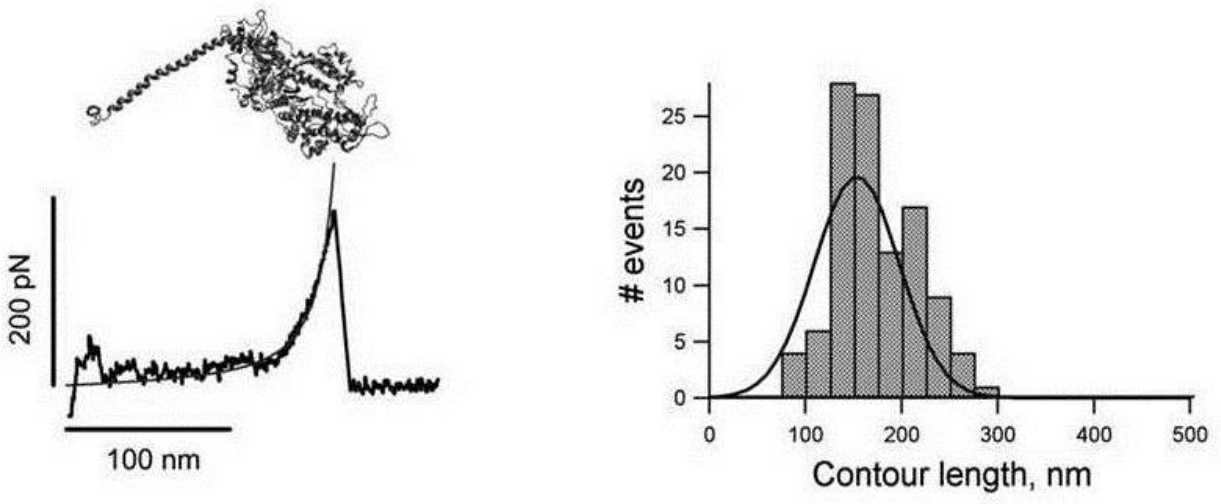

Figure II-3 .The force–extension trace for the myosin S1 unfolding. The left panel shows a representative example of a single unfolding trace of the myosin S1 molecule obtained by AFM. The right panel represents a histogram for contour lengths obtained from myosin S1 unfolding experiments. The mean value of the contour length, L_c = 171 ± 42 nm. The solid line in the right panel represents a fit to the worm-like chain equation using the persistence length, p = 0.39 nm (equation II-1). Adapted from (67) with permission .

The average contour length for the myosin S1 is significantly shorter, 171 ± 42 nm (n = 109) as depicted in **Figure II-2** and **Figure II-3**. These results correlate very well with known size of myosin. The full-length myosin is around 1385 amino acids long which correspond to the fully extended unfolded length of about 500 nm (we assume that each amino acid contributes 0.36 nm to the contour length of the protein). The myosin S1 alone is 845 amino-acids long thus its maximum unfolded length should be around 300 nm.

However, the experimental values are smaller than predicted from the unfolding of the full length protein. It is very unlikely that the tip binds to the precise end of the targeted protein and only in such situation the entire protein would be unfolded, yielding theoretical values of the contour length. In other words, these results can be explained by the fact that AFM tip interacts with proteins at random location on the protein molecule. Therefore, our AFM experiments indicate that myosin motor domain does not possess clearly defined mechanical unfolding fingerprint.

The titin molecular reporter

Because the AFM experiments described above showed that the myosin motor domain does not have an unambiguous mechanical fingerprint, we have decided to use the well-characterized titin I27 domain as a "mechanical reporter" (99, 107). The titin domains are one of the best characterize domain by single molecule AFM techniques (59, 67, 69). In a typical AFM experiment, one does not use a single titin domain, but a polyprotein composed of I27 tandem repeats (59, 69, 100). These macromolecules not

only unfold with a characteristic fingerprint but also refold through many repetitions cycles, without any signs of fatigue. Moreover, by utilizing multi-domain proteins we solve the problem of interpretation of the obtained force–extension curves. The source of the difficulty is in the fact that the obtained force peaks can originate from many sources such as detachment from the coverslip, or unspecific engagement of other molecules. However, the unfolding of polyproteins yield the characteristic force–extension pattern that resembles ‘‘saw-tooth’’ which describes the sequential unfolding of individual domains. Such periodicity of polyproteins allows the experimenter to unequivocally identify and select single molecules. Since recombinant expression of the myosin motor domain is very challenging, we could not just design the recombinant synthetic protein of myosin and titin. To tackle the problem, we performed chemical coupling reaction of the octameric I27 polyprotein to the specific site within the myosin motor domain (Materials and Methods).

The unfolded myosin motor domain interferes with titin I27 domains refolding

The myosin-I27 chimera was placed on the Ni^{2+}-charged NTA surface exposed to repeated mechanical stretching using AFM instrument **(Figure II-4**). After each stretching the protein was allowed to relax for 10 seconds. The unfolding of the titin I27 domains was detected during experiments with both full-length myosin and the motor domain protein chimeras (**Figure II-4**).

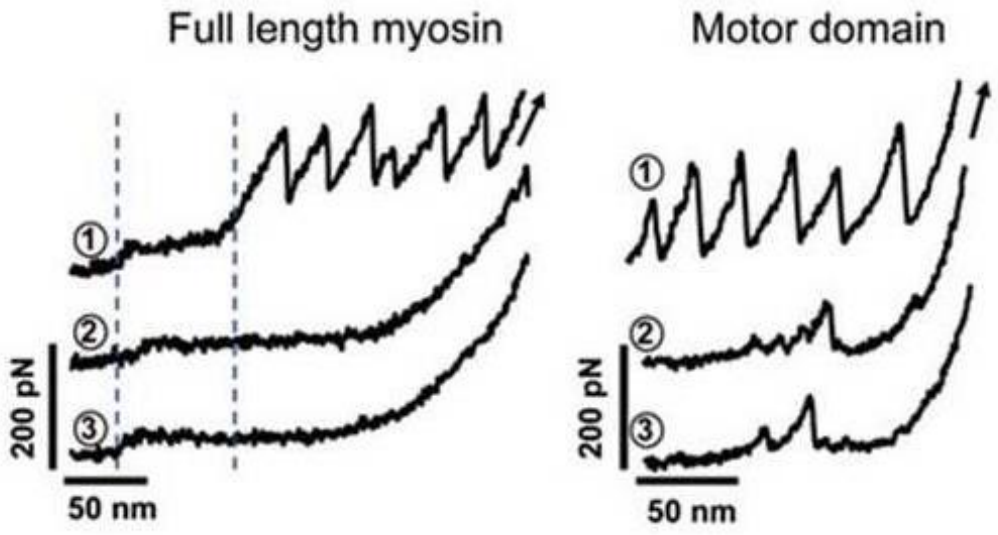

Figure II-4. The force-extension traces of the full-length myosin-I27 chimera and the myosin S1-I27 chimera. The left and right panels show the unfolding traces of a single molecule of full-length myosin-I27 protein chimera and myosin S1-I27 protein chimera. Each protein was subjected to repeated cycles of mechanical stretching. The typical titin I27 saw-tooth pattern is observed only in the first unfolding trace (1). In the subsequent traces (2 and 3) titin saw-tooth pattern is no longer observed, indicating that the unfolded motor domain interferes with refolding of the I27 domains. In the left panel all traces exhibit low-force plateau pattern associated with the tail domain. Notice also that the folding of the tail domain is independent from the motor domain. Adapted from (67) with permission.

Stretching the full-length myosin-I27 constructs reveals the existence of the long plateau at 30 pN force (the unravelling of the rod domain, **Figure II-4**). It should be noted that these results indicate that the force is applied across the titin I27 octamer, the motor and the tail domain, *i.e.*, validating our approach.

The most striking behaviour of the system was detected after repeated stretching of the same molecule. In this case, characteristic saw-tooth pattern of I27 domain unfolding, present in the initial pulling of the protein, disappeared (**Figure II-4** traces 2 and 3). The data imply that titin domain did not refold during the ten-second pause between the experiments. This is a significant result because I27 titin domains alone very easy refold within a few seconds. Therefore, behaviour of the chimera protein seems to be controlled by unfolding of the myosin motor domain. Similar results were obtained for both full-length myosin and myosin S1 (**Figure II-4**). This implies that the presence of the myosin motor domain affects the refolding of titin I27. Most likely, the refolding of titin domain is disrupted by interactions with covalently linked motor domain amino acids. Although behaviour of titin domain is a surprise, the inability of the myosin motor domain to refold was expected. Previous group already reported that myosin motor domain does not fold spontaneously (23, 90-92). Our data also showed that the rod domain folds independently from the motor domain since characteristic plateau at 30 pN was detected during repeated pulling cycles.

UNC-45 reverses the unfolding of titin I27 domains of myosin S1-I27 protein chimera

So far, all AFM experiments were performed in the absence of chaperones. However, it is well established that during *in vivo* folding process, myosin requires presence of the UNC-45 chaperone. We decided to repeat our AFM experiments with UNC-45 added to the reaction mixture (1 μM). In the **Figure II-5** we show the examples of three cycles of refolding. The presence of chaperone completely changes the outcome of the experiment. The refolding of titin I27 domains was completely restored in the presence of UNC-45. The control experiments showed that other proteins such as bovine serum albumin do not affect reversibility of I27–S1 refolding, as depicted in **Figure II-6**. Additional control experiments indicate that UNC-45 does not affect the refolding efficiency of the I27 domain alone. The data strongly suggest that UNC-45 prevents aberrant interactions between the unfolded polypeptides within the myosin - I27 protein chimera. The simplest interpretation of the results is that UNC-45 interacts with the myosin motor domain and stabilizes it. Therefore, our AFM experiments revealed an effect of the UNC-45 chaperone on myosin. The refolding of titin I27 domains was completely restored in the presence of the chaperone.

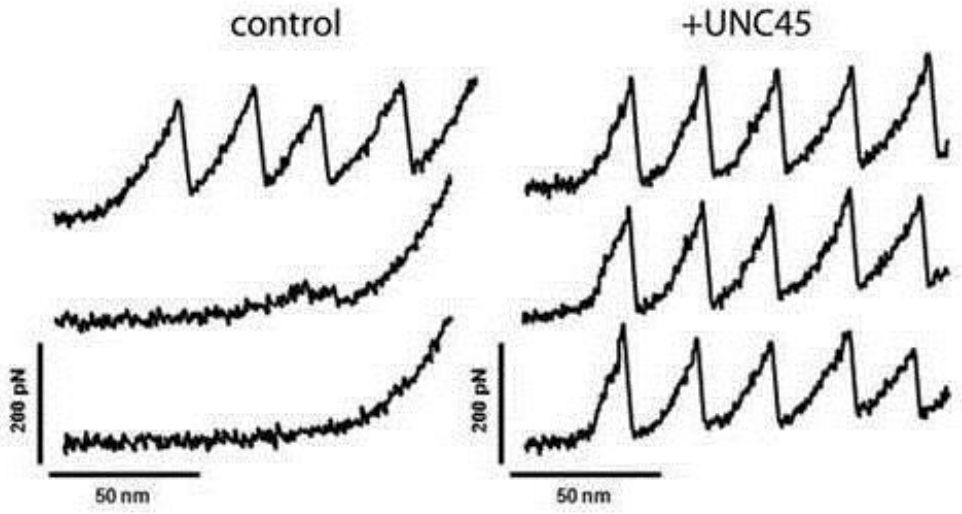

Figure II-5. The presence of the UNC-45 chaperone prevents misfolding of the titin mechanical reporter. Single molecule of myosin S1 - I27 was subjected to repeated cycles of unfolding. The left panel shows a series of repeated unfolding experiments in the absence of UNC-45 (control). The typical titin I27 saw-tooth pattern is observed only in the first curve, indicating that the unfolded motor domain affects with the refolding of the I27 titin domains. The presence of UNC-45 (1 mM), restores refolding of titin I27 domains (right panel). The data strongly suggest that UNC-45 prevents the interference between the myosin motor domain and titin I27 domains by binding to the myosin motor domain. Adapted from (67) with permission.

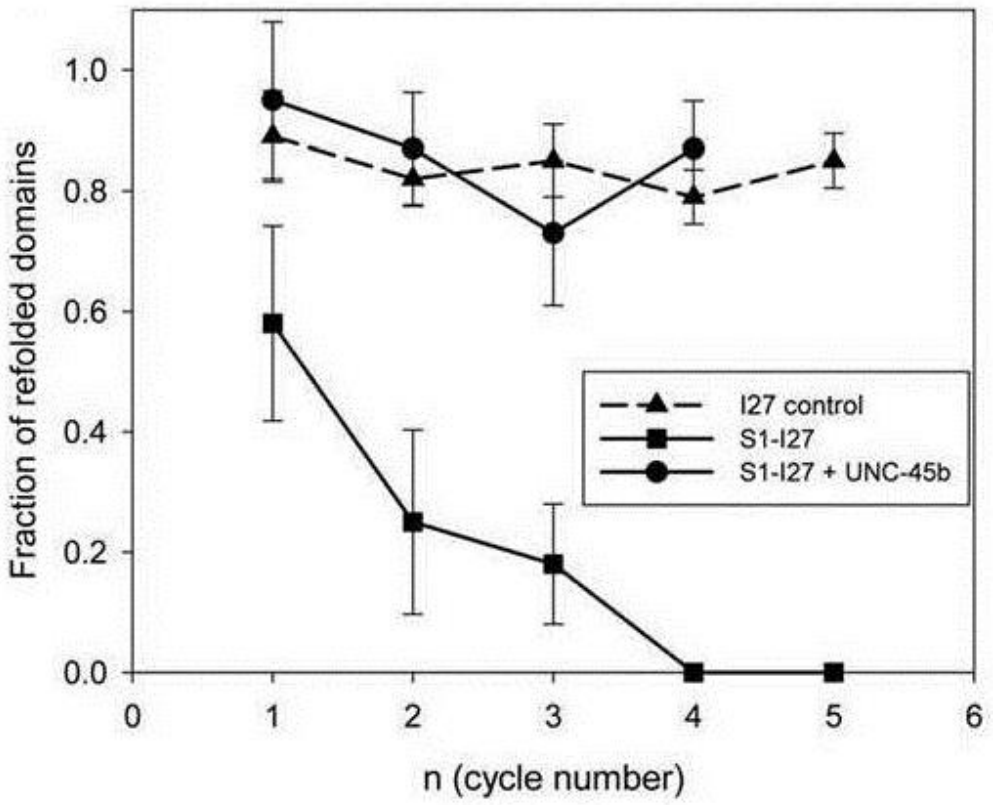

Figure II-6. The dependence of the fraction of refolded titin I27 domains of myosin S1-I27 chimera protein upon the number of refolding cycles. The single molecules of the I27 polyprotein (triangles; average of 18 molecules), myosin S1 - I27 protein chimera in the absence of chaperone (squares; average of 8 molecules), and myosin S1 - I27 protein chimera in the presence of 1 mM UNC-45 (circles; average of 12 molecules) were subjected to repeat cycles of unfolding. The error bars correspond to the standard deviations calculated, using the corresponding series of experimental data. Adapted from (67) with permission.

CONCLUSIONS

Myosins are structurally complex motor proteins that undergo significant structural rearrangements in order to perform their biological functions(94). Moreover, they are rather large macromolecules. If one combines their huge size and structural complexity, it is not surprising that they require additional assistance during folding process. Therefore, molecular chaperones are needed to navigate the myosin folding pathway into the native state. The UNC-45 protein was identified by different groups as a chaperone required for the folding of the myosin motor domain (24, 25, 91). Still, very little is known about the mechanism of the chaperone action on myosin.

Our studies are the first step in understanding how the UNC-45 chaperone affects the myosin motor domain folding. The AFM pulling experiments showed that the motor domain on its own does not fold after mechanical unfolding. Since myosin does not exhibit well defined mechanical fingerprint, detection of the domain misfolding or refolding events is a challenging task. Therefore, we utilize the titin I27 domains as a "mechanical reporter" to observe the effect of UNC-45 on the myosin motor domain. The experiments points to two major conclusions. First, the mechanical unfolding of the motor domain recruits very robust titin I27 domains into the misfolded state. Second, the refolding of the titin domains is restored in presence of the UNC-45 chaperone. In other words, the presence of UNC-45 prevents myosin misfolding into a state that might represent an off-pathway folding intermediate. Therefore, titin I27 domains act as a folding sensor that allows us to directly observe

the response of myosin S1 to interactions with the UNC-45 chaperone. In our opinion the approach discussed above is a novel and powerful tool to investigate effects of chaperones on myosin. We use it in our next studies of the biomolecular system (Chapter 3).

Chapter 3

UNC-45 Chaperone: the Role of its Domains in the Interactions with the Myosin Motor Domain

Modified from:

654 Biophysical Journal Volume 107 August 2014 654–661

Article

UNC-45B Chaperone: The Role of its Domains in the Interaction with the Myosin Motor Domain

Paul J. Bujalowski,[1,2] Paul Nicholls,[1,2] and Andres F. Oberhauser[1,3,*]
[1]Department of Neuroscience and Cell Biology, [2]Department of Biochemistry Molecular Biology, and [3]Sealy Center for Structural Biology and Molecular Biophysics, University of Texas Medical Branch, Galveston, Texas

Introduction

As discussed in the Introduction section, proteins must acquire a specific three-dimensional structure to perform their biological functions (89). For some proteins these folding processes occur spontaneously, for others additional help is required in the form of protein chaperones. The later situation is especially common in cases of larger and structurally more complex macromolecules (19). The existence of specialize protein that assist during the folding of other proteins has been known since 1970s (7). Protein chaperones are a specific case of enzymes, which interact with client protein intermediates, stabilize their structures, prevent potentially detrimental interactions and aggregation, but are not present in the final structure of a product. They can act as ATP-free catalyst (Hsp33) or as ATPases (GroEL/GroES)(108-111). During muscle development process several chaperones have been identified to play an important role for proper myosin assembly. These chaperones are Hsp70, Hsp90 and UNC-45 (112). Elucidation of mechanistic aspect of chaperone – myosin interactions is the major research challenge. Myosins compose a large superfamily of motor proteins that currently counts at least 24 different classes (51). Our work concentrates on the sarcomeric myosin that belongs to class II, the most studied type of myosins, engaged in muscle activities. It is built of the myosin head (motor domain), the neck and the tail domains (94). The active sites of the myosin II, which include the actin- and ATP-binding site, are located within the motor domain. Since the domain is structurally very complex, it does not fold spontaneously and requires presence of several molecular chaperones (23, 90-92).

The UNC-45 chaperone a member of the UCS (UNC-45/Cro1/She4p) family of proteins, was recognized as essential for folding and assembly of myosin into muscle thick filaments (112). Moreover, the UNC-45 protein was shown to prevent aggregation of thermally denatured myosin subfragment 1 (S1)(23). Furthermore, our data showed that the chaperone also stops misfolding of mechanically unfolded myosin S1 (**Chapter 2**)(67). The chaperone exists in two isoforms in vertebrates: the muscle specific UNC-45B and the general cell UNC-45A (29). It is built of three domains: 430 residue C-terminal UCS domain that is known to interact with the myosin motor domain, the 390 residue the Central domain of unknown function and the amino-terminal tetratricopeptide repeat (TPR) domain known to interact with the Hsp90 molecular chaperone (22, 23, 29) (**Figure I-1**). The biochemical and genetic data implies that the UCS domain plays a critical role in context of myosin function.

The last few years brought a tremendous progress in elucidating detailed structure of the UCS proteins with an atomic resolution. Different groups have determined crystal structures of She4p homolog, *Drosophila* and *C. elegans* UNC-45 (31-33). Nevertheless, the mechanism of the chaperone action is still not well understood. Particularly little is known about the nature of the interactions between different domains of UNC-45 and myosin. The biochemical data suggest that UNC-45 binds to myosin *via* the UCS domain. However, the energetics of the process has not been addressed. Moreover, nothing is known about the role of the Central domain in the myosin – UNC-45 complex formation.

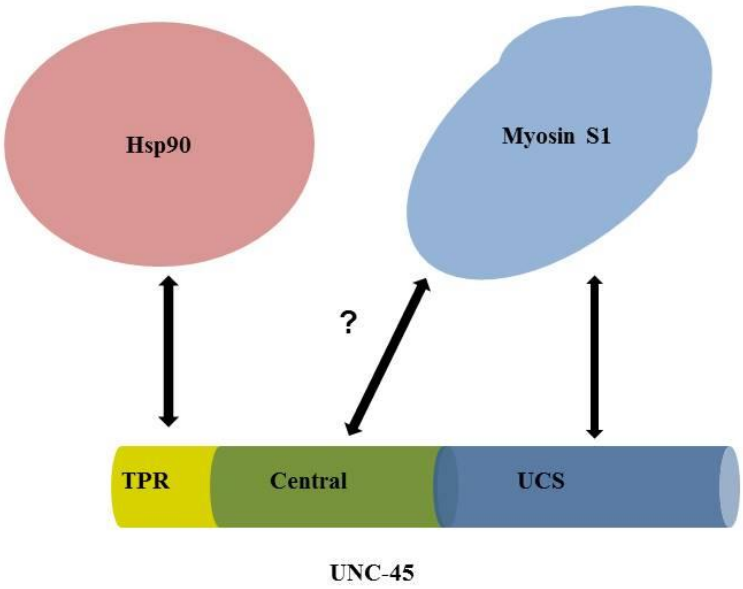

Figure III-1. Schematic structure of UNC-45B chaperone. The UNC-45B chaperone is built of three α-helical domains: The amino acid amino-terminal TPR domain that interacts with Hsp90 (yellow), the Central domain of unknown function (green) and the UCS domain that associates with the myosin motor domain (deep blue). Adapted from (67) with permission.

In our studies, we have combined an array of complementary experimental techniques (fluorescence titration of BADAN-labeled myosin with chaperone and its domains, dynamic light scattering, and single molecule AFM technique) to investigate the interactions of UNC-45B domains with the myosin motor domain (67). Our results imply that the UCS domain alone is sufficient to prevent myosin misfolding and aggregation. Therefore, the UCS domain most likely is essential for biogenesis and proper folding of the myosin motor domain. Furthermore, our data revealed that the total binding site of UNC-45B on myosin is built of two subsites, one engaging the UCS domain and the other one the Central domain. Thus not only the UCS domain but also the Central domain plays a role during myosin - UNC-45 complex formation.

MATERIALS AND METHODS

Myosin Purification

Myosin was purified from rabbit skeletal muscle using established protocol with small modification. The back and leg muscles were removed from freshly sacrificed rabbits. The dissection procedure was performed at 4° C. The obtained muscle tissue was washed and grinded three times through a course grinder and once through a fine grinder. The smoother grounding was achieved through adding ice cubes to both course and fine grinding processes. Subsequently, the extraction buffer (300 mM KCl, 100 mM KPO_4 pH 6.5, 20 mM EDTA, 5 mM $MgCl_2$, 1 mM ATP)

was added to the muscle (3 g/mL) and the sample left for 10 minutes. Next, the mixture was centrifuged at 9000g for 30 minutes. The supernatant was collected and its pH adjusted to 6.6 using ammonium bicarbonate (1M), which was followed by 10 volumes dilution in ice-cold glass distilled water. The glacial acetic acid was used to adjust pH back to 6.6. The sample was left to settle for 1 hour. The supernatant was discarded while the remaining material was centrifuged for seven minutes at 9000g. The obtained pellet was resuspended in 900 mL of the following buffer: 1M KCl, 60mM KPO4 at pH 6.5, and 25 mM EDTA. The solution was dialysed overnight in 10L of 0.6M KCl, 25mM KPO_4 at pH 6.5, and 10 mM EDTA and 1 mM DTT.

The next day, the dialysate was diluted 1:1 with the ice-cold glass distilled water and stirred for 30 minutes. Then, the solution was centrifuged for 50 minutes at 12,000 g. The pellet was resuspended in 30 mL of 2 M KCl. The KCl concentration of the mixture was adjusted to 0.5 M KCl using 2 M KCl solutions. The mixture was then stirred overnight. The solution was adjusted to 40% ammonium sulphate for 20 minutes and centrifuged for 11 minutes at 12,000 g. The resulting supernatant was first decanted and then adjusted to 50% ammonium sulphate, stirred again for an hour and centrifuged for 15 minutes. The obtained myosin pellet was stored under saturated ammonium sulphate at 4° C.

Myosin Subfragment 1 Preparation

Myosin subfragment-1 was prepared by dialysing the previously prepared myosin against 20 mM Tris, pH 8.5, 0.8 M NaCl, 0.3 mM EGTA and 1 mM DTT overnight. The resulting solution was then dialysed against 20 mM $NaPO_4$, pH 7.4,

120 mM NaCl, and 1 mM EDTA to form synthetic filaments. The resulting myosin solution of 20 mg/mL was then digested using 0.05 mg/mL of chymotrypsin for 10 minutes at 25^{o}C with careful constant stirring and was promptly quenched by adjusting the solution to 1 mM PMSF. The product was dialysed against 50 mM imidazole, 1 mM DTT, and 0.3 mM EGTA at pH 7.0 overnight, centrifuged for 1 hour at 12,000 g, and the pellet, containing rod-bearing fractions, was discarded. The supernatant was then adjusted to 150 mM NaCl and subjected to gel filtration over a GE 26/60 Superdex 200 (320 mL bed column) at a 1.5 mL/min flow rate. The S1 peaks were pooled, concentrated, dialysed against PBS buffer supplemented with 0.3 mM EGTA and 1 mM DTT, and stored at -80^{o}C with the addition of sucrose (1:2, sucrose : myosin, weight/weight) (113, 114).

UNC-45B constructs

Selections of domain boundaries for the UCS domain (500 to 931 amino acid) and the Central domain (100-499 amino acid) were based on the human UNC-45B sequence (Accession: Q8IWX7.1) and the published crystal structure of the protein(9, 27) (**Figure III-2**). UNC-45B is highly conserved among mammals. The alignment between human and mouse UNC-45B showed 95% identity and 98% similarity. Moreover, the human and mouse UCS domains show 99% identity and 99% similarity. Synthetic cDNA (GenScript, Piscataway, New Jersey) for the constructs were sub-cloned into a pProEx vector (Life Technologies, Carlsbad, CA) for UNC-45B, or pET28a vector (EMD Millipore, Billerica, MA) for the UCS and Central

domains. The N-terminus of the proteins had a hexa-histidine (His_6) tag. Protein expression in BL21 cells (Life Technologies, Carlsbad, CA) was induced by addition of 1 mM IPTG and shaking at 16° C overnight. The cells were resuspended in phosphate buffered saline (PBS, 10 mM sodium phosphate buffer, pH 7.4, 150 mM NaCl), and sonicated on ice in the presence of a protease inhibitor cocktail (1 mM PMSF and 1 mg/mL of trypsin inhibitor, chymostatin, pepstatin, leupeptin, *N*-benzoyl-L-arginine ethyl ester, and *p*-toluidinyl-L-arginine methyl ester). The proteins were purified over a His-Trap column (GE Healthcare, Piscataway, NJ), eluted with the gradient from 20 mM-500 mM imidazole over 20 column volumes.

The His_6-tags were cleaved using thrombin for the UCS and Central domains, or the TEV protease for UNC-45B. The purity of the proteins was confirmed by SDS-PAGE and was greater than 95% (**Figure III-3**). Full-length UNC-45B has a similar molecular mass to myosin S1 and runs at around 100 kDa whereas the UCS and Central domains run slightly below 50 kDa (molecular masses are 46 kDa and 44 kDa respectively).

Chimeric -myosin S1- I27 construct (S1-I27protein)

We used our previously published protocol to chemically couple an octameric I27 polyprotein to a specific site within the myosin motor domain S1 (25). The polyprotein harbored the N-terminal cysteine residue and the C-terminal His_6-tag.

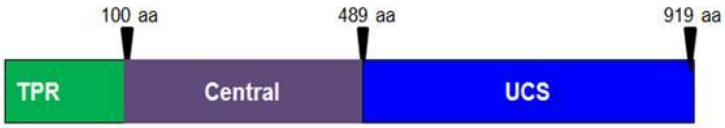

TPR

maeveavqlkeegnrhfqlqdykaatnsysqalkltkdkallatlyrnraacglktesyvqaasdasraidinssdikalyrrcqalehlgkldqafkdv

Central domain

qrcatleprnqnfqemlrrlntsiqeklrvqfstdsrvqkmfeilldenseadkrekaannlivlgreeagaekifqnngvalllqlldtkkpelvlaav
rtlsgmcsghqaratvilhavridricslmaveneemslavcnllqaiidslsgedkrehrgkeealvldtkkdlkqitshlldmlvskkvsgqgrdq
alnllnknvprkdlaihdnsrtiyvvdnglrkilkvvgqvpdlpsclpltdntrmlasilinklyddlrcdperdhfrkiceeyitgkfdpqmdknlnaiq
tvsgilqgpfdlgnqllglkgvmemmvalcgseretdqlvavealihastklsratfiitngvsllkqiykttknekikirtlvglcklg

UCS domain

saggtdyglrqfaegsteklakqcrkwlcnmsidtrtrrwaveglayltldadvkddfvqdvpalqamfelakagtsdktilysvattlvctnsydvke
vipelvqlakfskqhvpeehpkdkkdfidmrvkrllkagvisalacmvkadsailtdqtkellarvflalcdnpkdrgtivaqgggkaliplalegtdvg
iaavsnpdiafpgervyevvrplvrlldtqrdglqnyeallgltnlsgrsdklrqkifkeralpdienymfenhdqlrqaatecmcnmvl
hkevqerfladgndrlklvvllcgedddkvqnaaagalamltaahkklclkmtqvttqwleilqrlclhdqlsvqhrglviaynllaadaelakklvese
lleiltvvgkqepdekkaevvqtareclikcmdygfikpvs

Figure III-2. The amino acid sequences and boundaries of the domains of UNC-45. The TPR domain (1-99 amino acid) in green, the Central domain (100-489 amino acid) in purple, and UCS domain (490-919 amino acid) in blue. Adapted from (115) with permission.

Coupling to the myosin S1 was achieved *via* the reactive cysteines (SH1/SH2) within the motor domain. The cross-linking adduct was isolated by size exclusion chromatography on a Sephacryl S-300 column (GE Healthcare, Piscataway, NJ).

Circular Dichroism

The far UV CD measurements were performed with a Jasco J-815 Spectrometer. The protein concentration was 1 μM in 30 mM TRIS pH 7.4, 100 mM KCl, 1 mM $MgCl_2$, 1 mM TCEP buffer. A 0.2 cm path length cuvette was used. The data reported in **Figure III-4** correspond to the average of 3 scans obtained at a scan rate of 50 nm/min in the range of 190–260 nm. The K2D3 program (http://www.ogic.ca/projects/k2d3/) was used to estimate the content the protein secondary structures.

Fluorescence Measurements

The environmentally sensitive fluorophore BADAN (6-Bromoacetyl-2-Dimethylaminonaphthalene) attached to myosin S1 was used to study its interaction with the full length UNC-45B and its UCS and Central domains (Kaiser). The fluorescence titrations were done in presence of 100 mM KCl, 1 mM $MgCl_2$, 30 mM Tris, pH 7.4, and 1mM TCEP. Experiments were performed in a quartz cuvette (500 μl) into which the UNC-45B constructs (the full length UNC-45B, the UCS domain, and the Central domain) were added.

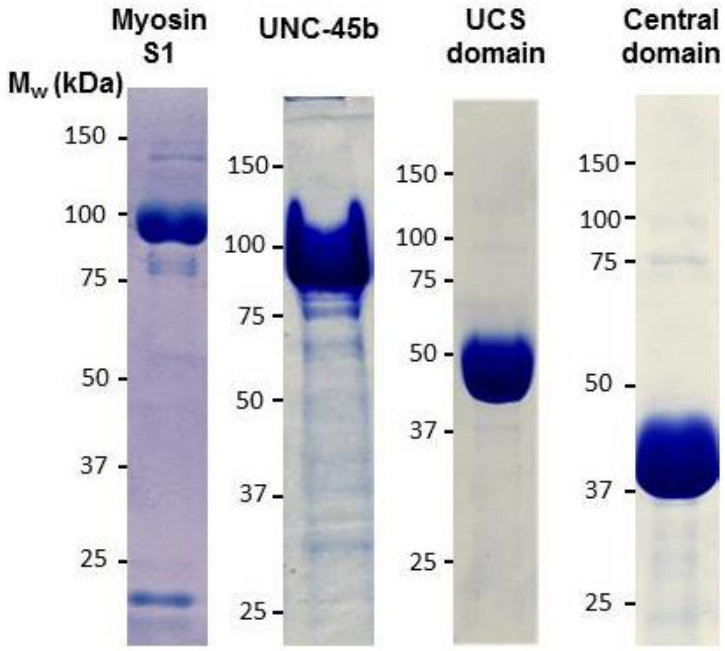

Figure III-3. The SDS PAGE gels confirm the purity of purified proteins. From the left: Myosin S1, UNC-45B, the UCS domain, and the Central domain Adapted with permission from (115).

Fluorescence emission of BADAN-S1 at 520 nm was measured at the excitation at 387 nm relative to a control sample that contained buffer instead of UNC-45B constructs. Each point of the titration curve corresponds to an average of 20 measurements. Steady-state fluorescence titrations were performed using an ISS PC1 spectrofluorometer (ISS, Urbana, IL). In order to avoid possible artifacts due to the fluorescence anisotropy of the sample, polarizers were placed in excitation and emission channels and set at 90 and 55° (magic angle), respectively. Non-linear Least Square fits were done using Kaleida Graph software (Synergy Software, PA) and Mathematica (Wolfram Research, IL).

Single-molecule Atomic Force Microscopy

The mechanical properties of single I27-S1 protein chimeras were investigated using a home-built single molecule AFM as previously described (99, 101-103). The spring constant of each individual cantilever (MLCT or Olympus OBL, Veeco Metrology Group, Santa Barbara, CA) was calculated using the equipartition theorem. A small volume of the purified I27-S1 chimera (~1-5 µl, 10-100 µg/ml) was allowed to adsorb Ni-NTA coated glass coverslip for about 10 min and then rinsed with PBS buffer, pH 7.4(38). Proteins were picked up randomly by adsorption to the cantilever tip, which was pressed down onto the sample for 1 - 2 seconds at forces of several nano-Newtons and then stretched for several hundred nm. All experiments were performed at room temperature (25° C) at a pulling speed of 0.5-0.7 nm/ms.

A two-pulse unfolding/refolding protocol was used to estimate the fraction of refolded domains (69, 99). After the first stretch, a single I27-S1 protein chimera was allowed to relax for time intervals of ~10 seconds. In the second pulling we counted the refolded domains. The number of the domains that refolded in the second pulling divided by the number of the unfolded domains in the first pulling gives the fraction of refolded I27 domains. In a typical experiment after picking up a protein, the AFM tip is moved away from the surface (~30-50 nm) in order to prevent the tip picking new proteins due to the cantilever drift.

Actin filament gliding assay

Actin gliding assays were performed with myosin S1 on nitrocellulose. Nitrocellose coated coverslips were prepared by depositing 1 μL of 1% nitrocellulose in amyl acetate on a glass cover slip and spread evenly with a pipette tip. Myosin S1 was concentrated to 0.2 mg/mL and was then placed on the coverslip in a TBS buffer for 2 minutes. Then the solution was washed with the buffer again to remove the unbound fraction. The coverslip surface was blocked by applying BSA (1 mg/mL) in G-actin buffer for 3 minutes. Then the solution was rinsed with the wash buffer (20 mM MOPS, pH 7.4, 80 mM KCl, 5 mM $MgCl_2$, and 0.1 mM EGTA).

The Alexa-594-phalloidin labeled actin was then added (20 nM) in the wash buffer and incubated for 60 seconds. The solution was then rinsed with the assay buffer (wash buffer accompanied with 0.7% methylcellulose, 1 mM ATP, 0.1 mg/mL glucose oxidase, 0.02 mg/mL catalase, 2.5 mg/mL d-glucose and 50 mM DTT)(114).

The flow cell was imaged using a Nikon Eclipse TE2000 microscope with the Nikon 40X 1.3 NA objective and the CoolSnapHQ camera. Images were taken every 1 - 5 seconds. Each frame was exposed for time of 200 ms. The Difference Tracker software (Babraham Bioinformatics, Cambridge, UK) in ImageJ software (NIH, Bethesda, MD) was used for analysis. The experiments were performed at room temperature.

Modified actin filament gliding assay

In order to test whether or not the motor domain in the I27-myosin S1 chimeric construct was active, we used the actin gliding *in vitro* motility assay (114). This assay reproduces the most fundamental property of the muscle, namely, the ability of myosin to translocate actin. The gliding assay was a modified version of Sellers (116). In our modification, we used Ni-NTA functionalized flow cells (59). Briefly, the I27-S1 protein was immobilized on a Ni-NTA coated coverslip, blocked with BSA (1mg/mL) in G-actin buffer, and washed with 10 mM MOPS pH 7.0, 0.1 mM EGTA, 3 mM NaN_3. Filamentous actin, labeled with Alexa Fluor 594 phalloidin, was added at 20 nM concentration and incubated for 1 minute. The initial buffer was exchanged with the buffer containing 1mM Mg-ATP, 0.7% methylcellulose, 50mM DTT, 2.5 mg/mL glucose oxidase, and 0.02mg/mL catalase to initiate gliding. Movement of Alexa-594-phalloidin labeled actin filament was then imaged using a Nikon TE2000 Eclipse microscope equipped with a Photometrics CoolSnap HQ camera using a 200 ms exposure time.

RESULTS

Characterization of the full-length UNC-45B and its UCS and Central domains secondary structures in solution

The secondary structure of the examined protein constructs was addressed using the far-UV Circular Dichroism spectroscopy. Wavelength dependence of the circular dichroism for all examined constructs show typical characteristics of the protein CD spectra with pronounced negative peaks at 220 and 210 nm (**Figure III-4**). The spectra and their analyses indicate that the overall secondary structure of the UNC-45B, the UCS domain and the Central domain constructs have predominantly α-helical secondary structures (**Figure III-4**). The nonlinear fits of the data using the K2D3 program (http://www.ogic.ca/projects/k2d3/) indicate 58 %, 69 % and 69 % content of the α-helix in UNC-45B, the UCS, and the Central domain. The results are consistent with the published crystal structure analyses, which clearly indicate that UNC-45B is composed almost entirely of α-helical armadillo repeats (33).

The UCS domain binding to the myosin motor domain

The myosin motor domain has been modified with the environmentally sensitive fluorescence marker, BADAN, to monitor its interaction with the UCS domain.

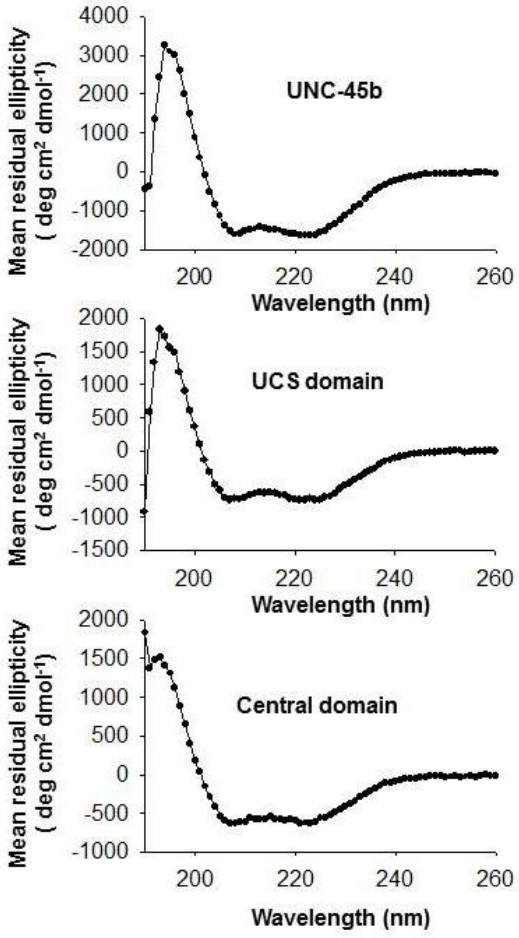

Figure III-4. Far-UV CD spectroscopy of the investigated proteins. At the top, full-length UNC-45B, the UCS domain (center) and the Central domain (bottom). The spectra are characteristic for the high α-helix secondary structure content with minima at 209 and 222nm (58%, 69 % and 69% for the full length UNC-45B, the UCS and the Central domains (K2D3 program (http://www.ogic.ca/projects/k2d3/)). Adapted with permission from (115).

The BADAN fluorophore reacts preferentially with the SH1 group on myosin, producing labeled myosin S1 (BADAN-S1). The fluorophore is attached at a specific site (Cys-707) within the myosin catalytic domain. The affinity of the UCS domain for the myosin motor domain has been determined using the fluorescence titration technique, where interactions are examined by monitoring the alterations of the recorded fluorescence intensity. We discovered that the presence of the UCS domain induced a decrease in BADAN fluorescence emission intensity, indicating changes in local environment of the fluorescent probe, due to interaction of BADAN-S1 with the UCS domain. The most plausible explanation of the signal alterations is the binding of UCS in the area near the catalytic site or binding at a distant site that induces allosteric conformation changes.

Figure III-5 shows the relative fluorescence intensity of the BADAN-labeled myosin S1, ΔF_{obs}, as a function of the UCS concentration in the sample. The concentration of the myosin S1 is 2.5 x 10^{-7} M. Binding of UCS induces quenching of the fluorescence intensity of the labeled myosin, with the maximum value of the quenching reaching 7%. The experimental data in **Figure III-5** have been analyzed using the following approach. The binding constant, K_1, for the UCS association with the myosin to form a complex, C_1, is defined as

$$K_1 = \frac{[C_1]_F}{[S1]_F [UCS]_F} \qquad (1)$$

The observed total fluorescence of the sample at any titration point is defined as

$$F_{obs} = F_F [S1]_F + F_C [C_1]_F \qquad (2)$$

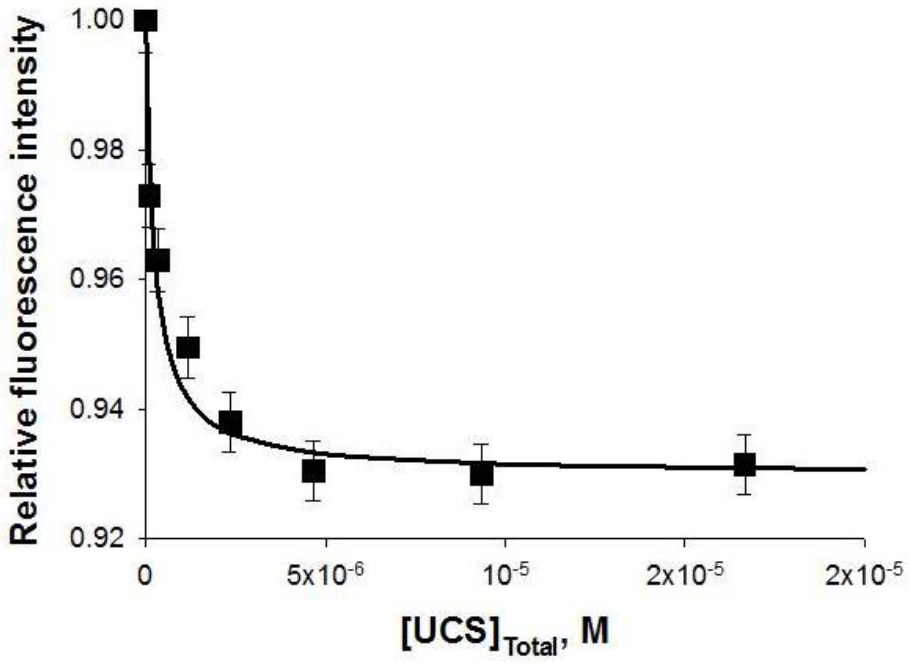

Figure III-5. The UCS domain binding to the UNC-45 chaperone. BADAN-S1 fluorescence emission as a function of the total UCS domain concentration; the solid line shows a fit of Equation 5 to the data assuming a complex formation with a 1:1 stoichiometry of UCS and BADAN-S1, yielding an apparent binding constant of $K_1=4.3x10^6$ M^{-1}. The BADAN-S1 concentration was $2.5x10^{-7}$ M. Adapted with permission from (115).

where F_F and F_C are the molar fluorescence intensities of the free myosin and the formed complex, respectively. Using equation1, one obtains

$$F_{obs} = F_F [S1]_F + F_C K_1 [S1]_F [UCS]_F \quad (3)$$

The mass conservation equation for the total myosin concentration in the sample is

$$[S1]_T = [S1]_F (1 + K_1 [UCS]_F) \quad (4)$$

By combining equations 3 and 4, one obtains the relative observed change of the observed myosin fluorescence, ΔF_{obs}, as

$$\Delta F_{obs} = \frac{F_{obs}}{F_F [S1]_T} = \frac{1}{1 + K_1 [UCS]_F} + \Delta F_{max} \left(\frac{K_1 [UCS]_F}{1 + K_1 [UCS]_F} \right) \quad (5)$$

where, $\Delta F_{max} = F_C/F_F$, is the maximum observed relative fluorescence quenching. The solid line in **Figure III-5** is the nonlinear least squares fit of the experimental titration curve to equation 5, with K_1 and ΔF_{max} as two fitting parameters, which provides $K_1 = (4.3 \pm 1.5) \times 10^6\ M^{-1}$ and $\Delta F_{max} = 0.930 \pm 0.005$.

The UCS domain competes with the UNC-45 chaperone for the myosin motor domain.

In our solution conditions, binding of the intact UNC-45 chaperone to the labeled myosin does not induce any change of the protein fluorescence. Therefore, the affinity of the intact UNC-45 for the myosin motor domain has been determined using the macromolecular competition titration method (117, 118) .

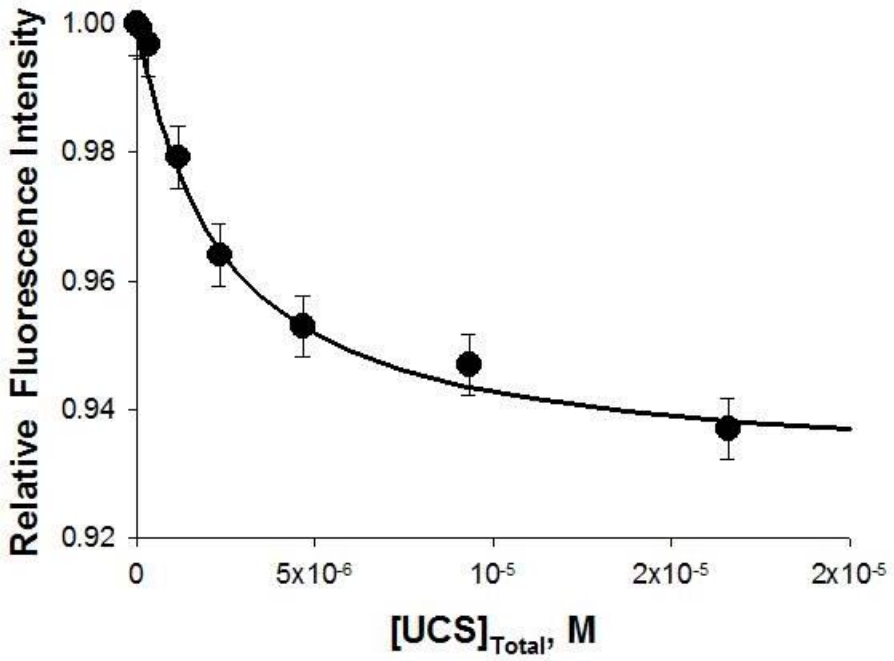

Figure III-6. Competition between UCS and UNC-45 for myosin. Titration of BADAN-S1 ($2.5x10^{-7}$ M) with the UCS domain in the presence of the full length UNC-45B ($3x10^{-6}$ M). The solid line is the nonlinear least squares fit to equation 9, with $K_2 = 2.8x10^6$ M^{-1}. The maximum fluorescence quenching is $\Delta F_{max} = 0.93$. Adapted with permission from (115).

The relative fluorescence intensity of the BADAN-myosin S1, as a function of the UCS concentration, in the presence of the 3 x 10^{-6} M UNC-45 is shown in **Figure III-6**. The total chaperone concentration, $[UNC\text{-}45]_T$, is in large excess over $[S1]_T$.

The curve is shifted toward higher UCS concentrations than in the absence of the chaperone (**Figure III-5**), indicating an efficient competition between the domain and the chaperone for the binding site on the myosin.

The binding constant, K_1, of the UCS association with the myosin to form a complex, C_1, is defined by equation 1. The binding constant, K_2, of the UNC-45 association with the myosin to form a complex, C_2, is defined as

$$K_2 = \frac{[C_2]_F}{[S1]_F[UNC45]_F} \qquad (6)$$

The fluorescence of the sample at any titration point is then

$$F_{obs} = F_F[S1]_F + F_F[C_2]_F + F_C K_1[S1]_F[UCS]_F \qquad (7a)$$

and, using equations 1 and 2, one has that

$$F_{obs} = F_F[S1]_F + F_F K_2[S1]_F[UNC45]_F + F_C K_1[S1]_F[UCS]_F \qquad (7b)$$

The mass conservation equation for the total myosin concentration in the sample is

$$[S1]_T = [S1]_F(1 + K_1[UCS]_F + K_2[UNC45]_F) \qquad (8)$$

Using equations 7b and 8, one obtains the relative observed change of the myosin fluorescence, ΔF_{obs}, in the presence of UNC-45 and the UCS domain as

$$\Delta F_{obs} = \frac{1}{1+K_1[UCS]_F + K_2[S1]_F[UNC45]_F} + \Delta F_{max}\left(\frac{K_1[UCS]_F}{1+K_1[UCS]_F + K_2[S1]_F[UNC45]_F}\right) \quad (9)$$

The maximum change of fluorescence signal, ΔF_{max}, is defined as in equation 5 and has been already determined (see above). As we stated above, because the total $[UNC\text{-}45]_T >> [S1]_T$, we can take $[UNC\text{-}45]_F \approx [UNC\text{-}45]_T$ and treat it as the known constant. The solid line in **Figure III-6** is the nonlinear least squares fit of the experimental titration curve to equation 9, with K_2 as a single fitting parameter, which provides $K_2 = (2.8 \pm 0.8) \times 10^6\ M^{-1}$.

The central domain interacts with the myosin motor domain.

The fact that the UCS domain interacts with myosin and the TPR domain binds to Hsp90 has been known before, although the energetics of the interaction has not been ever established (23). On the other hand, nothing is known whether or not the Central domain interacts with any potential client proteins, or about the domain function in the formation of the myosin - UNC-45 complex. Therefore, we addressed the interactions of the last uncharacterized domain of UNC-45 with myosin.

Similar to the intact UNC-45 chaperone, the isolated Central domain does not induce any change of fluorescence signal of the labeled myosin. Consequently, as discussed above, we used the macromolecular competition titration method to address the Central domain interactions with the myosin motor domain (118).

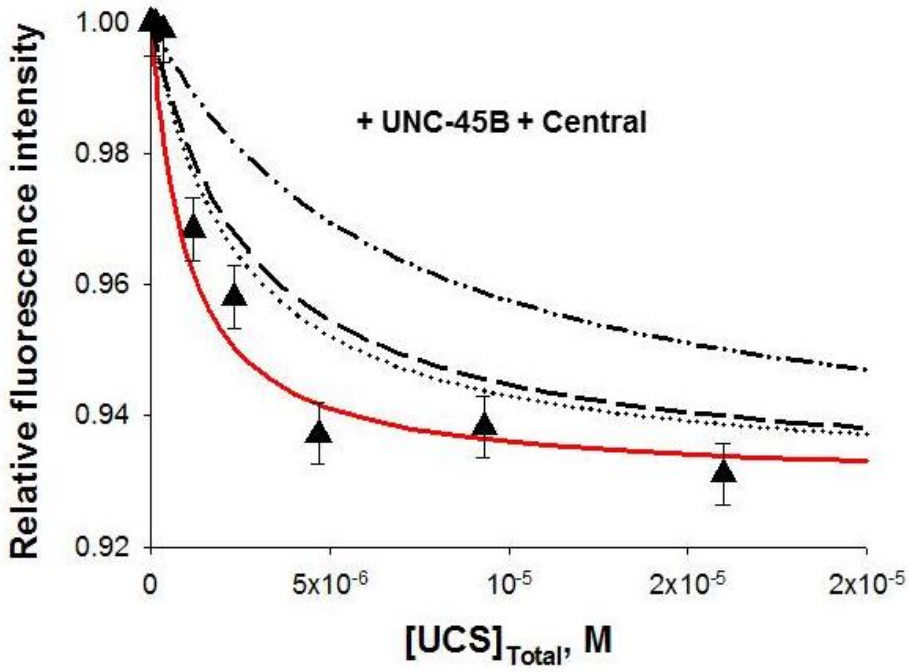

Figure III-7. Competition between the Central, UCS domains and UNC-45 for myosin. The graph represents BADAN-S1 ($2.5x10^{-7}$ M) fluorescence emission as a function of the total UCS domain concentration in the presence of full length UNC-45B ($3x10^{-6}$ M) and Central domain ($3x10^{-6}$ M). The dotted black lines represent the analysis of the experimental data using a triple competition single-binding site model (equation 15); the binding constants for UCS and UNC-45B, K_1 and K_2 respectively, were from the experiments shown in Fig. 3A, B. Each line correspond to different values for the association constant for the Central domain, K_3, ranging from $6x10^6$ to $6x10^3$. The solid red line corresponds to the best-fit to a triple competition two-binding site model (Equation 14) yielding a $K_3 = 6x10^5$ M^{-1}. Adapted with permission from (115).

The relative fluorescence intensity of the BADAN-myosin S1, as a function of the UCS concentration, in the presence of the 3 x 10^{-6} M UNC-45 and 3 x 10^{-6} M Central Domain, respectively, is shown in **Figure III-7** (black triangles). The behavior of the system is surprising. The presence of the Central domain shifts the titration curve toward the lower concentrations of the UCS domain, as compared to the [UCS], in the titration performed in the presence of the UNC-45 chaperone alone (**Figure III-6**).

There are two major aspects of these data. First, the data establish that the central domain binds to the myosin S1. Second, the results indicate that the three components of the binding system, UNC-45, UCS domain and the Central domain do not simply compete for a single site on myosin. The simple triple competition single binding-site model is shown in **Figure III-8A**. The predictions of the model where UNC-45B and its UCS and Central domains compete for the same binding site on the myosin motor domain are shown in **Figure III-7**. The dotted black lines represent the behavior of the examined system according to this model, using different values of the association constant, K_3, ranging from 6×10^6 to 6×10^3 M^{-1}, that characterizes the affinity between the Central domain and myosin (**Figure III-7** and **Figure III-8A**). Each dotted line was calculated using equation 15 (see below). It is evident that the triple competition single binding-site model does not describe the behavior of the system.

Next, we consider a model where the UCS domain and the Central domain bind to two different binding sites on the myosin, as depicted in **Figure III-8B**. In

other words, we analyzed the data using the triple-competition two binding-sites model, as defined by equation 14 (see below). The solid red line in **Figure III-7** is the nonlinear least square fit of experimental data to equation 14, yielding an apparent association constant, K_3, of $(6.0 \pm 2.1) \times 10^5\ M^{-1}$. It is evident that the model, which includes two different binding sites for the Central and UCS domains, reflects the experimental behavior of the system (**Figure III-8B**). Thus, our data and analysis clearly show that the Central domain binds to the myosin head and to a different site than the UCS domain.

The relevant thermodynamic relationship describing the fluorescence titrations for the triple-competition single binding-site model and the triple competition two binding-sites model have been derived using the following approach. The binding constant, K_1, characterizing the UCS association with its binding site on the myosin to form a complex, C_1, is defined by equation 1.

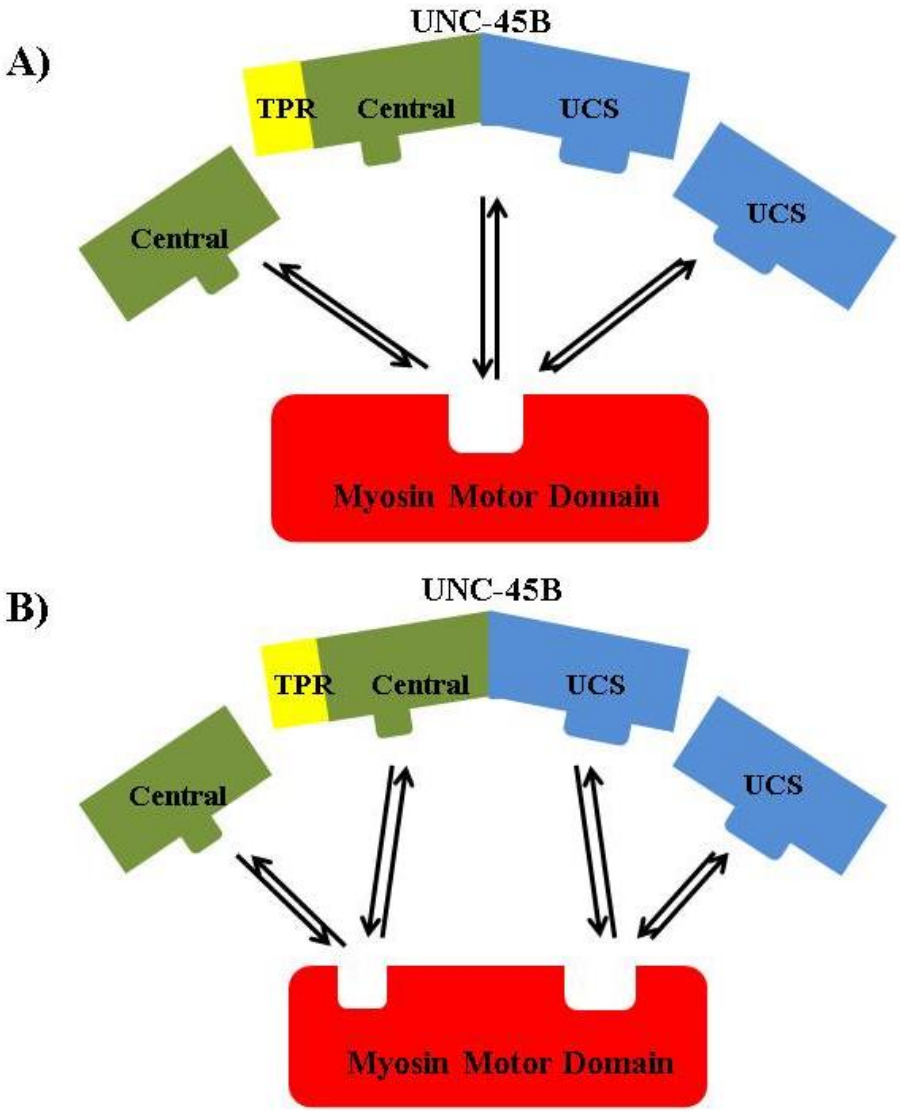

Figure III-8. Myosin – UNC-45 binding models. A) Triple competition single-binding site model. The UCS and Central domains compete for one binding site on myosin. **B)** Triple competition two binding-sites model. Both domains engage different sites on myosin. . Adapted with permission from (115).

The binding constant, K_2, of the intact UNC-45 association with the myosin to form a complex, C_2, is defined by equation 6. The association constant of the Central domain with its binding site on the myosin, K_3, is defined as

$$K_3=\frac{[C_3]_F}{[S1]_F[CD]_F} \tag{10}$$

In the case of the triple competition two binding-sites model (**Figure III-8B**), the observed fluorescence of the sample at any titration point, F_{obs}, is described by

$$F_{obs} = F_F[S1]_F + F_F K_2[S1]_F[UNC45]_F + F_F K_3[S1]_F[CD]_F + F_C K_1[S1]_F[UCS]_F + F_C K_1 K_3[S1]_F[CD]_F[UCS]_F \tag{11}$$

The mass conservation equation for the total myosin concentration in the sample is

$$[S1]_T = [S1]_F Z_{S1} \tag{12}$$

where

$$Z_{S1} = 1 + K_1[UCS]_F + K_2[UNC45]_F + K_3[CD]_F + K_1K_3[CD]_F[UCS]_F \tag{13}$$

is the partition function of the S1 system.

By combining equations 11 and 12, one obtains the relative observed change of the myosin fluorescence, ΔF_{obs}, as

$$\Delta F_{obs} = \frac{1 + K_2[UNC45]_F + K_3[CD]_F}{Z_{S1}} + \Delta F_{max}\left(\frac{K_1K_3[UCS]_F[CD]_F + K_1[UCS]_F}{Z_{S1}}\right) \tag{14}$$

where ΔF_{max} is defined as in eq. 5 (see above). As we stated above, because $[UNC\text{-}45]_T >> [S1]_T$ and $[CD]_T >> [S1]_T$ we can take $[UNC\text{-}45]_F \approx [UNC\text{-}45]_T$ and $[CD]_F \approx [CD]_T$ and treat them as the known constants.

In the case of the triple competition single binding-site model (**Figure III-8A**), the plots included in **Figure III-7** were obtained using the equation analogous to equation 14, as

$$\Delta F_{obs} = \frac{1 + K_2[UNC45]_F + K_3[CD]_F}{Z_{S1}} + \Delta F_{max}\left(\frac{K_1[UCS]_F}{Z_{S1}}\right) \qquad (15)$$

where partition function is defined, as

$$Z_{S1} = 1 + K_1[UCS]_F + K_2[UNC45]_F + K_3[CD]_F \qquad (16)$$

with a single fitting parameter, K_3.

The Central domain does not compete with the UCS domain for myosin

The analyses discussed above of the triple competition titration models indicated that the UCS domain and the Central domain bind to different binding sites on myosin, *i.e.*, they do not compete for myosin. In the final set of experiments, we directly addressed the competition between the UCS and the Central domain to confirm the conclusion that both domains bind to different binding sites. We carried out direct competition studies of the UCS binding to myosin in presence of the Central domain.

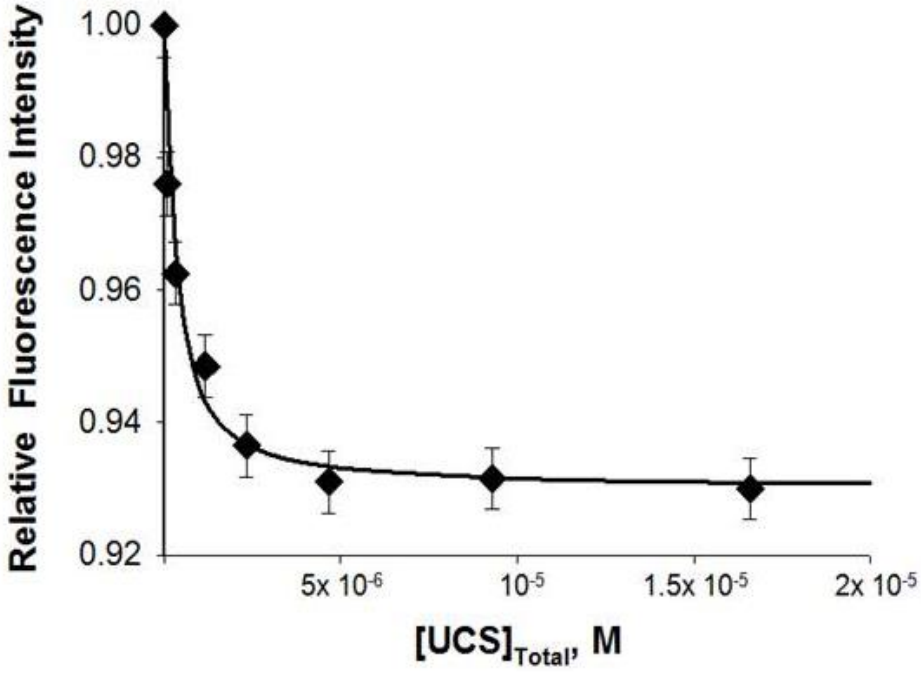

Figure III-9. Competition between the UCS and the Central domains for myosin. Titration of BADAN-S1 ($2.5x10^{-7}$ M) with the UCS domain in the presence of the Central domain ($3x10^{-6}$ M). Data show no competition between both domains. The solid line is the best-fit to the data yielding $K_1=(4.5 \pm 1.5) \times 10^6\ M^{-1}$ and $\Delta F_{max} = 0.930 \pm 0.005$. Adapted with permission from (115).

Figure III-9 shows the change of the relative fluorescence signal of BADAN-myosin S1 as a function of UCS concentration, in presence of the Central domain. The solid line is the nonlinear least squares fit of the titration curve to equation 5 which provides the affinity of UCS for myosin, $K_1 = (4.5 \pm 1.5) \times 10^6\ M^{-1}$ and $\Delta F_{max} = 0.930 \pm 0.005$. Both the binding constant and the maximum relative quenching of the labeled myosin fluorescence are, within experimental accuracy, the same as obtained in absence of the Central domain. Therefore, the data clearly demonstrate that the UCS domain and Central domain do not compete for binding site on myosin.

Allosteric interactions between the UCS and Central Domain in the UNC-45 chaperone

Having determined the intrinsic properties of the isolated domains and the intact chaperone, we can address the energetics of allosteric interactions between the domains in the intact chaperone using the general approach proposed by W. Jencks (119).

The determined free energy of the complex formation between the intact UNC-45 and myosin S1, ΔG_1, is defined as

$$\Delta G_1 = \Delta G_2 + \Delta G_3 - \Delta G_C \qquad (17)$$

where, ΔG_2 and ΔG_3 are intrinsic free energy changes accompanying the binding of the isolated UCS and central domains to the myosin S1, respectively. Therefore,

$$\Delta G_C = -\Delta G_1 + \Delta G_2 + \Delta G_3 \quad (18)$$

The additional intrinsic free energy change, ΔG_C, results from the allosteric conformational changes of the intact UNC-45 and the myosin S1, accompanying the complex formation. Because the values of ΔG_1, ΔG_2, and ΔG_3 are known, the value of ΔG_C can be readily determined. The obtained binding constants (see above) provide $\Delta G_C \approx 8$ kcal/mol. Thus, the data indicate that binding of the intact UNC-45 chaperone to the myosin S1 is accompanied by a significant conformational change of the formed complex, resulting in a dramatic decrease of the chaperone affinity for the myosin, as compared to the affinity of the two interacting domains of the protein.

The UCS domain acts as a chaperone and prevents myosin motor domain thermal aggregation

Chaperone activity of the UNC-45 is reflected in its ability to prevent the myosin aggregation. Myosin is known to aggregate around 43°C (22, 67). Thus, it was reported that aggregation of myosin motor domain at 43°C is prevented in presence of UNC-45 (23). We used dynamic light scattering to characterize effect of the UCS and Central domains on myosin motor domain aggregation. The dependence of the scattered light intensity of the myosin sample, containing BSA alone, upon time is shown in **Figure III-10**. In this control experiment, the strong increase of the scattered light intensity indicates the efficient formation of the myosin aggregates (23). On the other hand, the lack of the scattered light intensity increase in the

presence of the UCS domain (1 μM) alone clearly shows that the domain prevents aggregation of the myosin motor domain. This result is analogous to the effect of the presence of the intact UNC-45 on the time-dependence of the scattered light intensity of the myosin sample (**Figure II-10**). In other words, the UCS domain alone acts as a chaperone (**Figure III-10**).

The dependence of the scattered light intensity of the myosin sample, containing the Central domain alone, upon time is also shown in **Figure III-10**. The strong increase of the scattered light intensity clearly indicates the efficient formation of the myosin aggregates. Hence, although the Central domain binds to the myosin, it does not stabilize non-aggregated myosin, *i.e.*, it does not have the chaperone activity (**Figure III-10**). The results corroborate the findings discussed above that the UCS domain and the Central domain bind to different binding sites, *i.e.*, might differently affect the myosin structure. These data also suggest that despite the fact that the UCS domain and the Central domain are not energetically autonomous, they perform different biological function with regard to myosin.

The UCS domain prevents anomalous interactions of the unfolded motor domain with titin I27 domains

In chapter 2, we described the mechanical unfolding fingerprints of full-length myosin and myosin motor domain. These data showed that the myosin force extension curves exhibit two characteristic features.

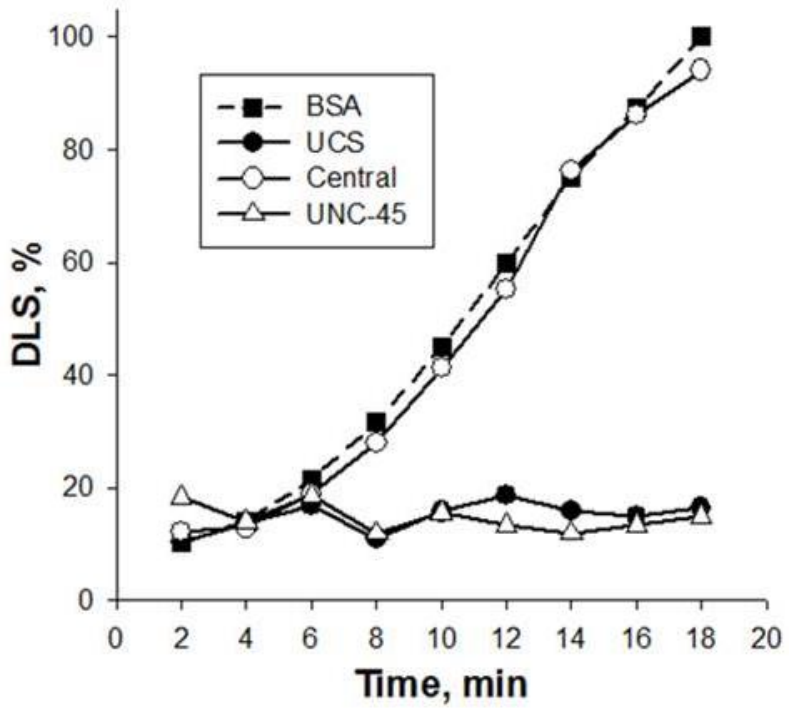

Figure III-10. The UCS but not the Central domain is sufficient to prevent aggregation of the myosin motor domain. Thermal aggregation of the myosin S1 (1μM) at 43°C measured by the dynamic light scattering intensity (532 nm) in presence of BSA (squares), UCS (filled circles), Central domain (open circles), and full length UNC-45 (triangles). The increase of the scattered light intensity is expressed as the percentile of its initial value at the zero time of the reaction. In all experiments, the concentration of each protein was 1 μM. Adapted with permission from (115).

A plateau at around 30 pN, which can be attributed to the rod domain and the poorly defined high force peak following the plateau. These data indicated that the motor domain does not unfold with a defined mechanical fingerprint (67) .

In this context, we have applied previously published titin reporter method to analyze the interactions between the UCS domain and the Central domain with myosin S1 (67). We synthesized chimeric proteins myosin S1-I27 and placed them on Ni^{2+}-charged NTA surface. These molecules were subjected to the repeated mechanical stretching using the AFM method. The pulling of the molecule was separated by 5 seconds time interval. The characteristic unfolding saw-tooth pattern of I27 titin domain is observed only during the initial stretching, as depicted in **Figure III-11A**. Clearly titin domains do not refold during the relaxation time, suggesting that they are affected by the presence of myosin motor domain. Moreover, the myosin motor domain does not refold spontaneously after denaturation and in absence of the chaperone protein.

However, the presence of the UNC-45 chaperone fully restores refolding of I27 domains. Therefore, AFM experiments assay revealed the UNC-45 chaperone activity. Using the same AFM assay, we wanted to elucidate which domain of UNC-45 is responsible for its chaperon like activity. As shown in **Figure III-11A**, the presence of the UCS domain fully restores the refolding of I27 domains.

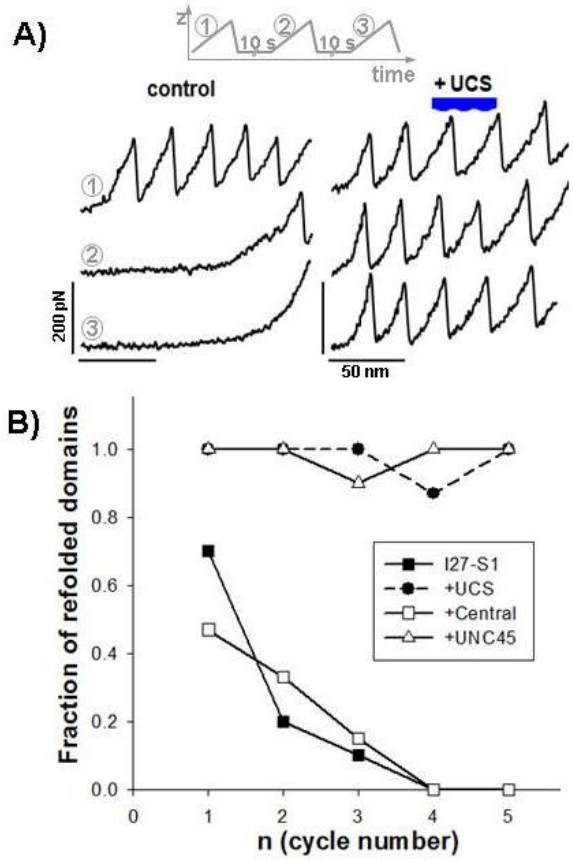

Figure III-11. The UCS but not the Central domain is sufficient to prevent misfolding of the myosin motor domain. A) Misfolding of the I27-S1 chimera is observed in the absence of the chaperone (left panel, control), whereas full recovery is observed in the presence of 1μM UCS domain (right panel). **B)** The dependence of the fraction of refolded I27 domains as a function of the number of refolding cycles. I27−S1 molecules in the absence of chaperone (filled squares), in the presence of 1μM Central domain (open squares), in the presence of 1μM full length UNC-45 chaperone (triangles), or in the presence of 1μM UCS domain (filled circles). Adapted with permission from (115).

The data strongly suggest that analogously to the intact UNC-45, the UCS domain inhibits aberrant interactions between the unfolded polypeptides within the myosin-I27 chimera, probably through interactions with the unfolded motor domain. Thus, the AFM assay enables us to observe refolding of titin I27 domains, which act here as molecular reporter (**Figure III-11A**). Consequently, AFM experiments assay revealed the chaperone activity of the UCS domain. It should be noted that the UCS domain does not affect the refolding efficiency of the I27 domain alone (data not shown). We have also found that proteins other than the UCS domain, such as bovine serum albumin, do not have an effect on the reversible induced unfolding/refolding of I27–S1.

The analysis of the AFM experiments showed that the UCS domain alone is as effective as the full-length UNC-45 chaperone in promoting the myosin refolding (**Figure III-11B**). The AFM results are in complete agreement with the light scattering experiments discussed above (**Figure III-10**), which showed that the UCS domain alone is sufficient to prevent aggregation of the myosin motor domain.

Actins gliding of the S1-I27 protein chimera reveal that the myosin motor domain in the construct preserves its functional activity

In order to address whether or not the myosin motor domain was functional in the myosin S1 – I27 protein chimera, we utilized the actin-gliding assay (116, 120). These experiments were performed in collaboration with Paul Nicholls from our laboratory. We used the modified motility assay developed by Sellers to investigate

the myosin capability to translocate actin. It allows tracking the translocation and sliding of actin filament by myosin bound to the surface of the coverslips cells. Movement of Alexa-594-phalloidin labeled actin filament is imaged, by monitoring the labeled protein fluorescence, using the Nikon TE2000 Eclipse microscope. In our modification of the assay, we have functionalized flow cells with Ni-NTA. The chimera protein S1-I27 is immobilized on the flow cell surface *via* Ni-NTA-His_6tag interactions. That creates a layer of myosin molecules that are capable of binding and translocating actin filaments. The translocation process is followed in the fluorescence microscope.

Figure III-12A shows two examples of movement of selected actin filaments. As a control, the experiment with denatured at 43^0C motor domain has also been performed, indicating the loss of actin translocating capacity by the denatured myosin (data not shown). **Figure III-12B** shows that comparison between the velocities of actin translocation performed by S1-I27 chimera protein and the denatured myosin. It is clear that the chimera-contained myosin has a significantly greater ability to translocate actin than the denatured protein. The experiments clearly indicate that the myosin motor domain as a part of the chimera construct is folded into its native state and can perform its main function, *i.e.*, binding and translocating actin. Moreover, the myosin capability to translocate actin was restored by addition of another chaperone, Hsp90(93). The inhibition by UNC-45 might be essential during the sarcomere development by preventing myosin power strokes from disrupting the precise alignment of the sarcomere until its formation is completed.

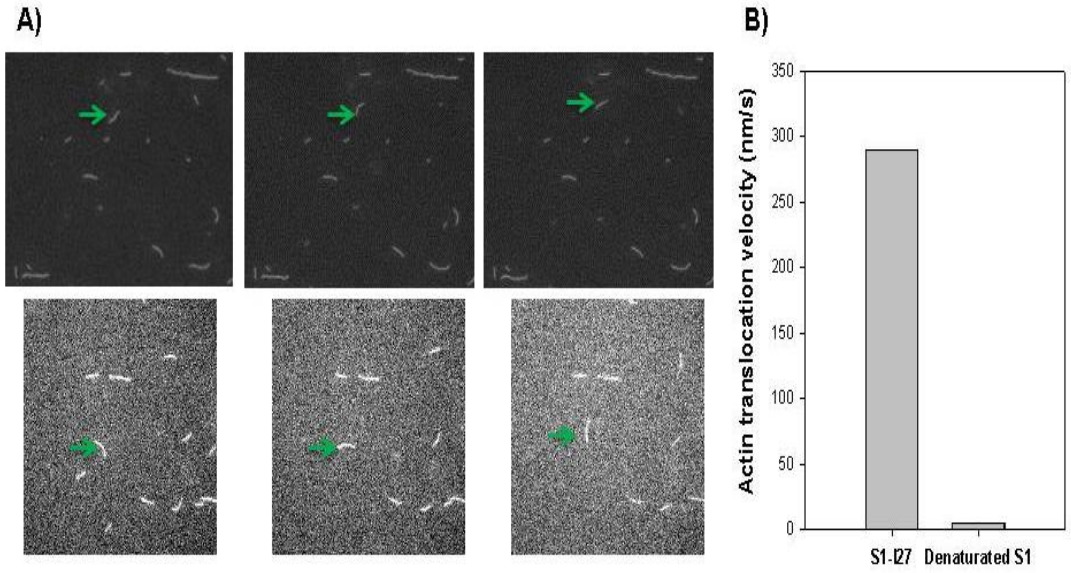

Figure III-12. The myosin motor domain in the I27-S1 chimera is functional and can translocate actin filaments. A) Photographs of the microscope images of two examples of actin gliding images (green arrow). The chimera protein displaces the selected actin molecules. The movement of the actin filaments clearly shows that the myosin motor domain within the chimera construct is capable of binding and translocating actin filaments. **B)** Comparison of actin translocation velocity of the native I27-S1 and heat denatured I27-S1. The native I27-myosin chimera translocates actin with velocity v= 0.29 (±0.0161) microns/s. The recorded velocity of the actin filament in the presence of the denatured myosin is within the experimental error of the measurement. Adapted with permission from (115).

CONCLUSIONS

Our studies revealed that the UNC-45 is a unique chaperone. It is built of three domains with clearly defined different functions. The UCS domain binds to myosin heads stabilize them and prevents their aggregation, as revealed by light scattering data. Thus, it can alone perform the chaperone functions. On the other hand, the Central domain also interacts with myosin but both thermal aggregation assay and AFM experiments showed that it does not exhibit chaperone activities. Moreover, the third domain, TPR, does not bind to the client protein but interacts with another chaperone Hsp90, which plausibly function as a co-chaperone in that system.

We have demonstrated that the myosin motor domain possesses two binding sites, which engage two different domains of the UNC-45 chaperone. In other words, the UCS domain and the Central domain bind to different binding sites on myosin (**Figure III-14**). The results suggest different roles of both domains in the myosin-UNC-45 complex. Our data show that affinities of myosin S1 - UNC-45, S1 - UCS domain, and S1 - Central domain complexes are $(2.8 \pm 0.8) \times 10^6\ M^{-1}$, $(4.3 \pm 1.5) \times 10^6\ M^{-1}$, and $(6 \pm 1.5) \times 10^5\ M^{-1}$. Interestingly, the UCS domain binds to myosin stronger than the full-length UNC-45. Moreover, the affinity of UNC-45 to myosin is not a simple sum of its domains affinity to myosin. That implies existence of allosteric interactions between UNC-45 domains in the complex with myosin. We have determined that intrinsic free energy change that is a result of the allosteric conformational changes is, $\Delta G_C \approx 8$ kcal/mol.

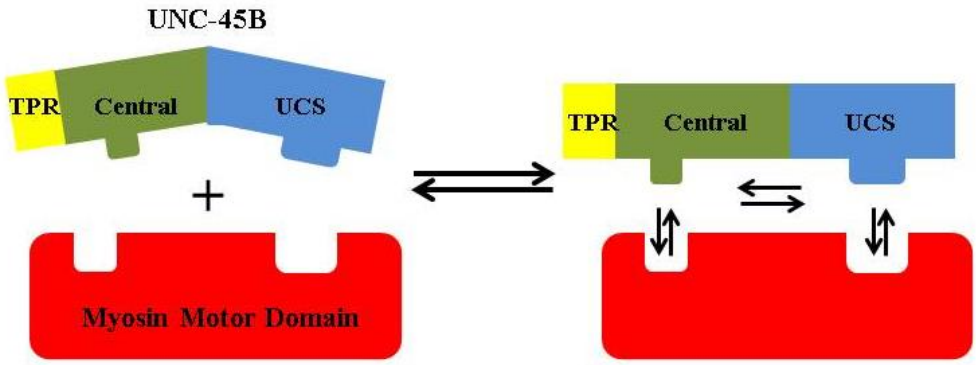

.

Figure III-13. Schematic model for the UNC-45 - Myosin Motor Domain Complex Formation. Each UNC-45 domain engages different binding sub-sites on the myosin client protein. The formation of the UNC-45 - motor domain complex is accompanied by allosteric conformational transitions. Adapted with permission from (115).

The significant energetic penalty of engagement of two UNC-45 domains with myosin indicates the occurrence of large conformational changes in the proteins in the myosin-UNC-45 complex. In other words, the UCS domain and the Central domain are not thermodynamically autonomous and that they induce the conformational changes in the myosin-UNC-45 complex that decrease the chaperone affinity for the myosin, as compared to the affinity of the two interacting domains alone.

The results obtained using the dynamic light scattering and single molecule AFM pulling experiments indicate that the UCS domain alone is responsible for chaperone-like activity of UNC-45. Interestingly, although we established that the Central domain binds to myosin S1, the domain does not possess chaperone properties. Notice, the allosteric interactions between the UCS domain and the Central domain, which weakens the full-length UNC-45 affinity for myosin, do not seem to be critical for chaperone properties localized in the UCS domain. Nevertheless, our results indicate that the Central domain is always involved in the UNC-45 interactions with myosin, suggesting a different function of the Central domain than the UCS domain. Indeed, the actin gliding experiments showed that the Central domain plays a critical role during myosin power stroke (Oberhauser et al., unpublished data). Thus, the data suggest that the domain can inhibit myosin translocation of actin and most likely allowing the UCS domain to perform its chaperone action on myosin without any disturbances.

Chapter 4

Physiologically relevant temperature induces structural changes within the chaperone domain of UNC-45 that may allow it to act as a thermosensor

Modified from:

FEBS Letters 589 (2015) 123–130

ELSEVIER

FEBS Letters

journal homepage: www.FEBSLetters.org

Thermally-induced structural changes in an armadillo repeat protein suggest a novel thermosensor mechanism in a molecular chaperone

Paul J. Bujalowski[a,b,1], Paul Nicholls[a,b,1], José M. Barral[a,b,c,*], Andres F. Oberhauser[a,b,c,*]

[a] Department of Neuroscience and Cell Biology, University of Texas Medical Branch, Galveston, TX 77555, USA
[b] Department of Biochemistry Molecular Biology, University of Texas Medical Branch, Galveston, TX 77555, USA
[c] Sealy Center for Structural Biology and Molecular Biophysics, University of Texas Medical Branch, Galveston, TX 77555, USA

INTRODUCTION

As we discussed above, the UNC-45 chaperone belongs to the UCS protein family (112, 121). The protein exists in two isoforms known as UNC-45A (general cell) and UNC-45B (striated muscle)(29). UNC-45 chaperone is built of three domains: the UCS domain, the Central domain and the TPR domain (**Figure IV-1**)(22). In *in vivo* experiments, UNC-45 was identified as a critical factor involved in the sarcomere assembly (21). Subsequent biochemical experiments showed that UNC-45 could suppress the thermal aggregation of myosin (23, 67). This ability reveals the UNC-45 chaperone activities. Furthermore, the structural and solution studies imply that UNC-45 forms a scaffold, which helps to organized action of other chaperones involved in the myosin folding process, such as Hsp90 and Hsp70 proteins. The crystal structure of UNC-45 has been determined up to 2.9 Å resolution (33).

The UCS domain has been the most studied domain of UNC-45 since it is structurally the most conserved and its domain homologues have been found in many other proteins belonging to fungi and metazoa kingdoms (22). Moreover, UCS was identified as the myosin-binding domain (23, 67). Furthermore, other members of the UCS protein family were shown to be functionally linked to many classes of myosins (121). While eukaryotic UCS domains are critical for structural folding of myosin I, II, and V (20, 24, 26, 30), the yeast homologues are required for proper function of already folded myosin II (24).

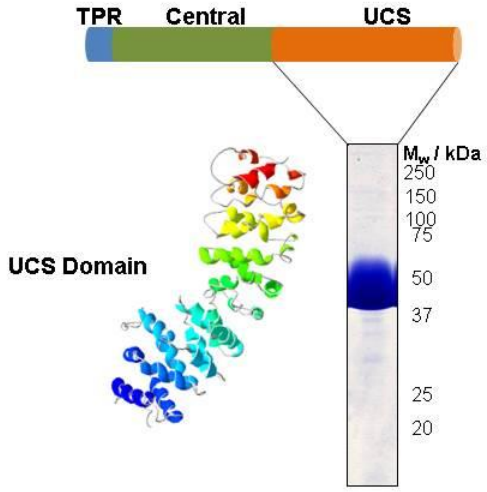

Figure IV-1. Schematic domain Structure of the UNC-45 chaperone and the crystal structure of its UCS domain. UNC-45 is built of three domains: The UCS domain, the Central domain and the TPR domain. The UCS domain predominantly has the α-helical secondary structure, which is organized into armadillo repeats. The x-ray crystal structure shown in the panel (4i2z.pdb) is adapted from Gazda et al (2013). The UCS domain near homogenous purity was confirmed by SDS-PAGE gel. Adapted with permission from (122).

The chaperone activities of the UCS domain have been identified using variety of different techniques ranging from thermal aggregation assays to single molecule atomic force spectroscopy (67) (Chapter 3). Furthermore, these findings are supported by the results of *in vivo* studies, which showed that UCS domain can partially rescue the motility defect in thermally sensitive e286 worms (123).

Chaperones have been discovered as factors that help protein folding process. However, they are also part of the protein quality control system thus they play critical role in maintaining protein homeostasis (124). Every organism must survive a variety of stressful conditions, including rapid temperature increases that can damage cellular structures and cause misfolding of cellular proteins. Considering myosin function one must take into account the harsh environment inside sarcomere. There, proteins can be constantly affected by chemical, thermal or mechanical stress. Thus, maintaining protein homeostasis is a serious challenge. Therefore, it should be of no surprise that as a response to stress, cells develop a system of heat stress proteins that are activated under these conditions. For example the Hsp70 chaperone has been identified to be involved not only during development of sarcomere but later on as well, where it protects proteins from stress inflicted by environmental conditions.

Crucial *in vivo* experiments shedding light on UNC-45 mechanism of action were performed in *Dario rerio* model organism (58). They revealed that the UNC-45 localization in sarcomere might depend on stress conditions and showed that chaperone is migrating in the response to the environmental pressure. Although during muscle development UNC-45 is localized near the A-band (sarcomere center), later it is shuttled to the Z-line (sarcomere periphery). The studies indicated that during sarcomere

assembly, UNC-45 is present in close proximity of its client protein, myosin. After formation of the sarcomere is completed, the chaperone presence is no longer needed and it migrates to the ends of sarcomere. However, when thermal or chemical stress is applied, UNC-45 is shuttled back from the Z-line to the A-band. These results indicate that the chaperone is not only needed during assembly process but also plays a critical role in maintaining protein homeostasis in sarcomere (58). In other words, UNC-45, in addition to being necessary factor during myosin folding process, is also required later on during stress conditions, when it helps in the refolding of the damage myosin. Moreover, the data also implies that UNC-45 undergoes some transitions under heat stress. The migration from Z-line to A-band under increased temperatures suggests a decreased affinity towards the Z-line complemented with an increased affinity for its client protein. The results strongly suggest that the temperature could control the function of the UNC-45 chaperone.

During the recent decade significant progress has been made in understanding the effects of the environmental stress on the molecular chaperones activities. This may be of general importance for any chaperone, including UNC-45. For example, recent studies revealed that the Hsp26 chaperone is activated by the temperature increase, which also affects the protein structure (56, 125, 126). These environmental changes induce structural rearrangements within the middle domain of the protein, which triggers the switch from the chaperone-inactive to chaperone-active state. Another protein that undergoes thermally induced structural changes is Hsp22 (127). In this case it was shown that even the secondary structure of the protein is significantly affected by the temperature increase. Inducing the thermal stress results in significant reductions of the

α-helical and β-sheets content and is accompanied by the increase of intrinsically disordered structure within some regions of the chaperone molecule (127). The disordered regions of protein might be critical for chaperone activities. In addition to temperature, the chemical stress can also affect chaperones structure as shown in a recent study done with Hsp33 (57). Oxidative stress catalyzes the oxidation of disulphide bonds which induce structural changes within the protein. This state is characterized by existence of intrinsically disordered regions which seems to be essential for the recognition of targeted folding intermediates. The process is reversed by the reduction of disulphide bonds, which ends in releasing the substrate and in an altered conformation of Hsp33 (57).

The UNC-45 chaperone is built of armadillo repeat motifs (ARM) where each motif is composed of 42 amino acids with high degree of residual variability (32, 33). Each repeat forms 3 helices which are arranged into a superhelical structure. Studies of proteins containing ARM show that they bind to wide variety of clients. Moreover, the nature of the interactions can range from electrostatic to hydrophobic. Additionally, mechanistic studies of the protein structures imply that the intrinsic flexibility of proteins with the ARM seems to play a significant role in discriminating between substrates (128). Computational simulations performed on structurally similar HEAT repeat proteins (both ARM and HEAT class of proteins belonging to α-solenoid protein group) revealed the high flexibility of the protein, even within the hydrophobic core, while the general solenoid structure remained undisrupted (129).

Although, ARM three-dimensional structures are very similar, they differ significantly with regard to amino acids sequences and physical properties. Moreover,

these features seem to be correlated with localization within the protein. The ARM helices that form the core of the protein are hydrophobic, while the helices localized at the ends of the macromolecule (capping regions) possess both hydrophobic residues and hydrophilic residues. Interestingly, the modification of the residues within the capping regions can change the properties of the ARM proteins. For example, the mutations can enhance thermal stability and provide protection from harmful factors such as chemical denaturants (130).

MATERIALS AND METHODS

Protein Expression and Purification

The UCS domain was obtained as described in chapter 3. The purity of the domain was confirmed by SDS-PAGE and was greater than 95% (**Figure IV-1**).

ANS Fluorescence

The UCS domain (1μM) was equilibrated with 8-anilino-1-naphthalenesulfonic acid (ANS) (10μM) in PBS buffer. The solution was heated at 1K/min in a quartz cuvette. All experiments were performed using Fluorolog fluorescence spectrometer (Horiba Jobin Yvon, Kyoto, Japan) equipped with a 40W temperature controller (Wavelength Electronics, Bozeman, MT). The samples were exited at 370 nm and emission spectra were collected in range of 400-600 nm at various temperatures. As a control we performed experiments at the same temperatures but with 10μM ANS in PBS but in

absence of the UCS domain. The final spectra were obtained by subtraction of the control spectra (ANS alone) from the spectra recorded in presence of the UCS domain.

Circular Dichroism

The far UV CD spectra of the UCS domain were recorded using a Jasco J-815 Spectrometer. The protein was equilibrated (1 μM) in 30 mM phosphate pH 7.4, 100 mM KCl, 1 mM $MgCl_2$, 1mM TCEP buffer. The cuvette was heated slowly at 1K/min and the ellipticity at 222nm was recorded at 1K temperature increase. The cuvette with 0.1 cm path length was used.

Limited Pulsed Proteolysis

The UCS domain (1μM) was mixed with 1μM L-1-Tosylamide-2-phenylethyl chloromethyl ketone (TPCK) treated trypsin (Worthington Biochemicals, Lakewood, NJ). The solution was incubated at different temperatures for 60 seconds (**Figure IV-4**). The reaction was quenched by addition of SDS-PAGE sample buffer and boiling for 5 mins. The products of proteolysis reaction was examined by SDS-PAGE and staining the gels with Coomassie blue. The intensity of the bands was analyzed using lane densitometry using ImageJ (NIH, Bethesda, MD).

Limited Trypsin Proteolysis and Mass Spectroscopy

The UCS domain (1μM) was mixed and incubated with trypsin in 1:10 000 ratios at 37°C. The reaction was rapidly quenched with SDS-PAGE sample after appropriate time intervals ranging from 0 to 30 minutes (**Figure IV-8**). Samples were then quenched with of SDS-PAGE sample buffer and boiled for 10 minutes. The reaction products were analyzed by SDS-PAGE stained with Coomassie blue. Easily identifiable bands were cut from the gel and analyzed by MALDI-TOF-TOF mass spectroscopy using an Applied Biosystems 4700 Proteomics Analyzer (Life Technologies, Carlsbad, CA). Peptides that were recognized as significant by Mascot analysis with a p value < 0.05 were used to examine the content of the bands. Combination of availability of trypsin digestible sequences in loops and MS data allowed the estimation of probable digest sites. High-resolution gel images were obtained by using a tricine gel system and silver stained (131) (**Figure IV-8**).

RESULTS

In chapter 3, we have shown that the UCS domain is responsible for chaperone properties of the UNC-45 chaperone *e.g.* preventing aggregation of the client protein (67) (Chapter 3). However, the detailed mechanism of the UCS domain action remains uncharacterized. Chemical nature of the chaperone interaction with the client proteins and localization of binding site on the UCS domain are unknown. Analysis of electrostatic surface potential and qualitative assessment of its surface polarity based on the crystal structure of UNC-45 *Drosophila melanogaster* demonstrated that 17-21 ARM helices form a nonpolar groove (32). Therefore, it was suggested that this region is responsible

for interactions with client proteins (32). Nevertheless, docking simulations suggested that electrostatic interaction also play a role in stabilization of the UNC-45 - myosin complex (132). In this context, protein-binding sites in small heat shock proteins have been proposed to become available after conformational changes within the chaperones macromolecule. It was suggested that these rearrangements are induced by environmental stress (56). These experiments triggered the idea that thermal stress may not only cause migration of UNC-45 into close proximity of myosin, but also might induce a conformational change in the chaperone, which plays a critical role for its function. The myosin easily aggregates in higher temperatures (chapter 3). Since the most probable mechanism of aggregation involves appearance of hydrophobic loops, the UNC-45 mechanism might include the unrevealing of the hydrophobic areas of the protein, in response to the temperature stress.

Therefore, we decided to investigate the appearance of hydrophobic surfaces of the UCS domain, *i.e.*, the domain predominantly responsible for the chaperone activity of UNC-45. In order to address the issue, we have utilized the ANS fluorescence probe. The dye is a common and standard reagent used to examine the hydrophobic patches on proteins (133). The fluorescence intensity of ANS is well known to undergo a large increase as a result of placing the dye in the hydrophobic environment, due to the decrease of the solvent quenching processes.

As an example, in our standard experiments, we have mixed 10 μM ANS with 1 μM of the purified UCS domain. The sample was equilibrated at room temperature until a stable fluorescence intensity of the dye was recorded. The solution was then heated to the following temperatures 25°C, 37°C and 41.5°C. At each temperature, the fluorescence

emissions spectra of the sample were recorded. Analogous spectra were recorded for the sample containing ANS alone and subtracted from the spectra of the mixture with UCS. In the presence of the UCS domain, the increase of the temperature induced a large increase of the ANS fluorescence intensity, as depicted by the corresponding emission spectra in **Figure IV-2**. The effect of the temperature on the ANS fluorescence alone was negligible and within experimental accuracy of the measurement. It is evident that the increase of the fluorescence signal originates from the ANS molecules binding to the protein. Furthermore, our results show that the ANS spectra are shifted towards the shorter wavelength values (blue shift) which a characteristic effect of the ANS binding to hydrophobic surfaces (**Figure IV-2**). In the examined temperature range, the ANS fluorescence intensity increases three times at 37°C and six times at 41.5°C, as compared to the fluorescence intensity of the sample at 25°C (**Figure IV-2**). These data indicate that the temperature increase induces the appearance of hydrophobic areas of the UCS domain, previously inaccessible to the ANS binding. In other words, the enhancement of temperature induces a structural rearrangement within the UCS domain.

To further investigate the correlation between temperature and conformational changes of the UCS domain, we examined the entire series of the different temperatures on the fluorescence of ANS - UCS sample. 10 μM ANS was mixed with 1 μM of the UCS domain and the fluorescence signal was recorded within the temperature range from 20°C to 45°C, with the excitation wavelength set at 370 nm and emission at 470 nm.

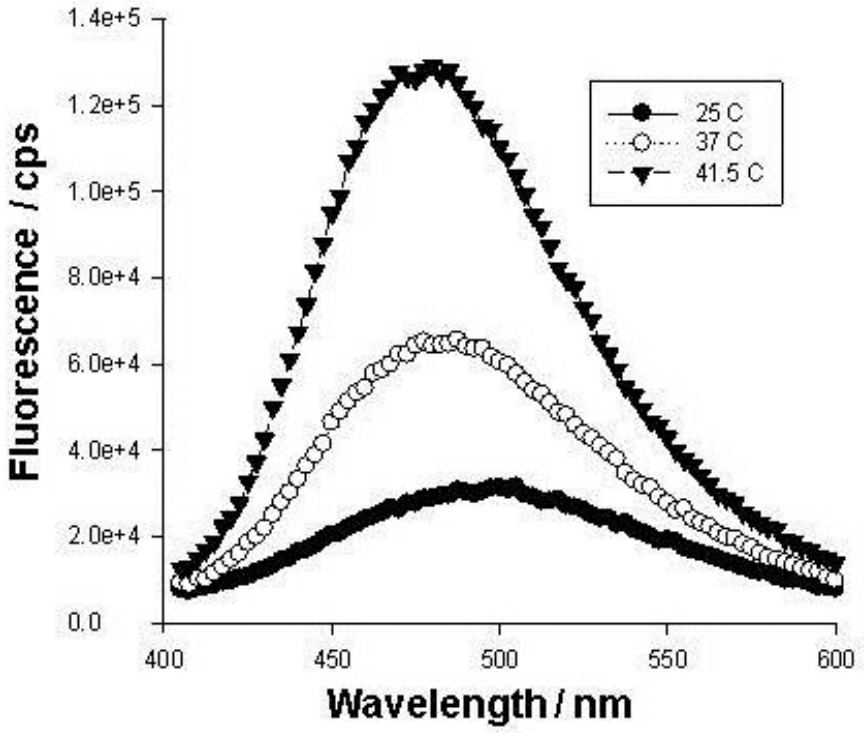

Figure IV-2. The increase of the ANS fluorescence intensity reveals greater solvent accessibility of hydrophobic regions at physiological temperatures. The recorded fluorescence intensity spectra of the sample containing ANS (10μM) and the UCS domain (1μM) at three different temperatures: 25°C (the black circles), 37°C (open circles) and 41.5°C (triangles). Adapted with permission from (122).

The dependence of the sample fluorescence as a function of the temperature is depicted in **Figure IV-3**. The data show that after initial plateau, the fluorescence intensity strongly increases between 35°C to 42°C. Above ~42°C, the signal reaches the next plateau (**Figure IV-3**). Clearly, at temperatures above ~35°C, the UCS domain undergoes a dramatic conformational change, which is saturated at ~42°C. Notice that the structural rearrangements of chaperone domain occur at physiological temperature level. The dramatic conformational shift occurs between the temperature of the resting muscle (35°C), and the temperature of the muscle during the extensive exercises that can reach 41°C (134). Observe also that similar temperature of ~41°C is reached in the case of high fiver in humans. Thus, the temperature stress around 41°C is a very likely circumstance in nature.

When the temperature reaches elevated values, it becomes dangerous for the protein stability in cell (124). Our data shows that exactly at these harmful conditions, the deeply buried hydrophobic areas of the chaperone domain of UNC-45 become accessible to the solvent. Thus, the protein can interact with and stabilize any appearing regions of myosin heads, which due to the high temperature became unstable and prone to misfolding. The reported thermosensor properties of the UCS domain seem to be critical to prevent the myosin aggregation. We would like to point out that our data shows that UCS domain undergoes precisely the kind of structural changes that helps the domain to perform its chaperone functions.

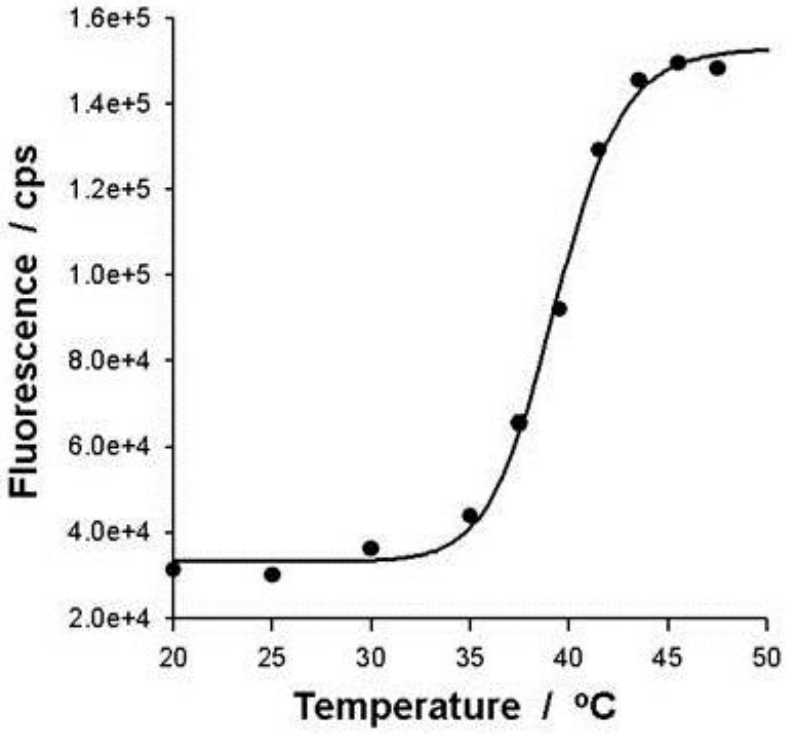

Figure IV-3. Thermally induced structural rearrangements within the UCS domain monitored by changes in ANS fluorescence intensity. The fluorescence intensity of the sample containing ANS (10μM) and UCS domain (1μM) is increasing in temperature above 37°C (excitation 370 nm, emission 470 nm). The intensity of ANS fluorescence signal reaches plateau around 42°C. Each dot represents an average of three measurements performed at a given temperature. The solid line is the nonlinear least squares fit of the data to the single temperature-induced conformational transition model (Equation IV-2, see below in the thermodynamic analysis of the UCS domain structural transitions section). Adapted with permission from (122).

Exposure of deeply buried loops in the UCS domain examined using the trypsin digestion pulse assay

Trypsin is a very potent protease that cleaves peptide bond. Trypsin digestion assays have been widely used to detect the existence of protein domains in the tertiary structure and occurrence of conformational transitions induced by examined interactions. In this context, the enzyme is also applied to reveal existence of solvent accessible loops that are disordered or the clearly defined secondary structures. Since our ANS fluorescence data indicate that the UCS domain undergoes a significant temperature-induced structural transition, we have addressed the UCS conformational transition using the trypsin digestion pulse method in the analogous temperature range (~20°C to ~43°C). The method is specifically adjusted to examine equilibrium conformational changes of a protein by using a very high concentration of the protease and very limited time of the digestion reaction (135). In these conditions, any available loops containing the cleavage sites are instantaneously and catalytically cleaved. In other words, protease accessibility of targeted loops is the determining factor of the reaction and the effect of temperature on trypsin activity can be neglected. The method is analogous to the nucleic acid foot-printing technique used to determine nucleic acid conformational transitions, formation of the equilibrium complexes with a ligand, and mapping the location of the ligand-binding site.

In our standard assay, we used a modified version of the assay where concentrations of the 1μM UCS domain and 1μM trypsin, respectively (135). Trypsin and the UCS domain (1:1 molar ratio) have been incubated for one minute followed by quenching of the reaction with SDS-PAGE sample buffer. Subsequently, the products of the reaction were analyzed using the SDS-PAGE gel as depicted in **Figure IV-4**. As a control, testing different trypsin concentration and digestion time provide the same pattern of the cleavage reaction (data not shown). The plot in **Figure IV-4** showed very low extent of the digestion of the UCS domain at lower temperatures. As the temperature increases above ~30°C, the extent of the digestion strongly increases reaching the plateau at ~37°C, where the intact UCS domain becomes undetectable. Clearly, loops which are inaccessible at lower temperatures become available for the trypsin cleavage above ~27°C. The cleavage reaction reaches plateau above ~37°C indicating the saturation of the temperature-induced conformational transition, which induces the exposure of the protein loops. Notice, that the conformational transition, as recoded using the trypsin digestion pulse assay, occurs in the lower temperature range than the structural change recorded using the ANS fluorescence assay (**Figure IV-3** and **Figure IV-4**). Nevertheless, the data corroborate ANS fluorescence experiments that the UCS domain undergoes complex temperature-induced structural transitions.

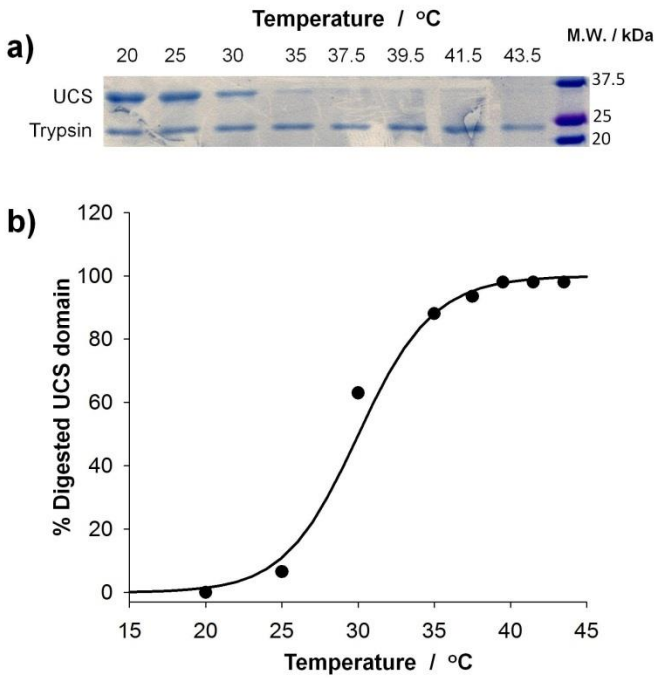

Figure IV-4. The temperature-induced conformational transition of the UCS domain as recorded by the trypsin digestion pulse assay. A) The SDS-Page gel of limited pulsed proteolysis of the UCS domain by trypsin mixed at 1:1 molar ratio (1 μM : 1 μM), recorded at the specified temperatures. The digestion reaction was quenched after one-minute incubation by the addition of the SDS-Page sample buffer. **B)** The dependence of the percentage of the digested UCS domain determined by lane densitometry in ImageJ program as a function of the temperature. The solid line is the nonlinear least squares fit of the experimental data to equation A-1 in Appendix 1. Adapted with permission from (122).

.

The chaperone secondary structure is preserved under thermal stress

Two independent techniques (ANS fluorescence and limited trypsin digestion) showed that the UCS domain undergoes complex conformational transitions as a result of thermal stress in the physiological temperature range. We decided to investigate structural nature of these changes. In other words, we decided to determine to what extent the temperature affects the secondary structure of protein. We tackle this problem using far- UV circular dichroism spectroscopy. The circular dichroism spectrum of the UCS domain is shown in **Figure IV-5**. The data indicate that α-helical structure constitutes a predominant part of the UCS domain secondary structure, as also evident in the protein crystal (**Figure IV-5**) (33). The obtained mean residue ellipticity spectrum is characterized by typical negative minima values at 208 nm and 222 nm (chapter 3).

The dependence of the mean residue ellipticity at 222 nm of the UCS domain upon the temperature is shown in **Figure IV-6**. Within experimental accuracy, the mean residue ellipticity remains unchanged in the physiological level of temperature (up to ~43°C). The melting process of the UCS secondary structure begins at around 45°C and it is completed when temperature reaches 50°C (**Figure IV-6**). Since the observed secondary structure transition occurs in significantly higher temperatures than conformational changes reported in the ANS fluorescence and the limited trypsin digestion pulse experiments, it is very likely that they are not responsible for availability of hydrophobic residues and disordered loops.

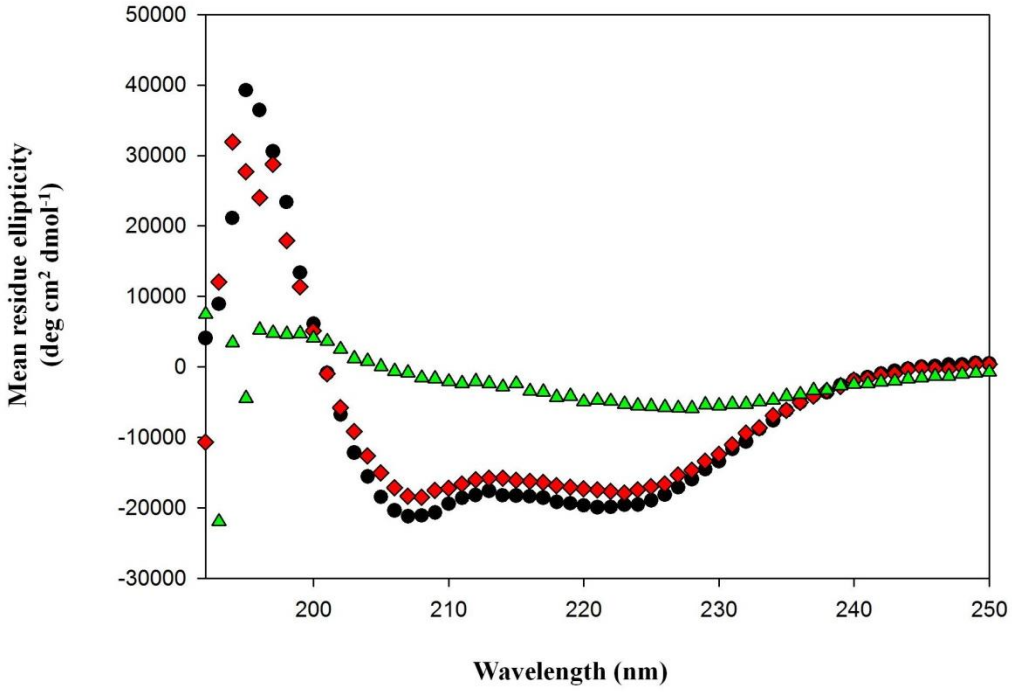

Figure IV-5. Far-UV CD spectrum of the UCS domain at 30, 40 and 50°C. The superimposed spectra of the UCS domain show that the α-helical secondary structure is preserved at 30 (black circles) and 40°C (red diamonds), but it is lost at 50°C (green triangles). Adapted with permission from (122).

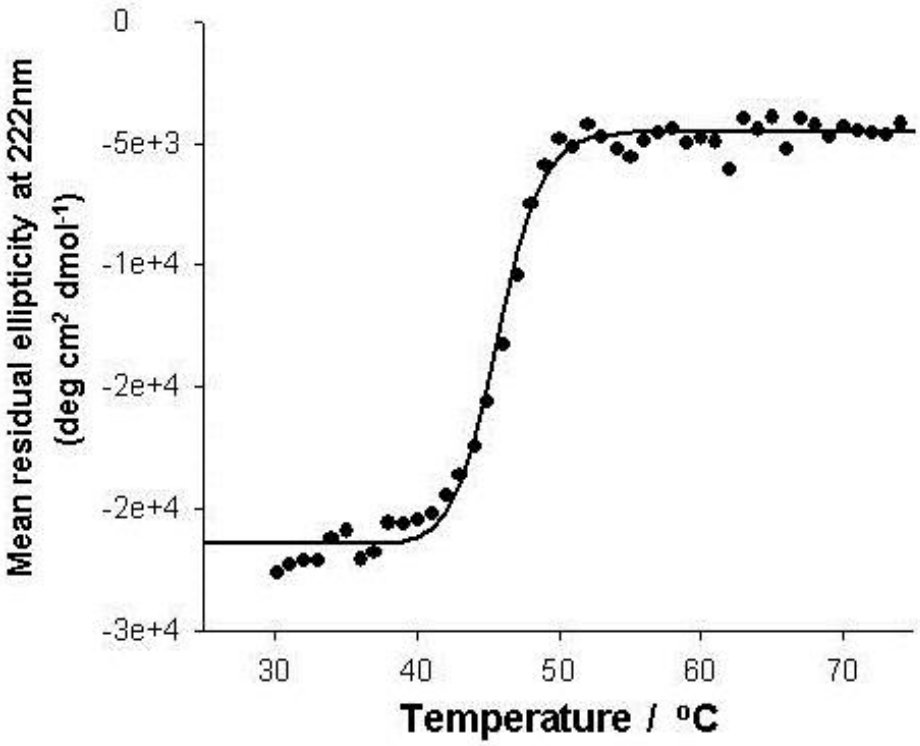

Figure IV-6. The dependence of the mean residue ellipticity of the UCS domain at 222 nm upon the temperature of the sample. The UCS domain (1 μM) was heated at 1K/minute rate and changes in the mean residue ellipticity at 222nm were recorded at different temperatures. The solid line is a nonlinear least squares fit of the experimental data to equation IV-2 (see below). The melting temperature of the transition, $T_m = 46^oC$. Adapted with permission from (122).

In other words, the data indicate that the secondary structure of the UCS domain remains intact in physiological temperatures, below 43°C. Therefore, the structural changes observed by ANS fluorescence and trypsin digestion experiments are outcomes of disruption of tertiary protein structure.

Thermodynamic analysis of the UCS domain structural transitions

The results of experiments described above imply that the UCS domain undergoes at least three conformational transitions under thermal stress. However, the transition in the lowest temperature range has been detected using a chemical reaction (trypsin digestion), while the remaining two transitions do not include any breaking of covalent bonds, *i.e.*, no new products are formed. Moreover, the separation of the conformational changes on the temperature scale, allows us to treat each transition independently (see below). In this context, we choose the most conservative approach and address only the two transitions that in their detection do not involved destruction of the covalent bonds of the protein substrate. For completeness, the analysis of all three transitions, also treated as a sequential reaction system, is described in Appendix 1.

The sigmoidal character of the UCS conformational transition recorded using the ANS fluorescence indicates that the simplest thermodynamic model of the structural change includes transformation between two states of the macromolecule, as

$$S_1 \Leftrightarrow S_2 \qquad \text{(IV-1)}$$

The dependence of the ANS emission intensity, ΔF_{obs}, is then described by equation IV-2, as

$$\Delta F_{obs} = \frac{1}{1+\exp((-\Delta H_{12} + T\Delta S_{12})/RT)} + \Delta F_{max}\left(\frac{[\exp((-\Delta H_{12} + T\Delta S_{12})/RT)]}{1+\exp((-\Delta H_{12} + T\Delta S_{12})/RT)}\right)$$

(IV-2)

where, ΔH_{12} and ΔS_{12}, are enthalpy and entropy changes characterizing the observed conformational transformation, R is the gas constant, and T is the temperature.

For easy comparison between different transitions, we have normalized the above equation, expressing the observed signal as a fraction of the total signal change, defined as

$$F_{Norm} = \frac{F_{obs}}{F_{max}} \qquad \text{(IV-3)}$$

where ΔF_{obs} is defined by equation IV-2. The solid red line in **Figure IV-7** is the nonlinear least squares fit of equation IV-3 to the experimental data yielding ΔH_{12} = 120 ± 40 kcal/mol and a change in entropy of ΔS_{12} = 390 ± 90 cal/mol K.

The next conformational transition occurs at higher temperature range and involves the melting of the protein secondary structure, as monitored by circular dichroism (expressed as mean residue ellipticity). Once again, the sigmoidal character of the transition indicates that the simplest thermodynamic model includes transformation between two states of the macromolecule, as

$$S_2 \Leftrightarrow S_1 \quad \text{(IV-4)}$$

The dependence of the mean residue molar ellipticity of UCS as a function of temperature is then described by equation analogous to equation IV-2, as

$$\Delta\Theta_{obs} = \frac{1}{1+\exp((-\Delta H_{23} + T\Delta S_{23})/RT)} + \Delta\Theta_{max}\left(\frac{[\exp((-\Delta H_{23} + T\Delta S_{23})/RT)]}{1+\exp((-\Delta H_{23} + T\Delta S_{23})/RT)}\right)$$

(IV-5)

where, ΔH_{32} and ΔS_{32}, are enthalpy and entropy changes characterizing the observed conformational transformation. The normalized mean residue molar ellipticity change is defined as

$$\Theta_{Norm} = \frac{\Theta_{obs}}{\Theta_{max}} \quad \text{(IV-6)}$$

The solid blue line in **Figure IV-7** is the nonlinear least squares fit of equation IV-6 to the experimental data yielding ΔH_{32} = 130 ± 40 kcal/mol and a change in entropy of ΔS_{32} = 410 ± 90 cal/mol K.

The enthalpy and entropy changes characterizing the melting of the protein secondary, as monitored using circular dichroism, are within the expected values for similar size proteins. For instance, other armadillo repeat proteins, which were examined by other groups, have similar, secondary structure melting temperatures, *i.e.*, the temperature at the mid-point of the conformational transition. Thus, the UCS domain

secondary structure melting curve has T_m = ~46°C, other armadillo repeat proteins such as α-importin has reported T_m of ~43°C (136).

On the other hand, the determined values of enthalpy and entropy changes for the transition, monitored using the ANS fluorescence may seem surprisingly large. Recall, this conformational change occurs *prior* to the secondary structure melting of the UCS domain (**Figure IV-3** and **Figure IV-6**). Nevertheless, ANS emission records the appearance of the protein hydrophobic areas (see above). Without disrupting the protein secondary structure, such a transformation would require a significant rearrangement of the protein tertiary structure, as indicated by the large enthalpy change. The observed large entropy of the transition suggests that the entire protein structure becomes more dynamic (more flexible, less ordered), as a result of the conformational transformation. Such flexibility could be crucial for the chaperone domain in adjusting to the structural requirements of the protein client.

The approximate topology of the active conformation of the molecular chaperone analyzed by trypsin digestion assay and mass spectroscopy

Our trypsin digestion pulse experiments (Figure IV-4) strongly suggested that increase of the temperature induces structural arrangements of the UCS, which make the protein loops available to the enzyme reaction.

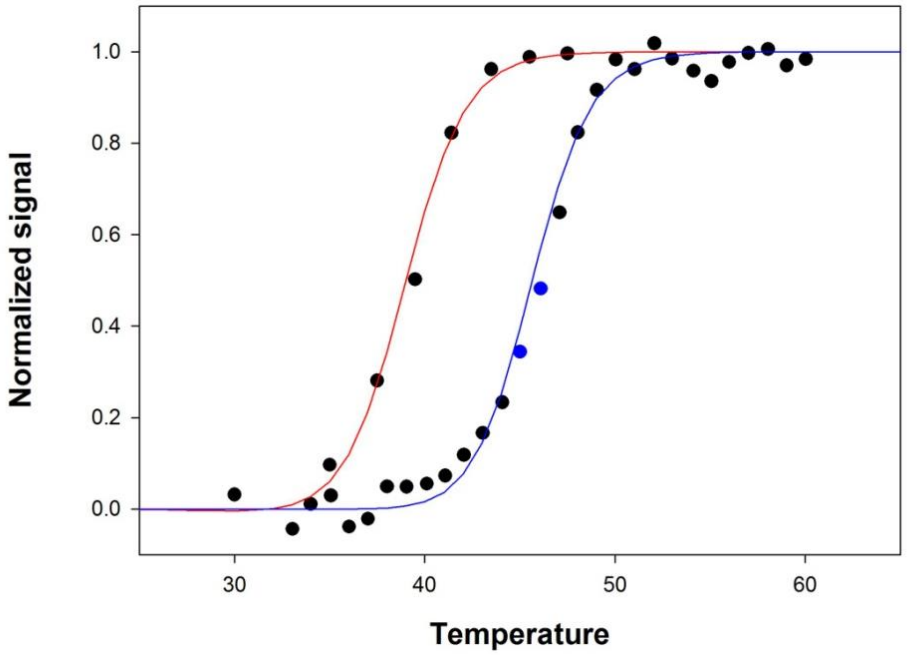

Figure IV-7. Thermally induced structural transitions of the UCS domain as monitored using the ANS emission and far UV CD. The dependence of the normalized signals, ANS fluorescence and Far-UV Circular Dichroism, as a function of temperature. The solid lines are nonlinear least squares fits of the curves to equations IV-3 and IV-6, with ANS fluorescence (red) and Circular Dichroism (blue).

. In order to further elucidate the structural rearrangements occurring within the UCS domain under thermal stress, we have examined the protein conformational changes using the limited trypsin digestion assay. The assay uses a catalytic low concentration of trypsin, which limits the enzymatic reaction to the exposed protein loops, containing the cleavage sites.

We incubated the trypsin - UCS domain mixture (1:10,000 ratio trypsin: UCS), at 37^{o}C for different time intervals, ranging from 1 to 30 minutes before quenching the reaction with SDS PAGE buffer. The results were analyzed by the SDS-PAGE gel, as depicted in **Figure IV-8**. Thus, we monitored the UCS domain proteolysis as a function of time. The first reaction product was formed after only 1 minute and has 37 kDa mass (**Figure IV-8**). Within the next 15 minutes three additional products were detected. They have molecular masses of 24, 18 and 14 kDa. Furthermore, the high resolution gel showed that the band with 14 kDa product contains two entities (**Figure IV-8**). Since we aimed at localization of these digestion products in the UCS domain structure, we used MALDI-TOF-TOF mass spectrometry at the UTMB mass spectrometry facility to identify their amino acid composition.

Analysis of the first digestion product (37 kDa) identified five peptide markers (**Figure IV-9**) (Mascott, Matrix Science, Boston, MA). The result enabled us to suggest the localization of a cleavage site between 10H3 and 11H1 helices (**Figure IV-9**). In order to deduce other digestion sites, we combine the data obtained from the analysis of limited trypsin digestion experiments, peptide markers identified by MALDI-TOF-TOF mass spectrometry, and *in silico* predicted cleavage sites. We applied the same approach to construe that the 24 kDa product is a result of cleavage between 11H2 and 11H3

helices. Furthermore, additional cleavage sites most probably exist between 13H2-13H3, 13H3-14H1 and 16H1-16H2 helices (**Figure IV-9**). They yielded 18 and 14 kDa products.

The data allowed us to elucidate structural changes occurring within the chaperone as a response to thermal stress. There are five major cleavage sites, which become available to the trypsin as a result of the temperature-induced transition. Moreover, the sites are located through the entire UCS domain, *i.e*., strongly suggesting that the response of the protein structure to the thermal stress involves the entire chaperone domain. In other words, the response seems not to be localized to any particular region of the domain. The results corroborate the thermodynamic analysis of the ANS fluorescence experiments, which indicate the presence of large enthalpy and entropy changes accompanying the thermal transition *prior* to the secondary structure melting, *i.e*., involving large parts of the UCS domain molecule.

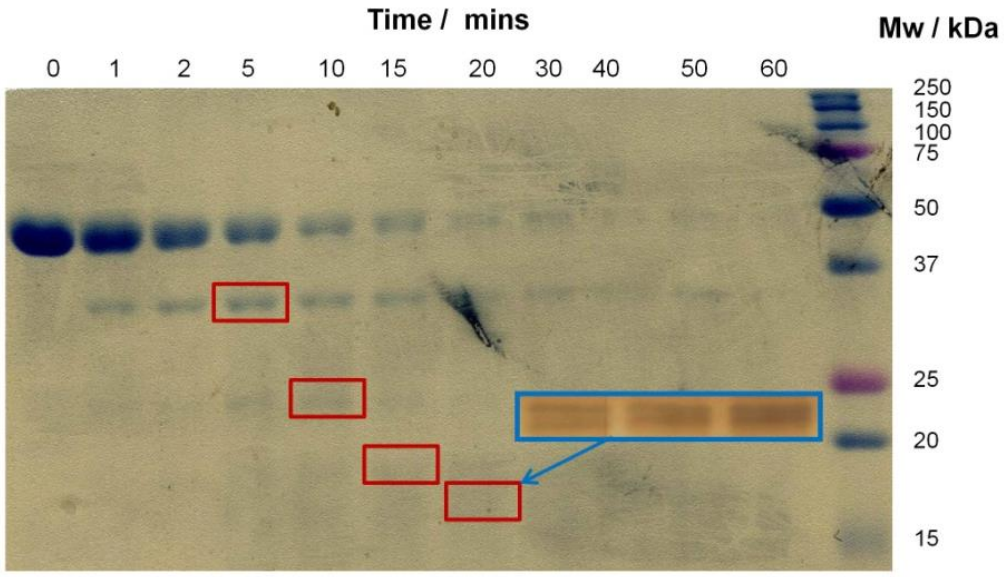

Figure IV-8. The SDS-PAGE gel of the limited trypsin digestion of the UCS domain. The UCS domain (1μM) was mixed in a 1:10,000 molar ratio with trypsin. The four indicated bands (red squares) were cut out and examined using the mass spectroscopy. The bands correspond to 37 kDa, 24 kDa, 18 kDa and 14 kDa products of the reaction. Inset represents a high-resolution tricine gel of the digest products, which was silver stained and shows that the 14 kDa band represents two distinct products. Adapted with permission from (122).

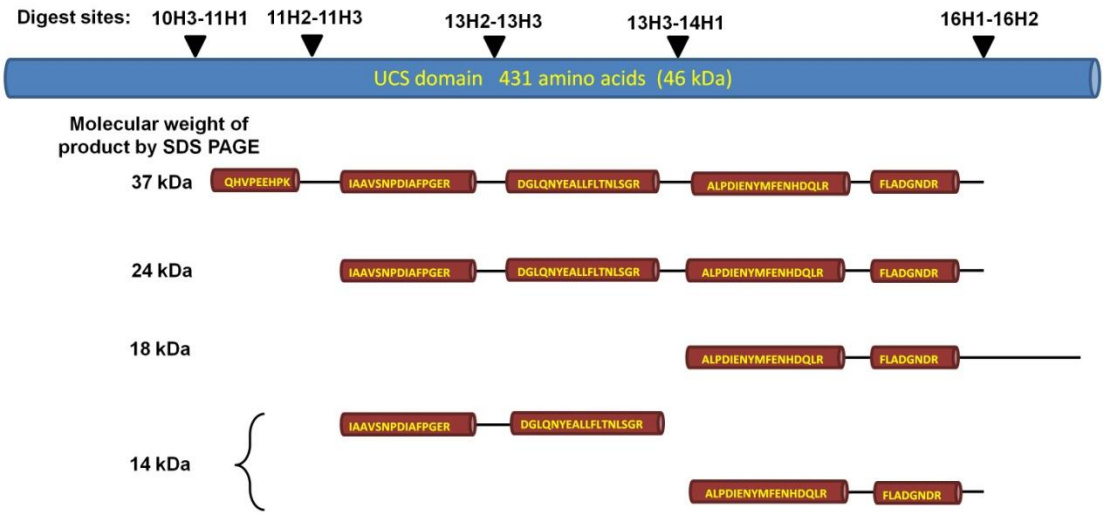

Figure IV-9. (MALDI-TOF-TOF) analysis of the UCS domain limited trypsin proteolysis. Peptides recognized as significant by Mascot (Matrix Science, Boston MA) are shown along with the approximate molecular weight of the product band from SDS-PAGE gel. Digest sites were deduced by combining results from the mass spectroscopy, known product size and constrained by protein surface availability estimated from the known X-ray crystal structure of the UNC-45 chaperone from *C. elegans* (4i2z). Adapted with permission from (122).

CONCLUSIONS

The UNC-45 chaperone is critical for the development and retaining of muscle function. The chaperone is localized in sarcomere where it can be subjected to significant thermal stress. The same thermal stress will also affect the client protein, myosin. In the human organism physiological ranges of temperature can reach 40-41°C. At these temperatures, the myosin molecules begin to aggregate. Therefore, in order to maintain protein homeostasis, cells should have a mechanism that would activate chaperones at the specific temperature conditions.

Our data revealed that the temperature induces conformational changes of the chaperone domain of UNC-45. Moreover, we have identified the critical structural changes occurring within the UCS domain as a response to heat stress. Our ANS experiments showed that in temperature ranges of 38-41°C, the hydrophobic moieties that were once deeply buried inside of protein core become accessible to solvent. Subsequently, the reported conformational changes occur at the temperatures corresponding to physiological heat shock conditions and environment of myosin aggregation. Additionally, the results of circular dichroism experiments showed that only the domain tertiary structure is affected by the temperature in the *homo sapiens* physiological ranges. In other words, the UCS domain secondary structure remains intact at thermal stress conditions.

The findings of ANS and circular dichroism experiments are supported by trypsin digestion of the UCS domain. Our data shows that there are loops within the UCS domain which as a result of thermal stress, start to lose their clearly defined

structure and become available for enzymatic cleavage. The results imply that at temperatures above 30°C the structure of the UCS domain becomes more flexible. This conclusion is supported by high entropy changes associated with the UCS domains conformational rearrangements.

The highly dynamic nature of the UCS domain is strongly linked to chaperone activities. Higher temperatures strongly affect myosin structure, which results in appearance of hydrophobic and aggregation-prone regions on the protein surface, as well as in greater flexibility of the entire myosin structure. These highly dynamic myosin molecules assume many conformations. Therefore, efficient chaperone should also exist in many dynamic conformations, which would enable it to bind different conformations of the client protein *i.e.*, myosin. Notice, these properties should be activated only at clearly defined conditions (38-41°C), otherwise UNC-45 could interact with too many proteins, which would be detrimental to its main chaperone functions.

As we discuss above, the temperature, which triggers the chaperone conformational changes and activates its function (38-41°C), is tuned to the temperature of the myosin aggregation. Moreover, we have concluded that high flexibility of the UCS domain structure is required for the chaperone function. The conclusion corroborates the *in vivo* experiments performed with *Danio rerio* model organism, which showed that heat stress (37° C) induces migration of UNC-45 from peripheries to the center of sarcomere, a region of high myosin concentration (from the Z-line to the A-band) (58). Therefore, both our and these *in vivo* experiments complement each other and indicate that the temperature is an environmental

parameter that controls the UNC-45 chaperone functions *i.e.*, the localization in the sarcomere and its conformational state.

Chapter 5

Conclusions and future directions

Understanding of the protein folding process as well as the mechanism by which protein homeostasis is maintained in cell is of pivotal biological and medical importance. The molecular chaperones are a major class of enzymes that play a critical role in these processes, and act as factors that prevent protein misfolding and aggregation. Therefore, elucidation of the mechanism of chaperone action has been one of the paramount challenges in molecular biology. Our research is focused on the UNC-45 chaperone, which is associated with the proper function of the sarcomeric myosin. We analyzed the UNC-45 chaperone - myosin interactions at single molecule level, using myosin S1- I27 protein chimera where I27 titin domains act as a folding sensor which allows us to observe the effect of UNC-45 on the myosin folding. This is a novel approach that can be used to examine how the presence of chaperones affects the folding of the client proteins. The obtained results, indicated that the chaperone can engage the partially folded myosin and prevent its misfolding. As a result of its chaperone action, UNC-45 also prevents the recruitment of the titin I27 domain into misfolded states.

In our studies we have examined the energetics of formation of the UNC-45 - myosin complex and addressed the role of the chaperone domains in the binding process. The obtained results revealed that both the UCS domain and the Central domain of UNC-45 interact with the myosin motor domain. Thus, we established that the Central domain binds to myosin. Moreover, the domains of the chaperone associate with two different binding sites on myosin. In other words, the myosin motor domain possesses two binding areas within the total binding site for UNC-45 and each area engages a different domain of the UNC-45 chaperone.

Using the fluorescence titration method we have quantified the intrinsic affinities between the myosin S1 and the full length UNC-45, the UCS domain, and the Central domain. The corresponding binding constants are $(2.8 \pm 0.8) \times 10^6$ M^{-1}, $(4.3 \pm 1.5) \times 10^6$ M^{-1}, and $(6 \pm 1.5) \times 10^5$ M^{-1}. Notice that the affinity of the UCS domain alone is even higher than the affinity of the full-length UNC-45. Therefore, the binding of both domains to myosin results in the decreased affinity of the full length UNC-45 for the client protein. Furthermore, these results also indicate that the free energy of interactions of UNC-45 with the myosin motor domain is not a simple sum of the free energies of interactions of its domains with myosin. Thus, the data indicate existence of allosteric interactions between the UCS domain and the Central domain during the formation of myosin - UNC-45 complex. Using our data, we were able to calculate the intrinsic free energy change accompanying the allosteric interaction, which amounts to $\Delta G_C \approx 8$ kcal/mol. The large energetic cost of the myosin - UNC-45 complex formation, with both domains bound to myosin indicates the presence of large conformational changes within the interacting proteins.

The presence of two different binding sites for the UNC-45 domains strongly suggests that the domains may perform different functions. In this context, our dynamic light scattering and single molecule AFM pulling experiments showed that the UCS domain is preventing myosin motor domains aggregation. Thus, the domain alone is responsible for chaperone activity of UNC-45.

On the other hand, despite the fact that the Central domain also interacts with myosin S1, the domain displays no effect on myosin aggregation, *i.e.*, it does not possess

the chaperone activities. Moreover, the allosteric interactions between the domains of UNC-45 do not affect the chaperone properties of the UCS domain.

This different behavior and the fact that the Central domain induces significant conformational changes within the myosin - UNC-45 complex through allosteric interactions, imply that the domain performs a different function than the UCS domain. The conclusion is strongly supported by recent actin gliding experiments. The data from Dr. Oberhauser's group show that the Central domain possesses the ability to stop actin translocation by myosin (unpublished results). In the context of sarcomere formation, the result suggests that inhibition of the actin translocation by the Central domain enables the UCS domain to bind and stabilize the myosin structure. In other words, the UCS domain can perform its chaperone function because the power stroke activities of myosin are blocked by the Central domain.

The results discussed above indicate a significant structural flexibility of the UNC-45 chaperone, which adjusts its interactions with the client protein through allosteric interactions. Moreover, some chaperones can be activated by application of environmental stress, which induces structural alterations in the protein molecule. In this context we have shown that the increasing temperature affects the structure of the chaperone domain of UNC-45. The UCS domain undergoes significant structural rearrangements as a function of the temperature that may play a critical role for its chaperone function (**Figure V-1**). Myosin, as the UNC-45 client protein, is also sensitive to the increase of temperature and starts to aggregate in 40-43°C. These temperatures are in physiological range of human organism. Therefore myosin has to be often subjected to the thermal stress. If nothing prevented the myosin aggregation, it would have to be

directed to proteosomal degradation. In turn, that would be a very energetically costly process for the organism. Subsequently, new myosin would have to be synthesized and assembled into sarcomeric thick filaments. The process would cost a lot of energy and resources. Therefore it is easy to appreciate that nature would design a process where thermosensing chaperone is activated at physiological temperatures to protect myosin from degradation.

The results of our experiments allowed us to identify crucial structural changes occurring within the UCS domain under heat stress. The increase of temperature towards the upper values of physiologically limits (~43°C) induces the structural alterations of the domain tertiary structure. At the same time, its secondary structure remains intact. Moreover, the ANS fluorescence experiments showed that at these elevated temperatures the hydrophobic surfaces become available to solvent. That implies that at low temperatures the hydrophobic binding sites are deeply buried within the protein core. Temperatures increase to 38-41°C brings them to the protein surface. This range of temperature is perfectly tuned with heat shock conditions occurring in the *homo sapiens* muscle. Therefore, we suggest that these rearrangements are of pivotal importance for the UNC-45 chaperone function.

Furthermore, additional data confirming structural rearrangements occurring within the UNC-45 chaperone were gained from trypsin digestion experiments. These experiments were ideal to analyze structural changes because trypsin easily cleaves physically exposed loops lacking defined secondary structure. Since we did not observe the digestion of the UCS domain at lower temperatures, in the limited digestion conditions, the protein in those temperatures does not possesses solvent exposed loops.

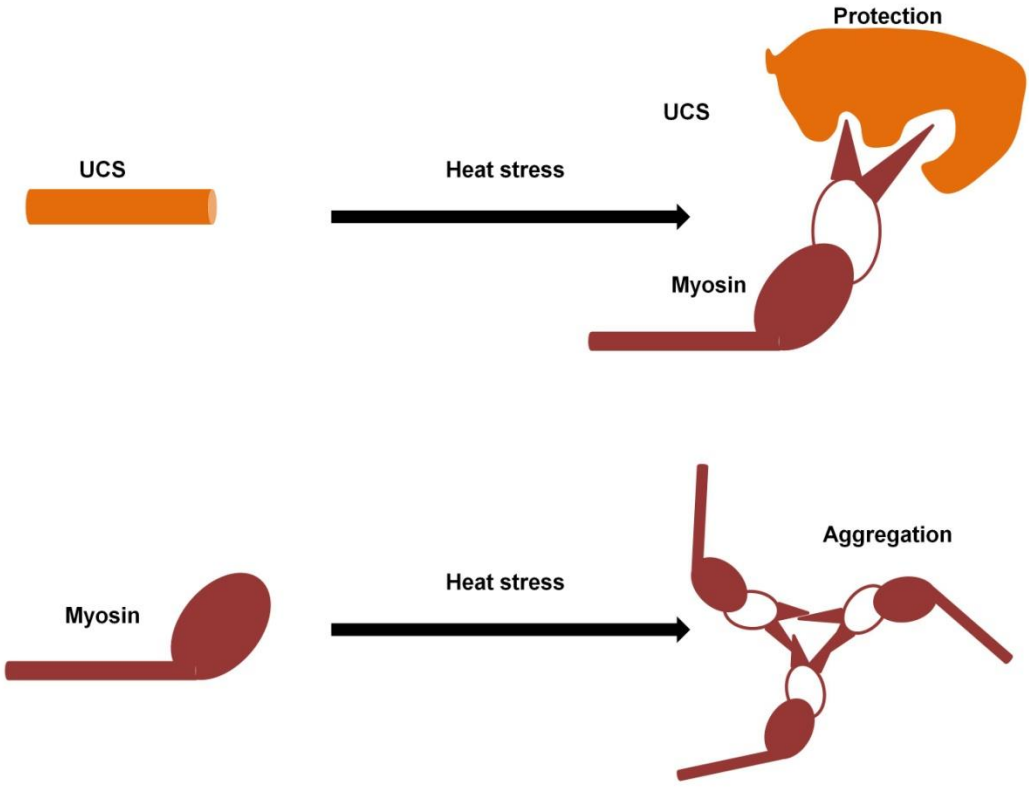

Figure V-1. Possible function of the UCS domain under physiologically relevant temperatures. The UCS domain undergoes significant structural rearrangements in response to thermal stress in the physiological range of temperatures of the human organism. Previously deeply buried hydrophobic moieties of the UCS domain become solvent exposed in response to heat stress. These structural changes may allow the chaperone to perform its function on the partially denatured myosin. In the absence of the UCS domain myosin easily aggregates, which is detrimental to its biological functions.

However, the situation is radically different at higher temperatures above 30℃, where trypsin-degradation of the protein is easily detected. Therefore, our data indicate that at physiological temperatures, several loops of the UCS domain start to lose some of their structural features and become more accessible to the trypsin cleavage. This indicates that the chaperone acquires more flexible and dynamic form at elevated temperatures, as indicated by high entropy changes characterizing the UCS structural transition. These properties are strongly linked to the chaperone activity. At higher temperatures, myosin starts to lose its internal structure and the wide range of hydrophobic and aggregation-prone regions are formed, and are exposed on the protein surface (**Figure V-1**). Since there is no a single clearly defined conformation of myosin at that state, it seems that the chaperone should also not possess one active conformation. That creates a need for existence of the structurally flexible chaperone. In other words, the flexible structure would allow the chaperone to bind to a variety of different conformations of myosin, *i.e.*, the states prone to aggregation.

Nevertheless, it is important to realize that chaperone should exhibit these properties only at biologically desired conditions, thus in the moments of stress. Otherwise, it could bind to too many substrates and that could negatively affect his activities for functionally target proteins.

Our data clearly shows that physiological temperatures are environmental parameter that induces active form of UNC-45. Notice, the chaperone-activation temperatures are perfectly tuned with temperatures where myosin (client protein) is

prone to aggregation. This gives us a very strong correlation between conditions that activates chaperone and the conditions that induce denaturation of the client protein. In our opinion, all these results indicate that intrinsically flexible chaperone is a required element of the mechanism of the UNC-45 function. These conclusions are also strengthened by *in vivo* experiments performed in *Danio rerio* (58). Under normal conditions (22°C) UNC-45 are localized along the Z line. However, when temperature was risen to 37° C, the protein was shuttled to the A-band where myosin is localized. Therefore, the UNC-45 localization in the sarcomere is controlled by temperature. The results are in excellent agreement with our findings about the thermosensor nature of UNC-45 activation. Moreover, both experimental results complement each other. Thus, experiments performed in *Danio rerio* indicate that UNC-45 under stress is moving into close proximity of myosin, whereas our data show that the chaperone additionally undergoes significant structural changes that adapt it to better perform it function.

Since our studies showed that both the UCS and Central domain binds to the myosin motor domain and determined energetic of formed complexes, in the future projects it would be very interesting to address the dynamics of complex formation. The fluorescence stop-flow method is an ideal technique to tackle the problem. The kinetic studies will provide information about the presence of specific intermediates dominating the recognition processes. Moreover, we will be able to determine whether or not the recognition mechanisms include specific conformational transitions of interacting protein molecules. Furthermore, the method allows us to

address which domain of UNC-45B recognizes the myosin motor domain and thus first interact with the client protein.

The ANS fluorescence, circular dichroism and trypsin digestion experiments clearly showed that the UCS domain undergoes significant structural rearrangements as a result of increase of temperature. The binding studies indicated that the formation of myosin – UNC-45B complex is accompanied by large structural rearrangements occurring within the formed complex. Nevertheless, the topology of the conformational changes occurring upon formation of the complex is not well understood. The fluorescence resonance energy transfer (FRET) technique is an exellent method to address that problem. It is very sensitive and allows the experimenter to determine intramolecular distances between different parts of the macromolecule, labeled with the fluorescence donor and the fluorescence acceptor. The method can be used to measure distances in the range of ~10 to ~80 Å. The observed changes in the FRET efficiency will provide estimates of distance changes between the location of the donor and the location of the acceptor, *i.e.*, the conformational changes occurring upon the formation of the myosin – UNC-45B complex.

The discovered thermosensing activities of human UNC-45 suggest that other UCS proteins could also possess similar properties. It would be very interesting to investigate whether UNC-45 chaperones present in species with body temperatures different from *homo sapiens* undergoes significant structural rearrangements when temperature is increased. The studies would allow us to answer whether different environmental condition such as lower temperature affected the evolution of the

UNC-45 chaperone in other species to such an extent that its thermosensing properties are tuned to different ranges of temperature.

Appendix 1

Thermodynamic analysis of the multiple sequential structural transitions of the UCS domain

Although the separation of the UCS conformational transition allows us to treat the transitions as independent events, a more complete analysis would require taking into account the sequential nature of the conformational changes of the UCS domain induced by the temperature. Moreover, such an analysis would include the transition observed in the trypsin digestion pulse experiments. The results of the experiments described in chapter 4 imply that the UCS domain undergoes at least three conformational transitions under thermal stress. The transition in the lowest temperature range was observed using the trypsin digestion pulse approach (**Figure IV-4**). At higher temperatures, another conformational change occurs, as followed by the ANS fluorescence technique (**Figure IV-3**). Finally, the melting of the UCS secondary structure occurs in the highest temperature range, as monitored by the far-UV circular dichroism (**Figure IV-6**).

The digestion reaction occurs almost instantaneously due to extremely high concentration of trypsin (135). The ANS fluorescence approach provides, within experimental accuracy, the same melting curves at different dye concentrations data not shown). Finally the CD melting curve could be reversed from the melting point to the initial value of the ellipticity. These features suggest that equilibrium structural

transitions of the protein are observed. The simplest thermodynamic model, which describes conformational changes of the UCS domain, is a sequential reaction

$$A \Leftrightarrow B \Leftrightarrow C \Leftrightarrow D \qquad \text{(A-1)}$$

where A is the initial state of the UCS domain at temperatures below ~25°C, B is the state of the domain in the plateau of the curve recorded by the trypsin digestion pulse method, C is the state of the protein in the plateau of the curve recorded by the ANS fluorescence intensity technique, and D is the state at the final plateau recorded by the mean residue molar ellipticity at 222 nm.

The degree of digestion, DG, as a function of the temperature in the transition, A <-> B, recorded by the trypsin digestion pulse experiments, is described by equation A-2, as

$$\Delta DG_{obs} = \frac{1}{1+\exp((-\Delta H_{AB} + T\Delta S_{AB})/RT)} + \Delta DG_{max}\left(\frac{[\exp((-\Delta H_{AB} + T\Delta S_{AB})/RT)]}{1+\exp((-\Delta H_{AB} + T\Delta S_{AB})/RT)}\right) \qquad \text{(A-2)}$$

where ΔDG_{obs} is the observed degree of digestion at a given temperature, ΔDG_{max} is the maximum value of the observed degree of digestion. This is a single-step conformational change characterized by the specific values of enthalpy, ΔH_{AB}, and entropy, ΔS_{AB}.

The conformational transition recorded by the ANS fluorescence, B <-> C, occurs at higher temperature *i.e.*, it follows the transition, A <-> B. Thus, the

conformational change recorded by the ANS fluorescence actually contains two conformational changes. Nevertheless, the sigmoidal character of the ANS fluorescence dependence upon the temperature indicates the first transition, A <-> B, does not contribute to the ANS fluorescence. The dependence of the ANS emission intensity, ΔF_{obs}, is then described by equation A-3, as

$$\Delta F_{obs} = \frac{1}{1+\exp((-\Delta H_{AB} + T\Delta S_{AB})/RT) + [\exp((-\Delta H_{AB} + T\Delta S_{AB})/RT][\exp((-\Delta H_{BC} + T\Delta S_{BC})/RT}$$

$$+\Delta F_{max}\left(\frac{[\exp((-\Delta H_{AB} + T\Delta S_{AB})/RT)][\exp((-\Delta H_{BC} + T\Delta S_{BC})/RT)]}{1+\exp((-\Delta H_{AB} + T\Delta S_{AB})/RT) + [\exp((-\Delta H_{AB} + T\Delta S_{AB})/RT)][\exp((-\Delta H_{BC} + T\Delta S_{BC})/RT)}\right)$$

(A-3)

This is a sequential, two-step conformational change characterized by specific values of enthalpies, ΔH_{AB} and ΔH_{BC}, and entropies, ΔS_{AB} and ΔS_{BC}.

The final conformational transition, C <-> D, recorded by the molar mean residue ellipticity follows the first and the second transitions, A<-> B and B <-> C, respectively. Therefore, the observed process actually contains three conformational changes. As in the case of the ANS fluorescence approach, the sigmoidal character of the CD dependence upon the temperature indicates that the first and second transitions do contribute to the circular dichroism changes. The partition function of the system, Z_{ABCD}, is then

$$Z_{ABCD} = 1+\exp((-\Delta H_{AB} + T\Delta S_{AB})/RT) + [\exp((-\Delta H_{AB} + T\Delta S_{AB})/RT][\exp((-\Delta H_{BC} + T\Delta S_{BC})/RT]$$

$$+[\exp((-\Delta H_{AB} + T\Delta S_{AB})/RT][\exp((-\Delta H_{BC} + T\Delta S_{BC})/RT][\exp((-\Delta H_{CD} + T\Delta S_{CD})/RT]$$

(A-4)

The dependence of the molar mean residue ellipticity, change, $\Delta\Theta$, as a function of the temperature is then described by equation A-5, as

$$\Delta\Theta_{obs} = \frac{1+\exp((-\Delta H_{AB}+T\Delta S_{AB})/RT)+[\exp((-\Delta H_{AB}+T\Delta S_{AB})/RT][\exp((-\Delta H_{BC}+T\Delta S_{BC})/RT]}{Z_{ABCD}}$$

$$+\Delta\Theta_{max}\left(\frac{[\exp((-\Delta H_{AB}+T\Delta S_{AB})/RT][\exp((-\Delta H_{BC}+T\Delta S_{BC})/RT][\exp((-\Delta H_{CD}+T\Delta S_{CD})/RT]}{Z_{ABCD}}\right)$$

(A-5)

This is a sequential, three-step conformational change characterized by specific values of enthalpies, ΔH_{AB}, ΔH_{BC}, and ΔH_{CD}, and entropies, ΔS_{AB}, ΔS_{BC}, and ΔS_{CD}.

For easy comparison between different transitions, we have normalized all transition curves, expressing the observed signal (ΔDG_{obs}, ΔF_{obs}, and $\Delta\Theta_{obs}$) as a fraction of the corresponding total signal change, as

$$\Delta DG_{Norm}=\frac{\Delta DG_{obs}}{\Delta DG_{max}} \qquad \text{(A-6)}$$

$$\Delta F_{Norm}=\frac{\Delta F_{obs}}{\Delta F_{max}} \qquad \text{(A-7)}$$

and

$$\Delta\Theta_{Norm}=\frac{\Delta\Theta_{obs}}{\Delta\Theta_{max}} \qquad \text{(A-8)}$$

Figure A-1 shows the normalized dependence of the degree of digestion of the UCS domain, the ANS fluorescence intensity of the ANS-UCS mixture, and the molar mean residue ellipticity of the UCS domain as a function of the temperature. The strong shift of the transition on the temperature scale is clearly evident with melting temperature corresponding to the midpoint of each curve as T_m = 30 °C, 39 °C, and 46 °C. The solid lines in **Figure A-1** are nonlinear least squares fits to equations A-6, A-7, and A-8 for the corresponding dependences of the degree of digestion, ANS fluorescence emission, and the molar mean residue ellipticity. The fits provide ΔH_{AB} of 75 ± 20 kcal/mol, ΔS_{AB} = 250 ± 70 cal/mol K, ΔH_{BC} of 120 ± 40 kcal/mol, and ΔS_{BC} = 390 ± 90 cal/mol K, and ΔH_{CD} of 130 ± 40 kcal/mol, and ΔS_{CD} = 410 ± 90 cal/mol K. As expected, because of the strong separation of the transitions on the temperature scale, these values are indistinguishable from the values of the corresponding parameters obtained by treating each transition independently.

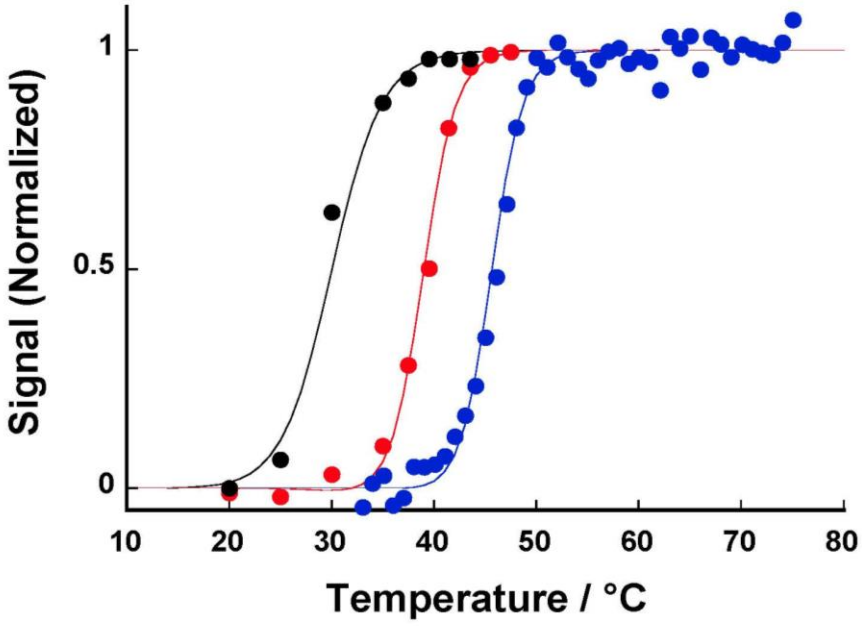

Figure A-1. The thermally induced structural transitions of the UCS examined using the trypsin digestion pulse method, ANS fluorescence of the ANS-UCS mixture, and the molar mean residue ellipticity. The dependence of the normalized signals; the degree of digestion (black), the ANS fluorescence (red) and the Far-UV molar mean residue ellipticity (blue) as a function of temperature. The solid lines in **Figure A-1** are nonlinear least squares fits to equations A-6, A-7, and A-8 for the corresponding dependences of the degree of digestion (black), ANS fluorescence emission (red) and the molar mean residue ellipticity (blue).

Appendix 2

Unpublished work

Tracking myosin – actin interactions, using a novel single molecule assay.

Our laboratory has demonstrated that in the presence of UNC-45, the myosin ATPase is uncoupled from actin translocation (74). In order to investigate the mechanism of the inhibitory effect of UNC-45 on actin translocation we have developed a novel single-molecule assay. The assay should allow us to investigate the size of the power stroke and the duration of the actin-bound state (dwell times) at different UNC-45 concentrations. We attached a biotinylated actin filaments to a streptavidin functionalized bead (4μm, Novascan) glued to an ultracompliant (20pN/nm) AFM cantilever (**Figure A-2**). The presence of actin filaments was verified by fluorescence microscopy. The biotin-streptavidin bond is mechanically strong (breaking at high forces of >100 pN, well above the actomyosin interaction forces, <10 pN). When the actin-coated AFM probe is brought into contact with a myosin coated coverslip there is a clear increase in the cantilever displacements, Δz, only in the presence of 1mM MgATP (**Figure A-2**). We detected staircase displacements (probably from multiple actin-myosin interactions) as well as transient displacements. These displacements are in the range expected for full-length skeletal myosin (137) (5-12nm). These promising initial experiments demonstrated that this assay may be applied to address the nature of the inhibition of actin translocation by UNC-45.

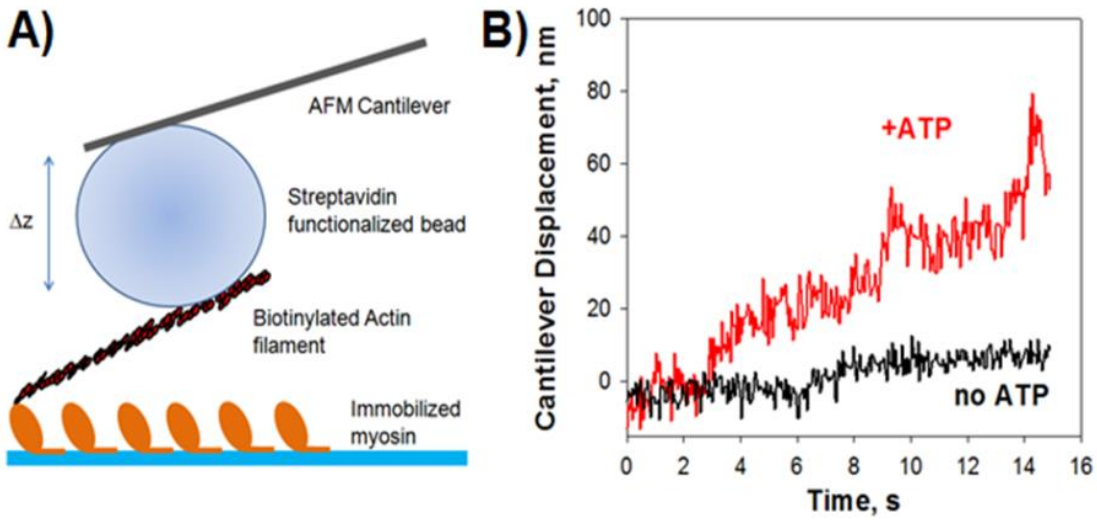

Figure A-2 Tracking actomyosin interactions using a novel single-molecule AFM based assay. A) Biotinylated actin was prepared by labeling F-actin with 1000:1 ratio of biotinylated phalloidin and Alexa 594 phalloidin. These ~10μm long filaments were briefly incubated with streptavidin-bead functionalized cantilevers and then rinsed. **B)** Example of cantilever displacement as a function of time in the absence and presence of 1mM MgATP, shows that, as expected, myosin-actin productive interactions are ATP-dependent.

REFERENCES

1. Anfinsen, C. B., E. Haber, M. Sela, and F. H. White. 1961. The kinetics of formation of native ribonuclease during oxidation of the reduced polypeptide chain. Proc Natl Acad Sci U S A 47:1309-1314.
2. Anfinsen, C. B. 1973. Principles that govern the folding of protein chains. Science 181:223-230.
3. Kubelka, J., J. Hofrichter, and W. A. Eaton. 2004. The protein folding 'speed limit'. Curr Opin Struct Biol 14:76-88.
4. Hartl, F. U., and M. Hayer-Hartl. 2002. Molecular chaperones in the cytosol: from nascent chain to folded protein. Science 295:1852-1858.
5. Bryngelson, J. D., J. N. Onuchic, N. D. Socci, and P. G. Wolynes. 1995. Funnels, pathways, and the energy landscape of protein folding: a synthesis. Proteins 21:167-195.
6. Dobson, C. M., and M. Karplus. 1999. The fundamentals of protein folding: bringing together theory and experiment. Curr Opin Struct Biol 9:92-101.
7. Laskey, R. A., B. M. Honda, A. D. Mills, and J. T. Finch. 1978. Nucleosomes are assembled by an acidic protein which binds histones and transfers them to DNA. Nature 275:416-420.
8. Pelham, H. R. 1986. Speculations on the functions of the major heat shock and glucose-regulated proteins. Cell 46:959-961.
9. Ellis, J. 1987. Proteins as molecular chaperones. Nature 328:378-379.
10. Beissinger, M., and J. Buchner. 1998. How chaperones fold proteins. Biol Chem 379:245-259.
11. Bukau, B., and A. L. Horwich. 1998. The Hsp70 and Hsp60 chaperone machines. Cell 92:351-366.
12. Zhu, X., X. Zhao, W. F. Burkholder, A. Gragerov, C. M. Ogata, M. E. Gottesman, and W. A. Hendrickson. 1996. Structural analysis of substrate binding by the molecular chaperone DnaK. Science 272:1606-1614.
13. Harrison, C. J., M. Hayer-Hartl, M. Di Liberto, F. Hartl, and J. Kuriyan. 1997. Crystal structure of the nucleotide exchange factor GrpE bound to the ATPase domain of the molecular chaperone DnaK. Science 276:431-435.
14. Panaretou, B., G. Siligardi, P. Meyer, A. Maloney, J. K. Sullivan, S. Singh, S. H. Millson, P. A. Clarke, S. Naaby-Hansen, R. Stein, R. Cramer, M. Mollapour, P. Workman, P. W. Piper, L. H. Pearl, and C. Prodromou. 2002. Activation of the ATPase activity of hsp90 by the stress-regulated cochaperone aha1. Mol Cell 10:1307-1318.
15. Hemmingsen, S. M., C. Woolford, S. M. van der Vies, K. Tilly, D. T. Dennis, C. P. Georgopoulos, R. W. Hendrix, and R. J. Ellis. 1988. Homologous plant and bacterial proteins chaperone oligomeric protein assembly. Nature 333:330-334.
16. Ostermann, J., A. L. Horwich, W. Neupert, and F. U. Hartl. 1989. Protein folding in mitochondria requires complex formation with hsp60 and ATP hydrolysis. Nature 341:125-130.
17. Cheng, M. Y., F. U. Hartl, J. Martin, R. A. Pollock, F. Kalousek, W. Neupert, E. M. Hallberg, R. L. Hallberg, and A. L. Horwich. 1989. Mitochondrial heat-shock protein

hsp60 is essential for assembly of proteins imported into yeast mitochondria. Nature 337:620-625.
18. Horwich, A. L., W. Neupert, and F. U. Hartl. 1990. Protein-catalysed protein folding. Trends Biotechnol 8:126-131.
19. Hartl, F. U. 1996. Molecular chaperones in cellular protein folding. Nature 381:571-579.
20. Epstein, H. F., and J. N. Thomson. 1974. Temperature-sensitive mutation affecting myofilament assembly in Caenorhabditis. Nature 250:579-580.
21. Landsverk, M. L., S. Li, A. H. Hutagalung, A. Najafov, T. Hoppe, J. M. Barral, and H. F. Epstein. 2007. The UNC-45 chaperone mediates sarcomere assembly through myosin degradation in Caenorhabditis elegans. J Cell Biol 177:205-210.
22. Barral, J. M., C. C. Bauer, I. Ortiz, and H. F. Epstein. 1998. Unc-45 mutations in Caenorhabditis elegans implicate a CRO1/She4p-like domain in myosin assembly. J Cell Biol 143:1215-1225.
23. Barral, J. M., A. H. Hutagalung, A. Brinker, F. U. Hartl, and H. F. Epstein. 2002. Role of the myosin assembly protein UNC-45 as a molecular chaperone for myosin. Science 295:669-671.
24. Lord, M., and T. D. Pollard. 2004. UCS protein Rng3p activates actin filament gliding by fission yeast myosin-II. J Cell Biol 167:315-325.
25. Lord, M., T. E. Sladewski, and T. D. Pollard. 2008. Yeast UCS proteins promote actomyosin interactions and limit myosin turnover in cells. Proc Natl Acad Sci U S A 105:8014-8019.
26. Wesche, S., M. Arnold, and R. P. Jansen. 2003. The UCS domain protein She4p binds to myosin motor domains and is essential for class I and class V myosin function. Curr Biol 13:715-724.
27. Toi, H., K. Fujimura-Kamada, K. Irie, Y. Takai, S. Todo, and K. Tanaka. 2003. She4p/Dim1p interacts with the motor domain of unconventional myosins in the budding yeast, Saccharomyces cerevisiae. Mol Biol Cell 14:2237-2249.
28. Melkani, G. C., R. Bodmer, K. Ocorr, and S. I. Bernstein. 2011. The UNC-45 chaperone is critical for establishing myosin-based myofibrillar organization and cardiac contractility in the Drosophila heart model. PLoS One 6:e22579.
29. Price, M. G., M. L. Landsverk, J. M. Barral, and H. F. Epstein. 2002. Two mammalian UNC-45 isoforms are related to distinct cytoskeletal and muscle-specific functions. J Cell Sci 115:4013-4023.
30. Hutagalung, A. H., M. L. Landsverk, M. G. Price, and H. F. Epstein. 2002. The UCS family of myosin chaperones. J Cell Sci 115:3983-3990.
31. Shi, H., and G. Blobel. 2010. UNC-45/CRO1/She4p (UCS) protein forms elongated dimer and joins two myosin heads near their actin binding region. Proc Natl Acad Sci U S A 107:21382-21387.
32. Lee, C. F., A. V. Hauenstein, J. K. Fleming, W. C. Gasper, V. Engelke, B. Sankaran, S. I. Bernstein, and T. Huxford. 2011. X-ray crystal structure of the UCS domain-containing UNC-45 myosin chaperone from Drosophila melanogaster. Structure 19:397-408.
33. Gazda, L., W. Pokrzywa, D. Hellerschmied, T. Löwe, I. Forné, F. Mueller-Planitz, T. Hoppe, and T. Clausen. 2013. The myosin chaperone UNC-45 is organized in tandem modules to support myofilament formation in C. elegans. Cell 152:183-195.
34. WL, D. 2002. The PyMOL Molecular Graphics System. DeLano Scientific, Palo Alto, CA.

35. Barral, J. M., S. A. Broadley, G. Schaffar, and F. U. Hartl. 2004. Roles of molecular chaperones in protein misfolding diseases. Semin Cell Dev Biol 15:17-29.
36. Chiti, F., and C. M. Dobson. 2006. Protein misfolding, functional amyloid, and human disease. Annu Rev Biochem 75:333-366.
37. Knowles, T. P., M. Vendruscolo, and C. M. Dobson. 2014. The amyloid state and its association with protein misfolding diseases. Nat Rev Mol Cell Biol 15:384-396.
38. Muchowski, P. J., G. Schaffar, A. Sittler, E. E. Wanker, M. K. Hayer-Hartl, and F. U. Hartl. 2000. Hsp70 and hsp40 chaperones can inhibit self-assembly of polyglutamine proteins into amyloid-like fibrils. Proc Natl Acad Sci U S A 97:7841-7846.
39. Jana, N. R., M. Tanaka, G. Wang, and N. Nukina. 2000. Polyglutamine length-dependent interaction of Hsp40 and Hsp70 family chaperones with truncated N-terminal huntingtin: their role in suppression of aggregation and cellular toxicity. Hum Mol Genet 9:2009-2018.
40. Schaffar, G., P. Breuer, R. Boteva, C. Behrends, N. Tzvetkov, N. Strippel, H. Sakahira, K. Siegers, M. Hayer-Hartl, and F. U. Hartl. 2004. Cellular toxicity of polyglutamine expansion proteins: mechanism of transcription factor deactivation. Mol Cell 15:95-105.
41. Hansen, J. J., A. Dürr, I. Cournu-Rebeix, C. Georgopoulos, D. Ang, M. N. Nielsen, C. S. Davoine, A. Brice, B. Fontaine, N. Gregersen, and P. Bross. 2002. Hereditary spastic paraplegia SPG13 is associated with a mutation in the gene encoding the mitochondrial chaperonin Hsp60. Am J Hum Genet 70:1328-1332.
42. Richardson, A., F. Schwager, S. J. Landry, and C. Georgopoulos. 2001. The importance of a mobile loop in regulating chaperonin/ co-chaperonin interaction: humans versus Escherichia coli. J Biol Chem 276:4981-4987.
43. Bazzaro, M., A. Santillan, Z. Lin, T. Tang, M. K. Lee, R. E. Bristow, I. M. Shih, and R. B. Roden. 2007. Myosin II co-chaperone general cell UNC-45 overexpression is associated with ovarian cancer, rapid proliferation, and motility. Am J Pathol 171:1640-1649.
44. Guo, W., D. Chen, Z. Fan, and H. F. Epstein. 2011. Differential turnover of myosin chaperone UNC-45A isoforms increases in metastatic human breast cancer. J Mol Biol 412:365-378.
45. Hansen, L., S. Comyn, Y. Mang, A. Lind-Thomsen, L. Myhre, F. Jean, H. Eiberg, N. Tommerup, T. Rosenberg, and D. Pilgrim. 2014. The myosin chaperone UNC45B is involved in lens development and autosomal dominant juvenile cataract. Eur J Hum Genet 22:1290-1297.
46. Kuhne, W. 1864. Unterschungen uber das Protoplasma and die Contractilitat. Leipzig.
47. Needham, D. M. 1942. The adenosinetriphosphatase activity of myosin preparations. Biochem J 36:113-120.
48. Szent-Gyorgyi, A. G. 1953. Meromyosins, the subunits of myosin. Arch Biochem Biophys 42:305-320.
49. Mueller, H., and S. V. Perry. 1962. The degradation of heavy meromyosin by trypsin. Biochem J 85:431-439.
50. Slayter, H. S., and S. Lowey. 1967. Substructure of the myosin molecule as visualized by electron microscopy. Proc Natl Acad Sci U S A 58:1611-1618.
51. Foth, B. J., M. C. Goedecke, and D. Soldati. 2006. New insights into myosin evolution and classification. Proc Natl Acad Sci U S A 103:3681-3686.

52. Reyes, B. A., J. S. Pendergast, and S. Yamazaki. 2008. Mammalian peripheral circadian oscillators are temperature compensated. J Biol Rhythms 23:95-98.
53. Takai, K., K. Nakamura, T. Toki, U. Tsunogai, M. Miyazaki, J. Miyazaki, H. Hirayama, S. Nakagawa, T. Nunoura, and K. Horikoshi. 2008. Cell proliferation at 122 degrees C and isotopically heavy CH4 production by a hyperthermophilic methanogen under high-pressure cultivation. Proc Natl Acad Sci U S A 105:10949-10954.
54. Altuvia, S., D. Kornitzer, D. Teff, and A. B. Oppenheim. 1989. Alternative mRNA structures of the cIII gene of bacteriophage lambda determine the rate of its translation initiation. J Mol Biol 210:265-280.
55. Narberhaus, F., T. Waldminghaus, and S. Chowdhury. 2006. RNA thermometers. FEMS Microbiol Rev 30:3-16.
56. White, H. E., E. V. Orlova, S. Chen, L. Wang, A. Ignatiou, B. Gowen, T. Stromer, T. M. Franzmann, M. Haslbeck, J. Buchner, and H. R. Saibil. 2006. Multiple distinct assemblies reveal conformational flexibility in the small heat shock protein Hsp26. Structure 14:1197-1204.
57. Reichmann, D., Y. Xu, C. M. Cremers, M. Ilbert, R. Mittelman, M. C. Fitzgerald, and U. Jakob. 2012. Order out of disorder: working cycle of an intrinsically unfolded chaperone. Cell 148:947-957.
58. Etard, C., U. Roostalu, and U. Strähle. 2008. Shuttling of the chaperones Unc45b and Hsp90a between the A band and the Z line of the myofibril. J Cell Biol 180:1163-1175.
59. Bujalowski, P. J., and A. F. Oberhauser. 2013. Tracking unfolding and refolding reactions of single proteins using atomic force microscopy methods. Methods 60:151-160.
60. Mashaghi, A., G. Kramer, D. C. Lamb, M. P. Mayer, and S. J. Tans. 2014. Chaperone action at the single-molecule level. Chem Rev 114:660-676.
61. Scholl, Z. N., W. Yang, and P. E. Marszalek. 2014. Chaperones rescue luciferase folding by separating its domains. J Biol Chem 289:28607-28618.
62. Oberhauser, A. F., and M. Carrión-Vázquez. 2008. Mechanical biochemistry of proteins one molecule at a time. J Biol Chem 283:6617-6621.
63. Greene, D. N., T. Garcia, R. B. Sutton, K. M. Gernert, G. M. Benian, and A. F. Oberhauser. 2008. Single-molecule force spectroscopy reveals a stepwise unfolding of Caenorhabditis. Biophys J 95:1360-1370.
64. Mashaghi, A., G. Kramer, P. Bechtluft, B. Zachmann-Brand, A. J. Driessen, B. Bukau, and S. J. Tans. 2013. Reshaping of the conformational search of a protein by the chaperone trigger factor. Nature 500:98-101.
65. Bechtluft, P., R. G. van Leeuwen, M. Tyreman, D. Tomkiewicz, N. Nouwen, H. L. Tepper, A. J. Driessen, and S. J. Tans. 2007. Direct observation of chaperone-induced changes in a protein folding pathway. Science 318:1458-1461.
66. Oberhauser, A. F., P. E. Marszalek, H. P. Erickson, and J. M. Fernandez. 1998. The molecular elasticity of the extracellular matrix protein tenascin. Nature 393:181-185.
67. Kaiser, C. M., P. J. Bujalowski, L. Ma, J. Anderson, H. F. Epstein, and A. F. Oberhauser. 2012. Tracking UNC-45 chaperone-myosin interaction with a titin mechanical reporter. Biophys J 102:2212-2219.
68. Bullard, B., T. Garcia, V. Benes, M. C. Leake, W. A. Linke, and A. F. Oberhauser. 2006. The molecular elasticity of the insect flight muscle proteins projectin and. Proc Natl Acad Sci U S A 103:4451-4456.

69. Rief, M., M. Gautel, F. Oesterhelt, J. M. Fernandez, and H. E. Gaub. 1997. Reversible unfolding of individual titin immunoglobulin domains by AFM. Science 276:1109-1112.
70. Cao, Y., M. M. Balamurali, D. Sharma, and H. Li. 2007. A functional single-molecule binding assay via force spectroscopy. Proc Natl Acad Sci U S A 104:15677-15681.
71. Moy, V. T., E. L. Florin, and H. E. Gaub. 1994. Intermolecular forces and energies between ligands and receptors. Science 266:257-259.
72. Engel, A., and D. J. Müller. 2000. Observing single biomolecules at work with the atomic force microscope. Nat Struct Biol 7:715-718.
73. Müller, D. J., F. A. Schabert, G. Büldt, and A. Engel. 1995. Imaging purple membranes in aqueous solutions at sub-nanometer resolution by atomic force microscopy. Biophys J 68:1681-1686.
74. Müller, D. J., M. Krieg, D. Alsteens, and Y. F. Dufrêne. 2009. New frontiers in atomic force microscopy: analyzing interactions from single-molecules to cells. Curr Opin Biotechnol 20:4-13.
75. Dufrene, Y. F., and P. Hinterdorfer. 2008. Recent progress in AFM molecular recognition studies. Pflugers Arch 456:237-245.
76. Hinterdorfer, P. 2002. Molecular recognition studies using the atomic force microscope. Methods Cell Biol 68:115-139.
77. Kodera, N., D. Yamamoto, R. Ishikawa, and T. Ando. 2010. Video imaging of walking myosin V by high-speed atomic force microscopy. Nature 468:72-76.
78. Mou, J., D. M. Czajkowsky, S. J. Sheng, R. Ho, and Z. Shao. 1996. High resolution surface structure of E. coli GroES oligomer by atomic force microscopy. FEBS Lett 381:161-164.
79. Vinckier, A., P. Gervasoni, F. Zaugg, U. Ziegler, P. Lindner, P. Groscurth, A. Plückthun, and G. Semenza. 1998. Atomic force microscopy detects changes in the interaction forces between GroEL and substrate proteins. Biophys J 74:3256-3263.
80. Viani, M. B., L. I. Pietrasanta, J. B. Thompson, A. Chand, I. C. Gebeshuber, J. H. Kindt, M. Richter, H. G. Hansma, and P. K. Hansma. 2000. Probing protein-protein interactions in real time. Nat Struct Biol 7:644-647.
81. Zhu, Y., J. Bogomolovas, S. Labeit, and H. Granzier. 2009. Single molecule force spectroscopy of the cardiac titin N2B element: effects of the molecular chaperone alphaB-crystallin with disease-causing mutations. J Biol Chem 284:13914-13923.
82. Kaiser, C. M., D. H. Goldman, J. D. Chodera, I. Tinoco, and C. Bustamante. 2011. The ribosome modulates nascent protein folding. Science 334:1723-1727.
83. Maillard, R. A., G. Chistol, M. Sen, M. Righini, J. Tan, C. M. Kaiser, C. Hodges, A. Martin, and C. Bustamante. 2011. ClpX(P) generates mechanical force to unfold and translocate its protein substrates. Cell 145:459-469.
84. Aubin-Tam, M. E., A. O. Olivares, R. T. Sauer, T. A. Baker, and M. J. Lang. 2011. Single-molecule protein unfolding and translocation by an ATP-fueled proteolytic machine. Cell 145:257-267.
85. Sharma, S., K. Chakraborty, B. K. Müller, N. Astola, Y. C. Tang, D. C. Lamb, M. Hayer-Hartl, and F. U. Hartl. 2008. Monitoring protein conformation along the pathway of chaperonin-assisted folding. Cell 133:142-153.
86. Hofmann, H., F. Hillger, S. H. Pfeil, A. Hoffmann, D. Streich, D. Haenni, D. Nettels, E. A. Lipman, and B. Schuler. 2010. Single-molecule spectroscopy of protein folding in a chaperonin cage. Proc Natl Acad Sci U S A 107:11793-11798.

87. Mapa, K., M. Sikor, V. Kudryavtsev, K. Waegemann, S. Kalinin, C. A. Seidel, W. Neupert, D. C. Lamb, and D. Mokranjac. 2010. The conformational dynamics of the mitochondrial Hsp70 chaperone. Mol Cell 38:89-100.
88. Kellner, R., H. Hofmann, A. Barducci, B. Wunderlich, D. Nettels, and B. Schuler. 2014. Single-molecule spectroscopy reveals chaperone-mediated expansion of substrate protein. Proc Natl Acad Sci U S A 111:13355-13360.
89. Bartlett, A. I., and S. E. Radford. 2009. An expanding arsenal of experimental methods yields an explosion of insights into protein folding mechanisms. Nat Struct Mol Biol 16:582-588.
90. Kachur, T. M., and D. B. Pilgrim. 2008. Myosin assembly, maintenance and degradation in muscle: Role of the chaperone UNC-45 in myosin thick filament dynamics. Int J Mol Sci 9:1863-1875.
91. Srikakulam, R., and D. A. Winkelmann. 1999. Myosin II folding is mediated by a molecular chaperonin. J Biol Chem 274:27265-27273.
92. Chow, D., R. Srikakulam, Y. Chen, and D. A. Winkelmann. 2002. Folding of the striated muscle myosin motor domain. J Biol Chem 277:36799-36807.
93. Nicholls, P., P. J. Bujalowski, H. F. Epstein, D. F. Boehning, J. M. Barral, and A. F. Oberhauser. 2014. Chaperone-mediated reversible inhibition of the sarcomeric myosin power stroke. FEBS Lett.
94. Sellers, J. R. 2000. Myosins: a diverse superfamily. Biochim Biophys Acta 1496:3-22.
95. Huxley, H. E. 1969. The mechanism of muscular contraction. Science 164:1356-1365.
96. Spudich, J. A. 2001. The myosin swinging cross-bridge model. Nat Rev Mol Cell Biol 2:387-392.
97. Pollard, T. D. 1982. Myosin purification and characterization. Methods Cell Biol 24:333-371.
98. Weeds, A. G., and B. Pope. 1977. Studies on the chymotryptic digestion of myosin. Effects of divalent cations on proteolytic susceptibility. J Mol Biol 111:129-157.
99. Carrion-Vazquez, M., A. F. Oberhauser, S. B. Fowler, P. E. Marszalek, S. E. Broedel, J. Clarke, and J. M. Fernandez. 1999. Mechanical and chemical unfolding of a single protein: a comparison. Proc Natl Acad Sci U S A 96:3694-3699.
100. Oberhauser, A. F., P. E. Marszalek, M. Carrion-Vazquez, and J. M. Fernandez. 1999. Single protein misfolding events captured by atomic force microscopy. Nat Struct Biol 6:1025-1028.
101. Bullard, B., W. A. Linke, and K. Leonard. 2002. Varieties of elastic protein in invertebrate muscles. J Muscle Res Cell Motil 23:435-447.
102. Oberhauser, A. F., C. Badilla-Fernandez, M. Carrion-Vazquez, and J. M. Fernandez. 2002. The mechanical hierarchies of fibronectin observed with single-molecule AFM. J Mol Biol 319:433-447.
103. Miller, E., T. Garcia, S. Hultgren, and A. F. Oberhauser. 2006. The mechanical properties of E. coli type 1 pili measured by atomic force microscopy techniques. Biophys J 91:3848-3856.
104. Root, D. D., V. K. Yadavalli, J. G. Forbes, and K. Wang. 2006. Coiled-coil nanomechanics and uncoiling and unfolding of the superhelix and alpha-helices of myosin. Biophys J 90:2852-2866.
105. Schwaiger, I., C. Sattler, D. R. Hostetter, and M. Rief. 2002. The myosin coiled-coil is a truly elastic protein structure. Nat Mater 1:232-235.

106. Taniguchi, Y., B. S. Khatri, D. J. Brockwell, E. Paci, and M. Kawakami. 2010. Dynamics of the coiled-coil unfolding transition of myosin rod probed by dissipation force spectrum. Biophys J 99:257-262.
107. Oberhauser, A. F., P. K. Hansma, M. Carrion-Vazquez, and J. M. Fernandez. 2001. Stepwise unfolding of titin under force-clamp atomic force microscopy. Proc Natl Acad Sci U S A 98:468-472.
108. Chakraborty, K., M. Chatila, J. Sinha, Q. Shi, B. C. Poschner, M. Sikor, G. Jiang, D. C. Lamb, F. U. Hartl, and M. Hayer-Hartl. 2010. Chaperonin-catalyzed rescue of kinetically trapped states in protein folding. Cell 142:112-122.
109. Hartl, F. U., A. Bracher, and M. Hayer-Hartl. 2011. Molecular chaperones in protein folding and proteostasis. Nature 475:324-332.
110. Brinker, A., G. Pfeifer, M. J. Kerner, D. J. Naylor, F. U. Hartl, and M. Hayer-Hartl. 2001. Dual function of protein confinement in chaperonin-assisted protein folding. Cell 107:223-233.
111. Tang, Y. C., H. C. Chang, A. Roeben, D. Wischnewski, N. Wischnewski, M. J. Kerner, F. U. Hartl, and M. Hayer-Hartl. 2006. Structural features of the GroEL-GroES nano-cage required for rapid folding of encapsulated protein. Cell 125:903-914.
112. Hellerschmied, D., and T. Clausen. 2014. Myosin chaperones. Curr Opin Struct Biol 25:9-15.
113. Weeds, A. G., and R. S. Taylor. 1975. Separation of subfragment-1 isoenzymes from rabbit skeletal muscle myosin. Nature 257:54-56.
114. Margossian, S. S., and S. Lowey. 1982. Preparation of myosin and its subfragments from rabbit skeletal muscle. Methods Enzymol 85 Pt B:55-71.
115. Bujalowski, P. J., P. Nicholls, and A. F. Oberhauser. 2014. UNC-45B chaperone: the role of its domains in the interaction with the myosin motor domain. Biophys J 107:654-661.
116. Sellers, J. R. 2001. In vitro motility assay to study translocation of actin by myosin. Curr Protoc Cell Biol Chapter 13:Unit 13.12.
117. Jezewska, M. J., S. Rajendran, and W. Bujalowski. 1998. Complex of Escherichia coli primary replicative helicase DnaB protein with a replication fork: recognition and structure. Biochemistry 37:3116-3136.
118. Bujalowski, W., and T. M. Lohman. 1987. A general method of analysis of ligand-macromolecule equilibria using a spectroscopic signal from the ligand to monitor binding. Application to Escherichia coli single-strand binding protein-nucleic acid interactions. Biochemistry 26:3099-3106.
119. Jencks, W. P. 1981. On the attribution and additivity of binding energies. Proc Natl Acad Sci U S A 78:4046-4050.
120. Kron, S. J., and J. A. Spudich. 1986. Fluorescent actin filaments move on myosin fixed to a glass surface. Proc Natl Acad Sci U S A 83:6272-6276.
121. Yu, Q., and S. I. Bernstein. 2003. UCS proteins: managing the myosin motor. Curr Biol 13:R525-527.
122. Bujalowski, P. J., P. Nicholls, J. M. Barral, and A. F. Oberhauser. 2015. Thermally-induced structural changes in an armadillo repeat protein suggest a novel thermosensor mechanism in a molecular chaperone. FEBS Lett 589:123-130.
123. Ni, W., A. H. Hutagalung, S. Li, and H. F. Epstein. 2011. The myosin-binding UCS domain but not the Hsp90-binding TPR domain of the UNC-45 chaperone is essential for function in Caenorhabditis elegans. J Cell Sci 124:3164-3173.

124. Haslbeck, M., T. Franzmann, D. Weinfurtner, and J. Buchner. 2005. Some like it hot: the structure and function of small heat-shock proteins. Nat Struct Mol Biol 12:842-846.
125. Franzmann, T. M., P. Menhorn, S. Walter, and J. Buchner. 2008. Activation of the chaperone Hsp26 is controlled by the rearrangement of its thermosensor domain. Mol Cell 29:207-216.
126. Haslbeck, M., S. Walke, T. Stromer, M. Ehrnsperger, H. E. White, S. Chen, H. R. Saibil, and J. Buchner. 1999. Hsp26: a temperature-regulated chaperone. EMBO J 18:6744-6751.
127. Kazakov, A. S., D. I. Markov, N. B. Gusev, and D. I. Levitsky. 2009. Thermally induced structural changes of intrinsically disordered small heat shock protein Hsp22. Biophys Chem 145:79-85.
128. Zhang, Z., K. Lin, L. Gao, L. Chen, X. Shi, and G. Wu. 2011. Crystal structure of the armadillo repeat domain of adenomatous polyposis coli which reveals its inherent flexibility. Biochem Biophys Res Commun 412:732-736.
129. Kappel, C., U. Zachariae, N. Dölker, and H. Grubmüller. 2010. An unusual hydrophobic core confers extreme flexibility to HEAT repeat proteins. Biophys J 99:1596-1603.
130. Parmeggiani, F., R. Pellarin, A. P. Larsen, G. Varadamsetty, M. T. Stumpp, O. Zerbe, A. Caflisch, and A. Plückthun. 2008. Designed armadillo repeat proteins as general peptide-binding scaffolds: consensus design and computational optimization of the hydrophobic core. J Mol Biol 376:1282-1304.
131. Schägger, H. 2006. Tricine-SDS-PAGE. Nat Protoc 1:16-22.
132. Fratev, F., S. Osk Jónsdóttir, and I. Pajeva. 2013. Structural insight into the UNC-45-myosin complex. Proteins 81:1212-1221.
133. Gains, N., and A. P. Dawson. 1975. 8-Anilinonaphthalene-1-sulphonate interaction with whole and disrupted mitochondria: a re-evaluation of the use of double-reciprocal plots in the derivation of binding parameters for fluorescent probes binding to mitochondrial membranes. Biochem J 148:157-160.
134. Saltin, B., A. P. Gagge, and J. A. Stolwijk. 1970. Body temperatures and sweating during thermal transients caused by exercise. J Appl Physiol 28:318-327.
135. Park, C., and S. Marqusee. 2005. Pulse proteolysis: a simple method for quantitative determination of protein stability and ligand binding. Nat Methods 2:207-212.
136. Figueroa, M., M. V. Hinrichs, M. Bunster, P. Babbitt, J. Martinez-Oyanedel, and J. Olate. 2009. Biophysical studies support a predicted superhelical structure with armadillo repeats for Ric-8. Protein Sci 18:1139-1145.
137. Tyska, M. J., and D. M. Warshaw. 2002. The myosin power stroke. Cell Motil Cytoskeleton 51:1-15.